Growth of SiC by High Temperature CVD and Application of Thermo-gravimetry for an In-situ Growth Rate Measurement

von der Fakultät für Ingenieurwissenschaften, Abteilung Maschinenbau

der Universität Duisburg-Essen

zur Erlangung des akademischen Grades

DOKTOR-INGENIEUR

genehmigte Dissertation

von

Ahmed Elhaddad

aus

Ägypten

Referent:Prof. Dr. rer. nat. Burak Atakan

Korreferent: Prof. Dr. rer. nat. Markus Winterer

Tag der mündlichen Prüfung: 02.08.2010

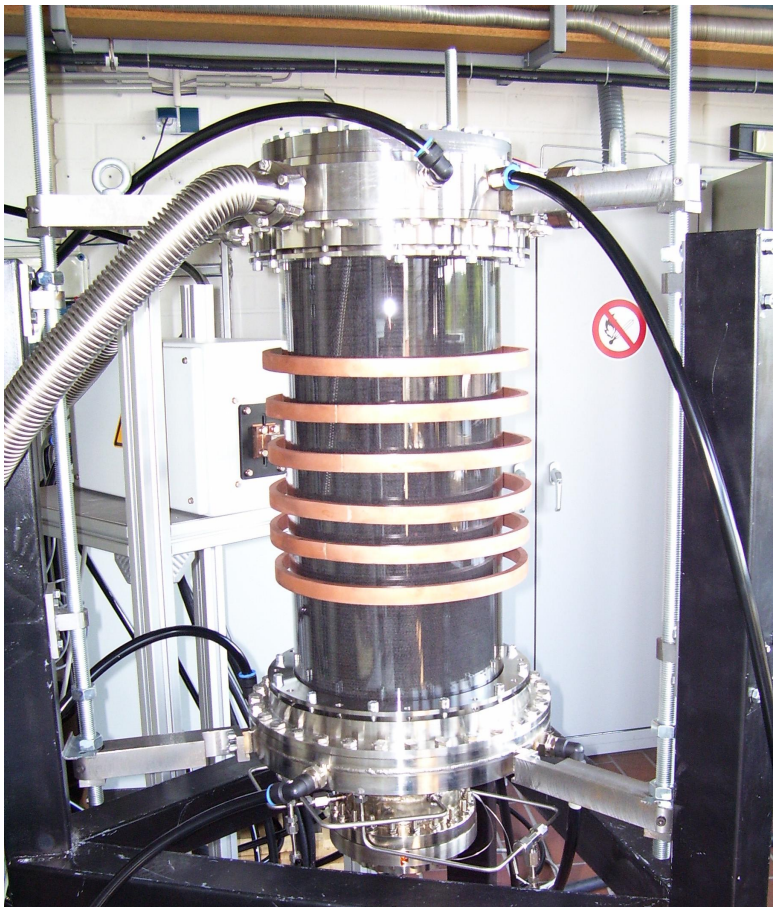

Abstract

Silicon Carbide (SiC) is an important compound with many benefits to man kind, ranging from early usage as an abrasive to its recent use as an intrinsic semiconductor. SiC is typically man made, since it rarely exists in nature in the form of the natural moissanite. The production of crystalline SiC with increasing size and high quality has been accomplished using Physical Vapor Transport (PVT) for the high power and low frequency applications. Although high quality crystals could be produced using this method, growth defects like micropipes, dislocations, etc., could not be completely inhibited. Thus, the preparation of the SiC powder used in this process requires additional energy, which makes the High Temperature Chemical Vapor Deposition (HTCVD) technique more attractive and could be considered as an efficient alternative to the PVT method, which requires lower throughput capacity than PVT due to saving the exergy destroyed in the powder formation process (used in the PVT method) and due to its low precursor's cost and their disposition for continuous feeding. Therefore, in this work, a vertical hot-wall reactor with an upward flow direction, was built and suited for the investigation of the epitaxial growth of low defect SiC single crystalline using the HTCVD technique. The gases are injected into the reactor through a water cooled flange and a nozzle including an optical access for the temperature measurement. The exhaust gases were removed by four openings at the top of the reactor. The substrates were fastened on a graphite seed-holder and hanged in the reactor using a graphite cord. The precursors used were silane (SiH_4), propane (C_3H_8) and hydrogen (H_2) while helium was used as a carrier gas. The temperature profile was measured by means of two color pyrometer. A maximum temperature of 2180°C was measured on the reactor walls, while a temperature of 2025°C was measured on the seed-holder,

which was hanged 18 cm below the outlet flange.

Non-seeded growth of polycrystalline SiC was carried out and used for indicating the growth parameters that were later used as a reference for the setup of the epitaxial growth experiments. In the epitaxial growth experiments the deposition was firstly performed on on-axis 6H-SiC seeds. At a temperature of 1995°C, a growth rate of 32 μm/h was achieved. This temperature was achieved at a substrate position of 30 cm below the outlet flange (5 cm above the middle plane of the inductive coil). Layers that grew on on-axis substrates were shown to have a plain surface morphology. The growth rate has shown a significant dependency on the C_3H_8 within low range of its concentrations. The *step flow* mechanism is activated when off-axis seed-crystals with a tilt angle of 3.5° and 8° are used. On the film layers that were grown on the off-axis substrate with a tilt angle of 3.5°, flat terraces with sharp edges could be recognized by optical microscopy. Instead, wavy surface morphology resulted on the films grown on the 8° off-axis seed. Increasing the temperature beyond 1955°C resulted in higher growth rates on the off-axis surfaces; meanwhile, no growth rate enhancement was obtained on the on-axis surfaces. A maximum growth rate of 100 μm/h was achieved at a growth temperature of 2060°C. The epitaxial growth of SiC by HTCVD was successfully carried out for long periods up to 3 hours using the hot-wall reactor.

The growth of thick epilayers of SiC can be realized at high growth rates for several hours, which makes it very important to measure the mass change of the substrate during deposition. On the other hand, investigating the growth rate for a wide range of the process parameters, can be accomplished by the application of an in-situ measuring

technique, which can save a lot of experimental time and cost. Accordingly, a magnetic suspension balance (MSB) was successfully integrated into the hot-wall reactor and used for the in-situ measurement of the mass change during deposition. In order to minimize the experimental cost, this technique was only applied during non-seeded growth experiments, where polycrystalline SiC was deposited directly on a graphite seed-holder with 50 mm diameter. The mass change could be successfully recorded at a growth temperature of 1950°C, flow velocity of 0.0075 m/s and a pressure of 800 mbar. The dependency of the growth rate on the precursor (SiH_4, C_3H_8 and H_2) concentrations was investigated individually while the mass change was recorded in-situ.

****

Dedication

TO

My parents

My wife

Acknowledgment

I want to express my sincere gratitude to my supervisor Prof. Dr. Burak Atakan. His kind, informative and encouraging supervision were always with me during the period i spent on my research. He always gave me time and answered my questions with great patience. The long discussions with him made it possible for me to understand and realize the research tasks.

I would like to thank Prof. Dr. Winterer for his tricky suggestions and friendly support.

Great thank goes to Dr. Ulf Bergmann for his continuous support during the whole research period and especially, for his help to write this dissertation.

I would like to express my gratitude to all those who gave his time and support to build the hot-wall reactor. I sincerely thank Dipl.Phys. Erdal Akieldiz for his appreciated support.

Finally I should not forget to give my special thanks to my wife Dorra whose patience and love enabled me to complete this work.

Duisburg, Feb. 2010

Ahmed Elhaddad

Contents

Chapter 1

Introduction

Most semiconductor applications today are using silicon based devices. According to the advanced process technology and development techniques, silicon crystals of high purity and crystalline quality can be produced in mass production. However, silicon has many limitations due to its physical properties: silicon is limited to a maximum operation temperature of 150°C and does not resist very high voltages. Therefore, SiC could be the better choice according to its supreme physical and electrical properties making it very promising for the next generation of semiconductors for extreme conditions, where their application in modern electrical engineering is essential. SiC has many remarkable properties which make it a very promising semiconductor material. Some of the potential applications of silicon carbide are in high-temperature, -frequency, and -power electronic devices. Others make use of the wide bandgap: UV radiation detectors and even blue-light lasers. Light emitting diodes (LEDs) have already been in commercial production for some years. Also some other electronic devices may become commercial in the near future. The large-scale manufacturing of

electronic devices requires a continuous production of good-quality wafers. In silicon carbide growth, there are still some basic problems to be resolved that limit the commercial utilization of the material. These problems are related to crystal size and both macroscopic and microscopic defects.

As reported in the PhD thesis of Peter Råback in [1], SiC is the only stable compound in the Si-C equilibrium system at atmospheric pressure. It was first observed in 1824 by Joens Berzelius. The properties and potential of the material were, of course, not understood at that time. The growth of polycrystalline SiC with an electric melting furnace was introduced by Eugene Acheson around 1885. He was also the first to recognize it as a silicide of carbon and gave it the chemical formula SiC. The only occurrence of SiC in nature is found in meteorites. Therefore, SiC cannot be mined but must be manufactured with elaborate furnace techniques.

In its polycrystalline forms, silicon carbide has long been a well proved material in high temperature, high-strength and abrasion resistant applications. Silicon carbide as a semiconductor is a more recent discovery. In 1955, Jan Antony Lely proposed a new method for growing high quality crystals which still bears his name [2]. From this point on, the interest in SiC as an electronic material slowly began to gather momentum; the first SiC conference was held in Boston in 1958. During the 60s and 70s SiC was mainly studied in the former Soviet Union. The year 1978 saw a major step in the development of SiC, the use of a seeded sublimation growth technique also known as the modified Lely technique. This breakthrough led to the possibility for true bulk crystal preparation. In section 2.2, a summary of the SiC growth techniques by CVD is presented in details.

Different crystal forms of the same chemical composition are called polymorphs. Poly-

morphism commonly refers to a three dimensional change affected by either a complete alteration of the crystal structure or a slight shift in bond angles. Polytypism is a special type of polymorphism which occurs in certain close-packed structures. In this phenomenon, two dimensions of the basic repeating unit cell remain constant for each crystal structure (polytype), while the third dimension is a variable integral multiple of a common unit perpendicular to the planes having the highest density (closest packing) of atoms. Silicon carbide is very rich in polytypism, as more than 170 different one-dimensional ordering sequences have been determined. For a theoretical treatment of SiC polytypes, see [3, 4].

SiC belongs to a class of materials commonly referred to as wide-bandgap semiconductors. This means that the energy gap between the valence and conduction band is significantly larger than in silicon. It implies, for example, that it is less probable that thermally excited electrons would jump over the gap. Therefore, SiC devices are less sensitive to high temperatures and should be able to operate at temperatures exceeding 500°C. The thermal conductivity of SiC is larger than that of copper. Thus the heat generated by the devices is efficiently removed. Also such properties as high electric feld strength and high saturation drift velocity are important for the device technology. Consequently devices can be made smaller and more efficient. SiC is a very hard material. This has resulted in a wide variety of applications using polycrystalline SiC. SiC is also chemically inert and extremely radiation resistant. It may thus be used in the most hostile environments, for example, near nuclear reactors and in outer space. Some of the properties of silicon carbide compared to some other semiconductors are listed in Table 1.1. It may be noticed that silicon is inferior to SiC in many respects. Diamond would be the ultimate semiconductor for power electronics, but problems related to its

use appear to be even larger than in the case of SiC. There are also some other potential wide-bandgap semiconductors that compete with SiC, for example, gallium and aluminum nitride.

Property	3C-SiC	6H-SiC	Si	GaAs	Diamond
Bandgap [eV]	2.2	2.9	1.1	1.4	5.5
Max. Temperature[°C]	873	1240	300	460	1100
Melting point [°C]	1800	1800	1420	1240	?
Physical stability	excellent	excellent	good	fair	very good
Thermal conductivity [W/cm.°C]	5.0	5.0	1.5	0.5	20
Sat. velocity [10^7*cm/s]	2.5	2.0	1.0	2.0	2.7

Table 1.1: *Properties of silicon carbide compared to other some semiconductor materials. GaAs stands for gallium arsenide.*

The use of SiC powder as a source material for the Lely method, which was improved to the Physical vapor transport (PVT) method using the seeded growth technique, demands further improvements to the reactor technology in order to achieve long deposition periods, wherein continuous feed of the source material is relatively difficult. Thus, the PVT method requires very high energy for the sublimation of the SiC powder at very high temperatures up to 2600°C. The resulting species of the sublimation process are transported in the gas-phase due to temperature gradients to nucleate on the surface of the seed-crystal. In high temperature chemical vapor deposition (HTCVD), the resulting species of the direct pyrolysis of the silane and one hydrocarbon (e.g. propane) in the gas-phase, are used here as an input for the growth of SiC. Due to the

use of this method, the exergy lost in forming the SiC powder can be saved. Accordingly, HTCVD can be considered as an energy efficient alternative for the PVT method. Another advantages of the HTCVD lie in its ability to the use of low cost volatile precursors and their disposition by continuous feed. Although high growth rates up to 1 mm/h could be reached using the HTCVD technique, solving growth defect problems like dislocations and the growth of hole cores (micropipes) are still requiring further research on this technique. According to this, a BWI project researching the growth characteristics of mono-crystalline SiC with high quality and growth rates was inspired and started at the University of Duisburg-Essen. The tasks of this project are divided into three parts. First, a part strives to design and build high temperature reactor to investigate the growth process of mono-crystalline SiC by the HTCVD technique, and the in-situ growth rate measurement via the integration of magnetic suspension balance (MSB) into the HTCVD reactor. The results attained in this part are presented in this work. Second comes the investigation of the crystal homogeneity by means of photoluminescence at the institute of experimental physics at the Technical University of the Bergakademie Freiberg. Finally, the particle generation in the gas-phase is being studied, by means of mass spectroscopy in the department of Nano-Particle Process Technology group University of Duisburg-Essen.

The dissertation is organized into six chapters. In the next chapter, a brief description of the SiC growth techniques, the HTCVD method and the techniques applied for the film analysis is presented. In chapter 3, the design of our HTCVD system, the experimental setup and procedure are discussed in detail. Chapter 4 is divided into two main parts. First, the observation of non-seeded growth of SiC on graphite substrates

was targeted to indicate the parameters setup required by the second part, where seeded growth of SiC was epitaxially aimed. The grown crystals were then analyzed by XRD, SEM and optical microscopy. In chapter 5, the in-situ growth rate measurement using a gravimetric technique is presented. The growth rate measurement was carried out for films grown by non-seeded HTCVD of polycrystalline SiC on a graphite seed-holder.

Chapter 2

Structure and Growth of SiC

2.1 Crystal Structure of SiC

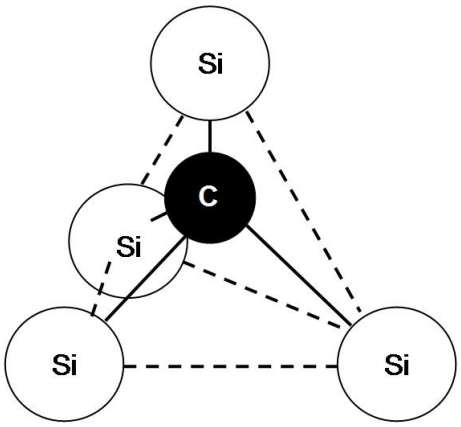

Figure 2.1: *Si and C atoms arranged in a tetrahedron, which is the smallest building block of the crystal structure, as found in [5].*

A brief description of SiC and its structure was introduced in the PhD thesis of Hina Ashraf in [5]. SiC has strong chemical bonds with a short bond length (1.89 Å) between Si and C atoms. The slight difference in electro-negativity between these two atoms gives 12 % ionicity to the otherwise covalent bonding, with the Si atom slightly

positively charged. The basic building block of the crystal is a tetrahedron consisting of a C (Si) atom in the middle and four Si (C) atoms at the four corners, as seen in Figure 2.1.

An important property of SiC is polytypism. Thus we can say that SiC is not a single semiconductor but a family of semiconductors. There are many polytypes of SiC but the simplest ones can be considered as natural super lattices. The Si-C double layer in the stacking order ABCABC leads to the zincblende structure (3C-SiC) as discussed in [6], while the stacking order ABAB leads to the wurtzite crystal structure (2H-SiC), as shown in Figure 2.2. Additionally, there is a huge number of hexagonal and rhombohedral polytypes with a higher complexity of their stacking order. The prevalent occurring polytype of SiC is 6H-SiC.

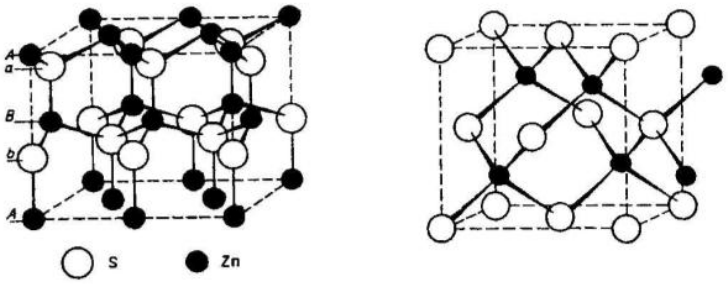

Figure 2.2: *Left: Wurzit Structure, Right: Zincblende Structure as found in [6].*

The freedom to choose between two different positions of the second layer and by creating an ordering in the stacking sequence of the layers, gives rise to a variety of different polytypes. The stacking of double layers is most conveniently viewed in a hexagonal system, as shown in Figure 2.3, with three different position of the atom pair labeled A, B and C. The c-axis is perpendicular to the basal plane, which lies in the plane of the close packed double layer. The three most common and important

polytypes of SiC are 3C, 4H and 6H, although 15R and 21R are also fairly common. Here, the Ramsdell notation is used, where the number represents the number of bi-layers per unit cell and the letter represents the type of Bravais lattice, i.e. H stands for hexagonal, C for cubic and R for rhombohedral. Consequently, there is no difference between the polytypes within the basal plane. It is the stacking sequence of double layers along the c- axis that gives rise to different polytypes.

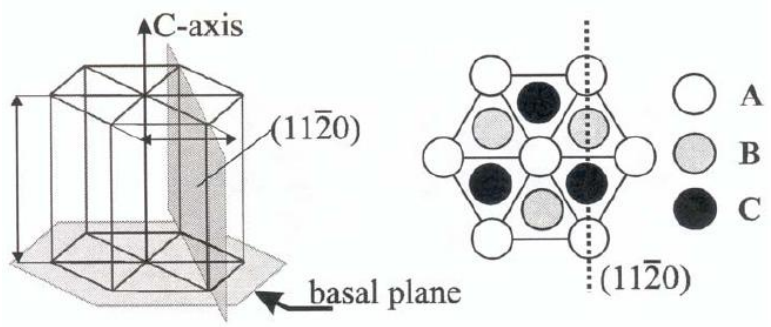

Figure 2.3: *The hexagonal system to describe different polytypes, as in [5], and the three different positions, A, B and C of the double layers, respectively.*

If the stacking sequence of the different polytypes is projected in the $\langle 11\bar{2}0 \rangle$ plane as indicated in Figure 2.4 and 2.5, we can observe difference in the local environment for different atomic sites. In the turning point (is a hexagonal local lattice which repeats its self within one structure of the polytype, in 4H and 6H there is one turning point), the local environment is hexagonal (h) and between the turning points, the local environment is cubic (k). 3C polytype has a cubic structure since there is no turning point, while the 4H polytype has one cubic and one hexagonal site (h,k). The 6H polytype has one hexagonal and two cubic sites (h,kB1B,kB2B). For the cubic and the hexagonal lattice site in 4H and 6H polytypes, the arrangement of the surrounding atoms differs from the second neighbors while the two cubic lattice sites kB1B and kB2B

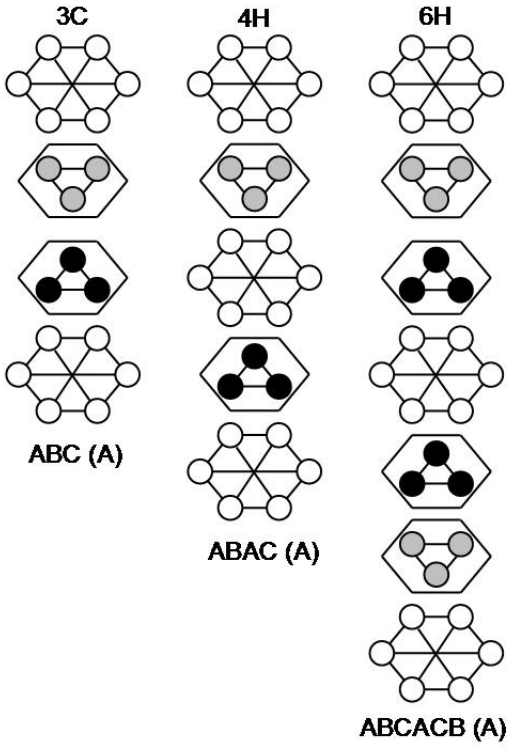

Figure 2.4: *One stacking period of three common polytypes 3C, 4H and 6H-SiC as in [5].*

differ firstly in the third neighbors.

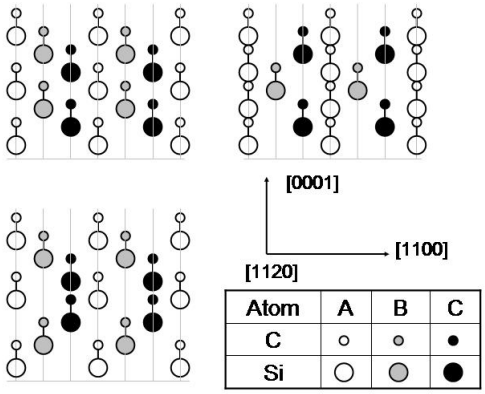

Figure 2.5: *The $\langle 11\bar{2}0 \rangle$ plane of the three polytypes 3C, 4H and 6H, as in [5].*

Cubic silicon carbide which is known as 3C-SiC, is also called beta SiC, while hexagonal SiC is called as alpha-SiC. The complete name of SiC polytype consists of a name (SiC), minus sign and a suffix. The suffix consists of a number and a capital letter. The number describes the stacking sequence and the letter the crystal system (cubic or hexagonal)[7].

2.2 SiC Growth Techniques

This section discusses mono-crystalline SiC growth techniques except HTCVD, which is discussed in details in section 2.3.

2.2.1 Growth from Melt

Most commercially utilized single crystal semiconductor boules are grown from a melt or solution, but this is not a feasible option for SiC growth. SiC does not have any liquid phase at normal engineering conditions. Calculations have indicated that stoichiometric melting is possible only under pressures exceeding 105 bar at temperatures

higher than 3200°C as mentioned in [1]. Even if the solubility of carbon in silicon melt ranges from 0.01% to 19% in the temperature interval from 1412 to 2830°C, at high temperatures the evaporation of silicon makes the growth unstable. The solubility of carbon can be increased by adding certain metals to the melt (e.g., praseodymium, terbium, scandium). This would, in principle, enable the use of crystal pulling techniques, such as Czochralski growth. Unfortunately there is no crucible material available that would be stable with these melts. It is also speculated that the solubility of the added metals in the growing crystal is too high to be acceptable in semiconductor materials [8, 9]. In spite of all the problems, SiC was grown from melt at 2200°C and 150 bar in a recent study. The crucible was made of graphite and it also acted as the carbon source. The technology is very expensive and seems to be economically not feasible. However, growing from a solution would avoid many of the problems related to the growth techniques from the gas-phase.

2.2.2 Lely Growth

The Lely growth method is used even nowadays to grow the crystals of the highest quality. The headstone of this method was placed in 1955 by the physicist Lely [2]. He used a crucible and porous cylinder of graphite to grow his first mono-crystal of SiC by heating SiC powder between the porous cylinder and the crucible at a temperature of 2500°C. Increasing the crucible temperature leads to vaporization of the SiC powder into gaseous species that flow through the cooler porous graphite. The problem he faced was to control the pressure and the temperature. A schematic Lely geometry is presented in Figure 2.6. In CVD the growth is driven by the initial gas composition, whereas in the Lely method the growth is controlled by temperature gradients within the system and by the chemical potential of the gas-phase species. The system is

close to chemical equilibrium, the SiC forming species have high partial pressures and low chemical potentials due to the applied high temperatures. This leads to a pressure gradient that results in mass transport from the hot parts to the cooler parts of the crucible [10, 11, 12, 13, 14]. In the Lely growth, the temperature distribution is such that in the cylindrical crucible the temperature minimum is at the inner side of the porous graphite cylinder. Therefore the gases travel towards its inner walls. The porous graphite holding the source provides nucleation centers for initially small seed crystals that eventually grow larger and usually obtain an energetically favorable hexagonal form. Unfortunately, the Lely grown crystals are limited and random in size, in average they are about the size of a nail (3-10 mm long). Because the Lely growth method does not require any seed crystals, it is the method from which all the other SiC crystals originate from. The resulting crystals have low defect and micropipe densities.

2.2.3 Seeded Sublimation Growth

The seeded sublimation growth, also known as physical vapor transport (PVT), is historically referred to as the modified Lely method, reported by Tairov and Tsvetkov [11] in 1978. PVT is a sublimation deposition process where the growth rate is proportional to, and the crystallization process is facilitated by, the supersaturation of the vapor phase. This method was further refined by Carter [15] and Stein [16] for producing larger SiC boules. The geometry of a PVT reactor was initially quite similar to the Lely geometry but the difference is the use of a seed crystal which results in a more controlled nucleation, see Figure 2.7.

The seeded sublimation process is nowadays the standard method for growing bulk

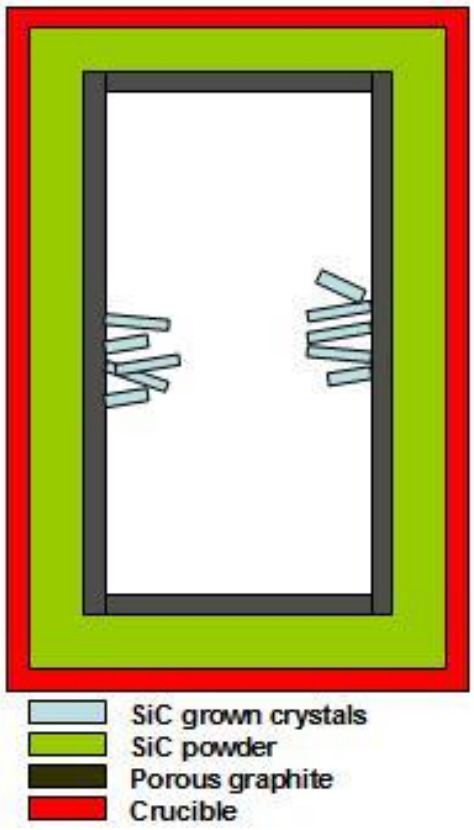

Figure 2.6: *A schematic drawing of the Lely growth method as found in [1].*

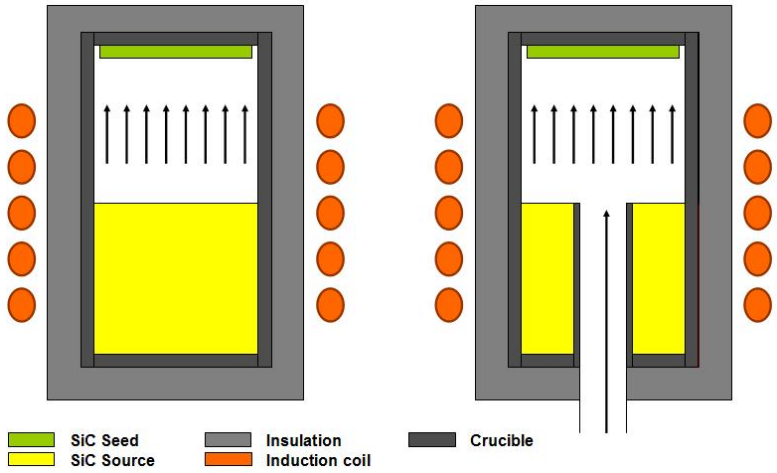

Figure 2.7: *(a) Modified Lely Method (PVT), (b) Modified (PVT) method, as found in [1].*

mono-crystalline silicon carbide [8, 17, 18, 19]. In this process polycrystalline SiC at the source sublimes at a high temperature, (1800-2600°C) and low pressure. The resulting gases travel through natural transport mechanisms (caused by natural convection, where the fluid motion is not generated by any external source like a pump, fan or suction device, etc, but only by density differences in the fluid occurring due to temperature gradients) to the cooler seed crystal where crystallization due to supersaturation takes place. The seed crystal is usually situated at the top of the crucible in order to prevent contamination by falling particles. Usually, the seed is produced by the Lely method or taken from previous growth, which was already produced by the PVT method.

Although the seeded sublimation growth is the most promising method for producing SiC crystals, and has been known for more than twenty five years, there are still some major difficulties involved in the process. The polytype formation and growth shape are poorly controlled and the doping is nonuniform. There are also severe defects, such

as micropipes and dislocations in the grown crystals.

2.2.4 CVD

Chemical vapor deposition is a widely used method for depositing thin or thick films with high quality and well defined chemical composition and structural uniformity. In a typical chemical vapor deposition process the substrate is exposed to one or more volatile precursors, which react and/or decompose on the substrate surface to produce the desired deposit. The activation energy for the reaction can be overcome by various methods, where the most common approach is to heat the substrate. Volatile byproducts are generally also produced, which are removed by the gas flow through the reaction chamber. The main benefit derived by a chemical vapor deposition process is the resulting uniform, adherent and reproducible films. Often the main disadvantages lie in the need to resort to dangerous and toxic chemicals to obtain the desired deposition along with the high temperatures necessary for some of the reactions. CVD technology opens possibilities to prepare new materials and structures for various applications for many industrial products.

Using this method, the direct growth of SiC from the gas-phase was achieved epitaxially at a temperature range of 1200-1700°C in a hot or cold wall reactor [20, 21, 22, 23, 24]. By the injection of SiH_4 and hydrocarbon diluted in carrier gas (Ar, He or H_2) into the reactor, the deposition of several micrometers of mono-crystalline SiC can be accomplished. By increasing the temperature, the growth rate increases, but currently problems related to the growth control , like temperature, pressure and the concentration of the gas-phase species, become more severe, and problems such as homogeneous nucleation in the gas phase may occur. These problems might be overcome by a very

careful control of the thermodynamic conditions.

However, the growth rate in the cold-wall reactor is limited to 3-5 μm/h [21, 23], while in the hot-wall reactor, the highest reported growth rate lies around 10 μm/h [22]. Vertical reactors have also been investigated. Both, rotating disk reactors [25] and a multi-wafer rotating planetary reactors [26], have been developed to improve layer uniformity and reactor throughput. Fast epitaxial growth using this technique was reached by Danielsson [20], who introduced the growth of 4H-SiC with high growth rates of 10-49 μm/h. Later on, two other groups also achieved growth rates above 10 μm/h using the vertical up-flow configuration in a chimney [27] or a radiation heated CVD reactor [28]. Fast epitaxial growth of high quality 4H-SiC in vertical hot-wall CVD reactor at 25-60 μm/h has been also reached by Fujihira [29].

A higher growth rate than 10 μm/h was investigated in a vertical hot-wall reactor. By the use of increased temperatures (1650-1850°C) and high reactant concentrations, this process is shown to enable growth rates up to 50 μm/h and demonstrates a material quality comparable to established CVD techniques until growth rates of 25 μm/h [30]. Generally, the growth rates in CVD are too low to allow boule production. Usually tens of micrometers an hour are attainable, which makes this method not very attractive for the application where single crystalline SiC is required to be produced at high growth rates.

2.3 SiC Growth by High Temperature CVD

The first successfully grown SiC crystal by HTCVD was introduced 1996 at the *Department of Physics and Measurement Technology of Linköping University* in Sweden [31]. They have constructed a prototype of a vertical hot wall reactor with relatively

small inner diameter (30 mm) of the crucible, see Figure 2.8. The reactor design based on the technology used in the modified PVT reactor. The basic difference lies in the use of an inlet duct at the bottom of the reactor to inject the process gases instead of using SiC powder as usual in the PVT method. The crucible is covered by a graphite lid with four small holes for the gas removal, while the substrate was glued on the center of the lid. The crucible is closed from the bottom by a graphite plate with one hole for the gas inlet. The temperature measurements are accomplished by a two-color pyrometer focused on the lid of the crucible. The crucible is inductively heated by a 50 kW middle frequency generator operating. All sides of the crucible are enclosed by graphite foam for thermal insulation and the assembly is placed on a quartz support inside an air-cooled quartz tube. H_2 and Ar or a mixture of both gases was chosen as a carrier gas. SiH_4 was used as a source for Si species, while small doses of C_3H_8 was carefully added to the mixture with small amounts, since at very high temperatures the decomposition rate of the crucible is further increased developing more hydrocarbons into the gas-phase. A maximum growth rate of 300 μm/h was reached at a temperature of 2300°C by this reactor. In 2004, a 2-inch, 15 mm thick SiC single crystal grown by HTCVD has been commercially introduced by Okmetic AB [32]. The 4H-SiC crystal demonstrated a micropipe density down to 0.3 cm^{-2}.

In this process, the precursors or the gas mixture is injected into the crucible through the bottom inlet. The higher the temperature the larger is the probability that the reactants will be thermally pyrolyzed producing species or radicals that will attach to the surface thus leading to epitaxial growth [1]. When the substrate temperature T_s is increased the probability of sticking increases, but also the etch rate from the surface increases. The growth rate is therefore determined by the desorption of the re-

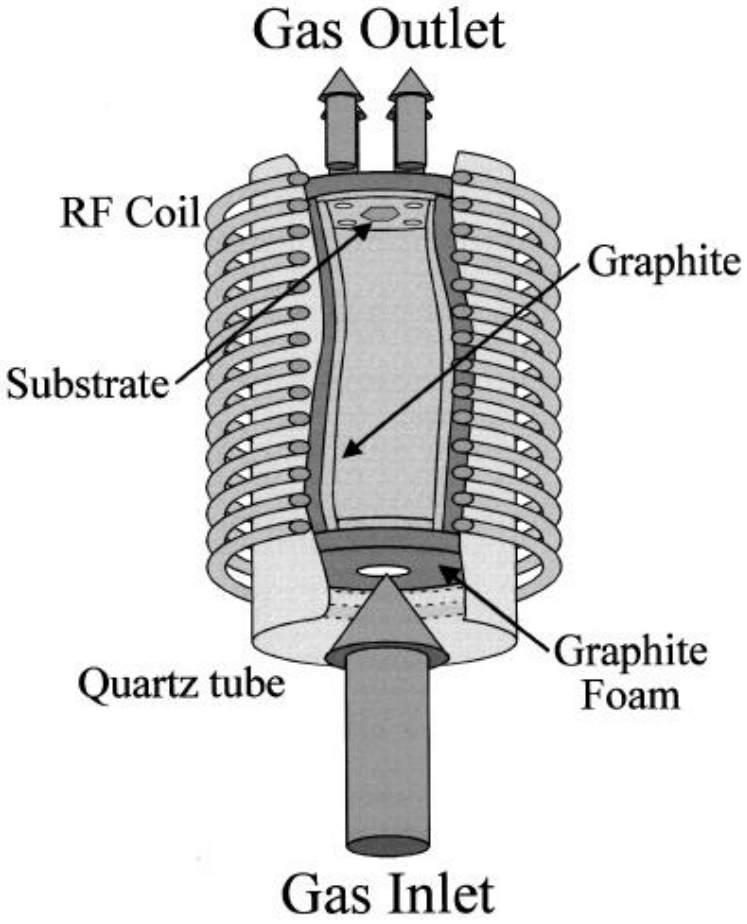

Figure 2.8: *Reactor prototype used for the HTCVD of crystalline SiC. The reactor was introduced by the Department of Physics and Measurement Technology of Linköping University in Sweden in 1996 [31].*

action products and by the etch rate of the surface, and by the diffusion dominated mass transport of the source molecules. The sticking coefficient S_c depends on both J_i the impingement flux rate and the rate constants due to this relation $S_c = R_r/J_i$ [33], where R_r is the desorption rate. R_r is dependent on the global activation energy and the temperature. If the activation energy is high enough ($E_{desorption}$-$E_{adsorption}>0$) the temperature must be increased to make the exponential term (E_r-E_d)/RT_s small. On other hand, the resorption rate $E_r < E_d$ will be decreased by increasing the surface temperature T_s. Inherent advantages of this technique include continuous supply of the source material, the relatively economical availability of high purity gases, the control of the C/Si ratio and the ability of pulling the growing crystal. Thus, the use of SiC powder in the Lely and PVT methods demands much energy, where high amount of the gases potential exergy are lost in the formation of the SiC powder. In HTCVD, the direct pyrolysis of the precursors into the process saves the exergy lost for the powder formation. That's why, the HTCVD method is considered as more energy efficient than both other methods of Lely and PVT.

2.3.1 Transport

The gross reaction equation for the HTCVD of SiC using both precursors, silane and propane, can be given due to the following reversible reaction:

$$3\ SiH_4 + C_3H_8 \Leftrightarrow 3\ SiC + 10\ H_2$$

The HTCVD process with silane and propane precusors is described in Figure 2.9 and explained particularly in the following four steps.

- The process gases (typically silane and a hydrocarbon diluted in a helium carrier gas flow) are transported upwards to a substrate or seed-crystal fixed on a seed-

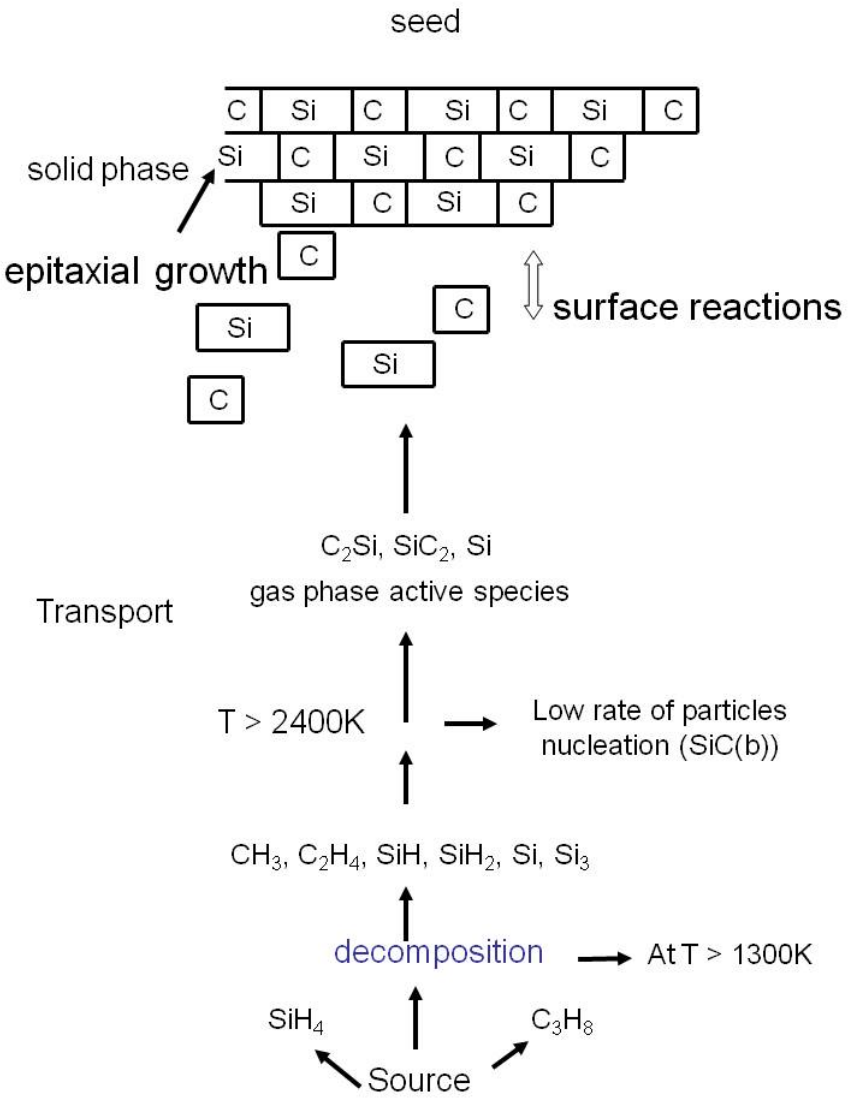

Figure 2.9: *A schematic description of the HTCVD process with SiH_4 and C_3H_8 as precursors.*

holder in a hot-wall reactor as presented in section 4.1.1.

- Gas-phase chemical reactions are initiated as the precursors flow through the hot zone of the reactor, typically made of graphite, which together with the design of the seed-holder will determine the growth species concentration and temperature-gradient profile near the seed surface. In this step, the temperature must be maintained very high so that Si and the hydrocarbon radicals do not react together and build stable SiC clusters, which normally depletes and fall in the opposite direction of the flow stream.

- The vapor species or radicals released by the hot zone are transported by flow system determined by the reactor design to the seed, which is maintained at lower temperature than the hot zone. Thus, the high temperature established in the hot-zone causes a reduction of the species chemical potential, which results in increased concentrations of the major species ensuring high supersaturation and growth rate. This and the chemical potential of the vapor species and radicals ensure high supersaturation and growth rate.

- Removal of by-product gases from the CVD chamber through the exhaust system.

2.3.2 Diffusion Limited Deposition

As previously explained in section 2.3, high temperature and precursor concentrations are required when fast epitaxial growth of crystalline SiC is desired. The influence of the temperature on the growth kinetics can be studied on the basis of an Arrhenius diagram, as shown in Figure 2.10, which presents three zones wherein the species

transport to the seed surface is controlled due to different mechanisms. In the low temperature region, the growth rate can be enhanced by increasing the temperature. This indicates a kinetically controlled process, where increased growth temperatures enhance the decomposition of Si_xC_y clusters and thus the diffusion to seed surface, which consequentially results in an enhanced supersaturation at the growing SiC surface. In the middle range where higher growth temperatures are applied, the growth rate follows a smoother dependence, which may be more ascribed to a mass-transport limited regime. The growth rate is then generally influenced by the temperature gradient applied to the seed crystal. In the highest temperature region, for a given temperature gradient, a further increase of the growth temperature decreases the net growth rate, which indicates the onset of equilibrium limit or the onset of film re-evaporation.

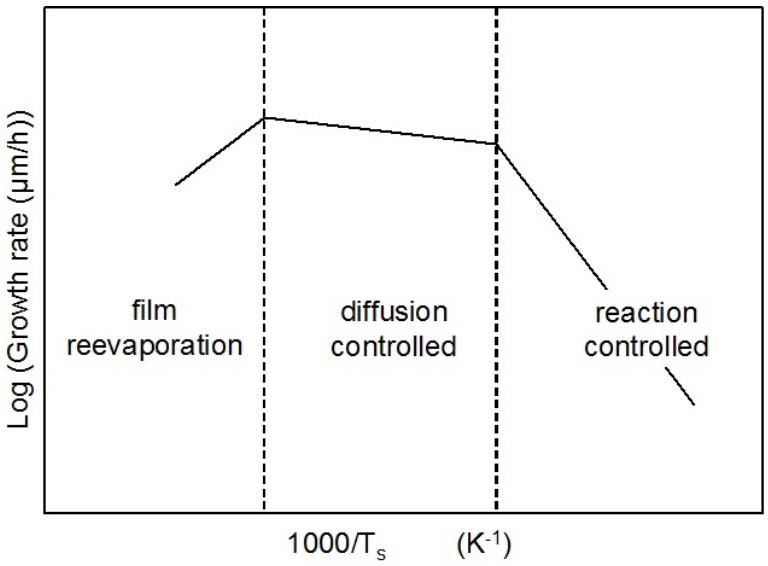

Figure 2.10: *A schematic description of the growth rate dependence on the temperature as discussed in [33]. In this diagram, three zones of the growth process are presented, which are individually explained in the text in reference to the HTCVD process of mono- crystalline SiC.*

The work introduced by Ellison [34] in 1999 observed that the growth process is lim-

ited by gas-phase chemistry within a seed temperature range of 2160-2230°C, where the growth rate is shown to be enhanceable by increasing the temperature in this range. Further increase of the temperature beyond 2230°C resulted in constant growth rate, which possibly indicates a growth mechanism limited by mass transport. In this case, increasing the precursor concentrations is usually favorable to increase the growth rate.

2.3.3 SiC Homoepitaxial Growth

The plane orientation of the seeds surface plays an important role in determining the SiC polytype that will grow. For example, a parallel plane to the crystalline layers (A or B) is normally coded by the number (0001) and usually called well oriented surface, which is known as basal plane. A misaligned surface to the [0001] direction with a small tilt angle to the well oriented surface develops a so-called off-axis surface. The growth mechanism on both surface planes is schematically depicted in Figure 2.11.

Homoepitaxial growth of SiC is basically determined by the polytype of the seed and its surface plane. Under both conditions, homoepitaxial growth of SiC can be accomplished by step controlled epitaxy [23, 35, 36]. Step controlled epitaxy is based upon the growing epilayers on, usually, 3.5° or 8° off-axis surfaces, resulting in a surface with atomic steps and flat terraces between steps. When growth conditions are properly controlled and there is a sufficiently short distance between steps, Si and C adatoms impinging onto the growth surface find their way to steps where they bond and incorporate into the crystal. Thus, ordered lateral (step flow) growth takes place, which enables the polytypic stacking sequence of the substrate to be exactly mirrored in the growing epilayer. When growth conditions are not properly controlled or when steps are too far apart (as can occur with SiC substrate surfaces that are polished at

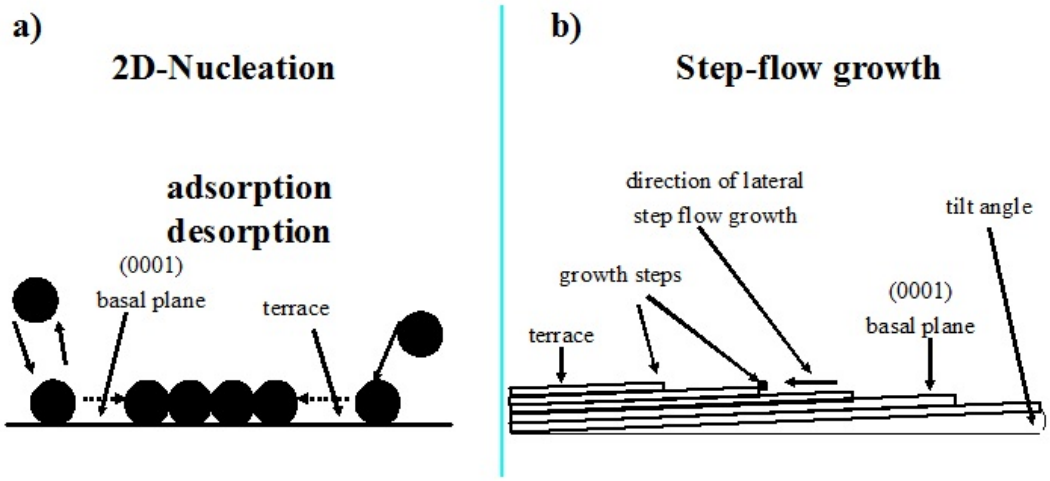

Figure 2.11: *a) On-axis surface: also called well-oriented. On these surfaces, the growth mechanism will perform on terrace area via two-dimensional nucleation, expanding laterally. b) Off-axis surface: the orientation of seed surface is misaligned to [0001] direction with a tilt angle of 3.5° or 8°, which develops high density of steps and narrowing terraces widths, which allows the replication of the epilayer structure. This mechanism is known as step-flow epitaxy [5].*

a tilt angle less than 1° to the basal plane), growth adatoms can nucleate and bond in the middle of terraces instead of at the steps, which leads to heteroepitaxial growth of poor-quality 3C-SiC [23, 26]. To help prevent 2D-nucleation of 3C-SiC (triangular inclusions) during epitaxial growth, most commercial 4H- and 6H-SiC substrates are polished to tilt angles of 8° and3.5° off the (0001) basal plane, respectively.

Chapter 3

Analytical Methods

The deposited film has to be analyzed in order to identify its physical and chemical properties where these properties are important in industrial applications. Morphology, phase composition and chemical composition are investigated in this study using techniques that include X-ray diffraction (XRD), microscopy, scanning electron microscopy (SEM) and energy dispersive X-ray spectroscopy (EDX).

3.1 Optical Microscopy

Microscopy is the technical field of using microscopes to view samples or objects. There are three well-known branches of microscopy, optical, electron and scanning probe microscopy. Optical and electron microscopy involve the diffraction, reflection, or refraction of electromagnetic radiation/electron beam interacting with the subject of study, and the subsequent collection of this scattered radiation in order to build up an image. This process may be carried out by wide-field irradiation of the sample (for example standard light microscopy and transmission electron microscopy) or by scanning of a fine beam over the sample (for example confocal laser scanning microscopy

and scanning electron microscopy). Scanning probe microscopy involves the interaction of a scanning probe with the surface or object of interest. The development of microscopy revolutionized biology and remains an essential tool in that science, along with many others including materials science and numerous engineering disciplines.

Optical or light microscopy involves passing visible light transmitted through or reflected from the sample through a single or multiple lenses to allow a magnified view of the sample. The resulting image can be detected directly by the eye, imaged on a photographic plate or captured digitally. The the system of lenses and imaging equipment, along with the appropriate lighting equipment, sample stage and support, makes up the basic light microscope. The optical microscope, often referred to as the "light microscope", is a type of microscope which uses visible light and a system of lenses to magnify images of small samples. Optical microscopes are the oldest and simplest of the microscopes. Digital microscopes are now available which use a CCD camera to examine a sample, and the image is shown directly on a computer screen without the need for expensive optics such as eye-pieces. Other microscopic methods which do not use visible light include scanning electron microscopy and transmission electron microscopy.

3.2 Scanning Electron Microscopy (SEM)

The surfaces morphologies of the films were analyzed by Scanning Electron Microscopy (SEM). The SEM is a microscope that uses electrons rather than light to form an image. There are many advantages of using the SEM instead of a light microscope according to its ease of sample observation, higher magnification and higher resolution. The principle of the SEM is to focus a beam of primary electrons onto a

sample, and to collect secondary electrons scattered from the sample. An image is created by scanning the sample surface point by point by a focused beam of electrons and to reconstruct the image from the scattered intensities. The sample is placed inside a vacuum chamber. After the chamber is evacuated, an electron gun emits a beam of high energy electrons. This beam travels down ward through a series of magnetic lenses designed to focus the electrons to a very fine spot. A set of scanning coils moves the focused beam back and forth across the sample, row by row. As the electron beam hits each spot on the sample, secondary electrons are scattered from its surface. A detector counts these electrons and sends the signals to an amplifier. The final image is built up from the number of electrons emitted from each spot on the sample. A scanning electron microscope purchased from FEI company was applied for analyzing the surface morphology of our grown crystals. The microscope has a type of 400 FEG Quanta. It has a magnification capacity of 7x - 1000,000 in high and ultra high vacuum. It has a resolution of 2-3.5 keV nm.

3.3 X-ray Diffraction

The films may be deposited in amorphous or crystalline phases. The atoms of a crystalline film are arranged in a regular pattern while the atoms of an amorphous film are arranged in a random way. The arranged atoms of a crystal form a series of parallel lattice planes separated from one another by a distance d, which varies according to the nature of the material. For any crystal, planes exist in a number of different orientations each with its own specific distance d. X-ray Diffraction (XRD) allows the identification of the phase composition of the analyzed films if they are crystalline or polycrystalline. X-ray diffractometers consist of an X-ray generator, a goniometer

(angle-measuring device), a sample holder, and an X-ray detector. X-rays can be generated within a sealed tube under vacuum. A tungsten filament is fixed within the tube and connected to high voltage transformer. When a voltage is applied to the filament at a current of 3 A, electrons are emitted and rapidly drawn to the target, often made of copper (λ= 1.5418 A). When these electrons hit the target, X-rays are produced. The emitted wavelength is characteristic for elements of that target. These X-rays are collimated and directed onto the substrate. The X-ray beam hits the sample and the detector records the X-ray intensity diffracted at the substrate. The distances between the adjacent lattice planes can be calculated by applying Bragg's Law, see Figure 3.1.

$$n\lambda = 2d * \sin\theta \tag{3.1}$$

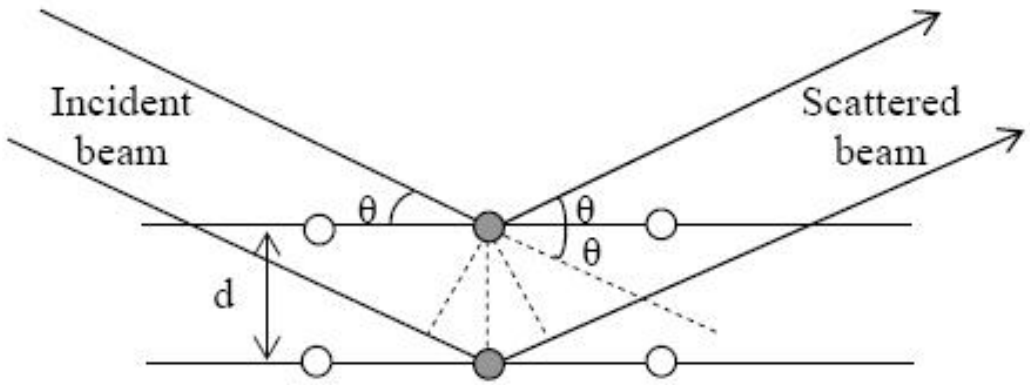

Figure 3.1: *Bragg's Law.*

where *n* is the order of diffraction (0,1,2,3,...), λ is the wavelength of the incident X-ray beam, *d* is the distance between adjacent lattice planes, and θ is the angle of incidence of the X-ray beam. The diffraction angle 2θ is equal to twice the incident angle θ. The goniometer is motorized and moves through a range of the angle 2θ. Each time the Bragg condition is satisfied, the detector measures the intensity of the reflected

radiation. An X-ray detector records the diffracted beam intensity as a function of the angle (2θ). Every crystalline material will give a characteristic diffraction pattern, which can be used for the identification of its structure. The plot of XRD patterns used to identify the type of material by comparing them with standard XRD patterns in a database. When XRD is applied for the characterization of powder or polycrystalline samples, each particle of the powder is a tiny crystal, or assemblage of smaller crystals, oriented randomly with respect to the incident beam. The result is that every set of the powder or the polycrystalline lattice planes can be capable of diffraction, but just in the case that its orientation is making a correct Bragg angle. In the XRD of single crystalline, the rotating crystal method is used, where the crystal is rotated about only one axis, which will lead to that only a particular set of lattice planes will, for an instance, make the correct Bragg angle for diffieration of the monochromatic incident beam and that instant a diffracted beam will be formed.

3.4 Energy Dispersive X-ray Spectroscopy (EDX)

Energy Dispersive X-ray spectroscopy (EDX) analysis was used for the deposited films in order to evaluate their chemical composition. The scanning electron microscope is also equipped by an EDX module. EDX is a micro-analytical technique that uses the characteristic spectrum of X-rays emitted by the sample after excitation by high energy electrons to obtain information about its elemental composition. During EDX analysis, the specimen is bombarded with an electron beam inside the scanning electron microscope. The bombarding electrons collide with the specimen atoms' own electrons, knocking some of them off in the process. A position vacated by an ejected inner shell electron is eventually occupied by a higher energy electron from an outer

shell. To be able to do so, however, the transferring outer electron must give up some of its energy by emitting an X-ray photon. The number and energy of the X-ray photon emitted from a specimen can be measured by an energy dispersive spectrometer. As the energy of the X-rays are characteristic of the difference in energy between the two shells, and of the atomic structure of the element from which they where emitted, this allows the elemental composition of the specimen to be measured. A quantitative analysis is possible using appropriate calibration. Elements of low atomic number such as hydrogen, which has only one electron that is impossible to be replaced by other when it is knocked off, are difficult to detect by EDX. An EDX system coupled to the laser electron microscope of type "Genesis 4000" was applied for analyzing our film's compositions.

3.5 In-situ Analysis of Mass Change

Laser reflectivity was used to measure the growth and etch rates in-situ during film deposition systems. Laser diffraction is an optical technique, which was widely introduced as convenient way to measure and detect the onset of grown layers in CVD systems. It was applied for the in-situ measurement of growth rate during CdTe single crystal growth from the vapour phase [37] and in plasma-enhanced chemical vapour deposition of vertically aligned multi-wall carbon nanotube films [38]. Such an optical technique is applicable when the substrates have a flat and transparent surface. Usually, films grow randomly three dimensional patterns. The films in this case have rough, non-flat surface morphologies that do not allow an accurate characterization using optical methods. Therefore, as the film starts to grow accumulatively with such a surface morphology, it becomes inaccurate to use such techniques for growth rate

measurement. In addition to this, optical techniques can not measure the growth rates directly in μm/h or g/h, since they can only measure the growth on definite portions of the substrates, where the laser beam is focused on, meanwhile on neighboring portions, more or less thick layers were already grown.

Gravimetric techniques are more adequate to be applied for direct growth rate measurement in CVD systems. They are applicable for relatively heavy substrates or substrate holders. According to the physical principle of the gravimetric technique a very stable vacuum environment is required according to its high sensitivity to the surrounding conditions. Gravimetric techniques were used for the study of kinetics in CVD systems, like graphite and diamond [39]. Weiner [40] and Evans [41] have used gravimetric microbalances extensively for determining the kinetics of diamond film growth. It was also used by Salifu [42] for the in-situ growth rate measurement in plasma processing of opaque materials. Till present, the gravimetric technique was not used at temperatures higher than 1300°C, where experimental difficulties are large. D. Neuschütz and his group have applied the microbalance in a hot-wall reactor to measure the growth rates of Al_2O_3 at a temperature range of 900-1200°C in [43].

The gravimetric microbalance has not been used previously in SiC HTCVD process. SiC HTCVD systems are difficult to combine with the gravimetric technique because the substrate must hang freely, the temperature is very high and the flow around the substrate should be stable to achieve accurate measurements. To overcome these problems a magnetic suspension balance MSB was coupled to our hot-wall reactor at laminar flow conditions for direct weight measurements during the growth of polycrystalline SiC. The work presented in this chapter focuses on the in-situ growth rate measurement of polycrystalline SiC in a non-seeded HTCVD process as an initial step

for its future application in seeded, epitaxial growth of SiC by HTCVD. The parameters used in these experiments were the same as applied in the experiments that were presented in the previous chapter.

3.5.1 The Magnetic Suspension Balance

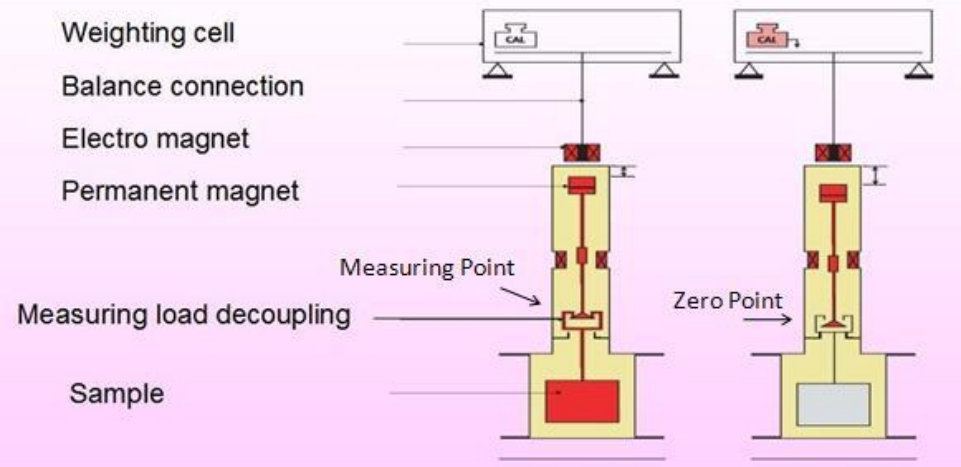

Figure 3.2: *Schematic description to the measuring principle of the magnetic suspension balance, see the MSB manual of Rubotherm GmbH.*

The Magnetic Suspension Balance (MSB) makes it possible to weigh samples contactlessly under nearly all environments with a balance located at ambient conditions. The sample is located in the measuring cell and can be (un)coupled specifically from/to the balance via a contactless magnetic suspension coupling. An electromagnet is attached to the bottom of the balance. It lifts a so-called suspension magnet, which consists of a permanent magnet, a sensor core and measuring load decoupling cage. The electromagnet, which is attached to the weighing hook of the weighing cell, maintains a freely suspended state of the suspension magnet via an electronic control unit. Thereby different vertical positions are possible. First the zero point position (ZP) in which the

suspension part suspends alone and contactlessly and thus represents the unburdened balance. And second the measuring-point position (MP), in which the suspension part reaches a higher vertical position, thereby the sample is coupled to the balance and the balance and transmits the weight of the sample to the balance transmitting the weight of the sample to the balance. This principle is illustrated in the following picture. A schematic presentation of the MSB principle is shown in Figure 3.2.

3.5.2 Experimental setup

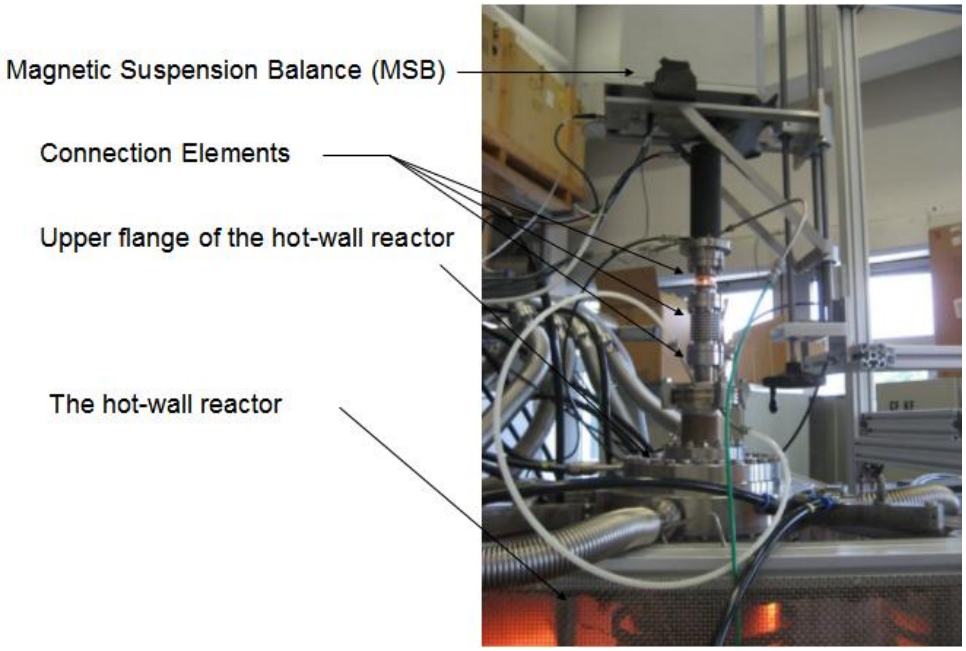

Figure 3.3: *Picture of the MSB coupled with the HTCVD reactor during the growth process of polycrystalline SiC.*

The MSB was connected to the HTCVD reactor as illustrated in Figure 3.3, the temperature was measured twice on the inner walls of the susceptor, firstly with a zero flow and secondly with only a helium flow of 0.0075 m/s. A non-constant distribution of the susceptor temperature was recognized showing a trivial temperature difference

between both flow conditions. A maximum temperature of 2460 K could be reached on the inner susceptor walls. The MSB is connected to the upper flange, as seen in Figure 3.3. An additional helium flow of 300 sccm was used for purging the MSB and its connection elements.

As known for the growth of mono-crystalline SiC by HTCVD, seed crystals are necessary for the epitaxial growth, which were usually fixed on a graphite lid or seed-holder. The design of the hot-wall reactor deals with a seed-holder, which has a geometry of a disc with 50 mm diameter, thickness of 8 mm and a density of 1.83 g/cm3. In the seeded growth experiments presented in the previous chapter, the graphite disc (seed-holder) was hanged freely inside the reactor by means of a graphite cord, which was tied to the outlet flange, while in non-seeded growth experiments, the graphite cord was tied to the hook of the MSB. A distance of 30 cm was measured between the bottom of the outlet flange and the seed-holder. A growth temperature of 1950°C was achieved after a heating period of 30 minutes. Thereafter, both precursors SiH_4 and C_3H_8 were added at flow rates of 20 sccm and 150 sccm leading the concentration values of 0.132 mol/m^3 and 0.994 mol/m^3, respectively. Both concentrations were chosen according to the results published by Elisson in [44], whereby it was observed that a very low ratio of C_3H_8/SiH_4 (nearly 1:8) is necessary for an optimal growth rate of SiC. Helium was chosen as a carrier gas and added at 6 slm with a flow velocity of 0.0075 m/s. As reported by B. Sundqqvist in [32], thick epitaxial layers of SiC could be successfully grown at a pressure of approximately 1 atm. Therefore, a value of 800 mbar was used in our experiments to avoid any danger that can be caused due to the pressure increase, which can be caused due to a sudden breakdown of the pump or the pressure controller.

In order to check the accuracy of the MSB, the mass of the seed-holder was measured

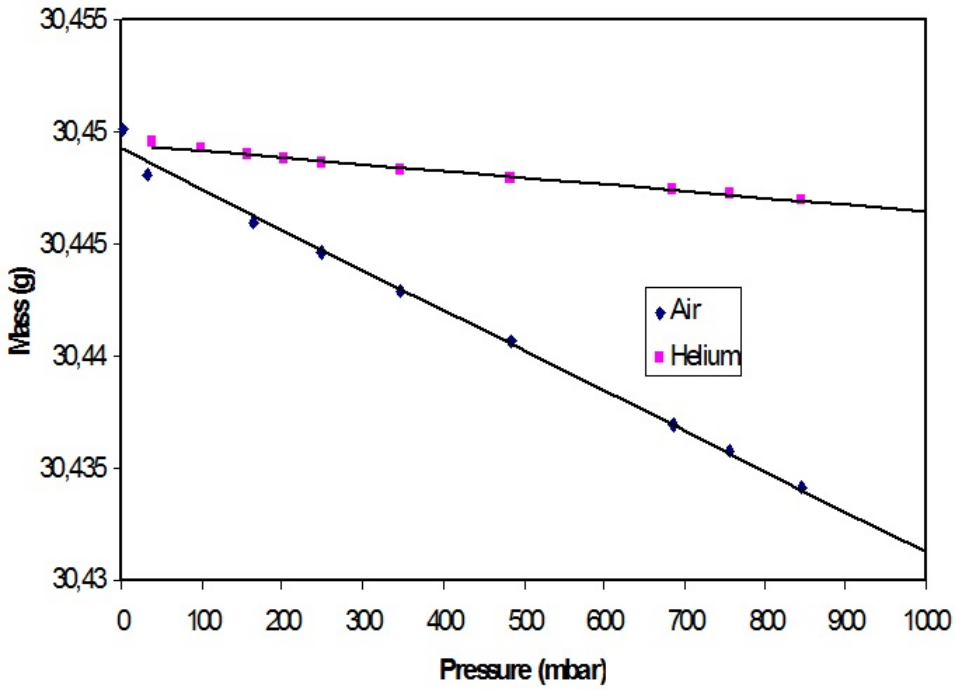

Figure 3.4: *The seed-holder mass (in g) is plotted versus a pressure range of 1-1000 mbar in helium and air atmospheres in order to check the measurement's accuracy of the MSB at room temperature.*

at different pressures in helium and air, individually. Figure 3.4 shows the seed-holder mass recorded versus the pressure in both cases. At low pressures the density of the medium is reduced, which reduces the buoyancy force and consequentially reduces the mass recorded for the seed-holder. The difference between the measured values at pressures of 40 mbar and 1 atm is 0.02 g in air and 0.003 g in helium. The latter value is much less than the one measured in air, which is expected due to the lower density of helium compared with air, which results in a lower buoyant force. Another experiment was carried out to check the accuracy of the MSB under flow. The seed-holder mass was measured at different flow rates as shown in Figure 3.5. The mass was firstly measured at 800 mbar in a stationary environment. Afterwards, the flow velocity was increased in steps by 0.0025 m/s (2 slm) every minute. The first flow acceleration from 0 slm to 2 slm had the most violent impact on the values recorded for the seed-holder mass. Instable mass values were recorded in this period. A further increase of the flow velocity has shown a smaller effect on the mass recorded. However, increasing the flow velocity by increasing the flow rate every minute leads to pressure fluctuations around the set point of 800 mbar, which leads to oscillating values of the mass recorded. Such an instability requires a small period of time till this effect disappears.

The direct growth of polycrystalline SiC on the 2-inch seed-holder was analysed on the basis of the mass change, which was recorded by means of the MSB. In order to investigate the influence of the precursor concentrations on the growth rate of polycrystalline SiC, five experiments were carried out. The mass change was recorded in-situ for analyzing the influence of variating the precursor concentrations on the growth rate.

- Firstly, the mass change was recorded during 45 minutes including a total deposition period of 20 minutes. SiH_4 and C_3H_8 were added at flow rates of 200

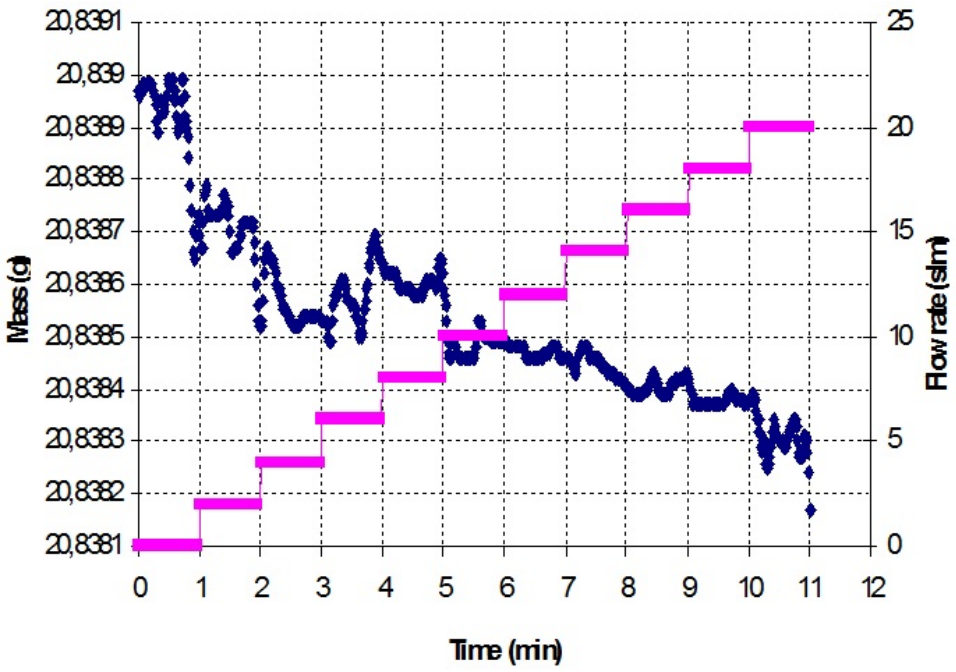

Figure 3.5: *The seed-holder mass is recorded at different carrier gas flow velocities. The flow velocity was increased by increasing the flow rate by 2 slm after a period of one minute. Fluctuations of the weight values that are visible in the diagram are caused by the sudden increase of the flow rate, which lead to a pressure disturbances and finally results in low accuracy of the weight measurement.*

sccm and 20 sccm in a carrier gas of helium leading to both concentrations of 1.315 mol/m^3 and 0.132 mol/m^3, respectively.

- Afterwards, the C_3H_8 concentration was held at a constant value of 0.132 mol/m^3, while the SiH_4 was added in gradual increase every 10 minutes at five different concentrations of 0.668, 0.994, 1.315, 1.631, 1.941 and 2.247 mol/m^3.

- In the third experiment, the SiH_4 concentration was held at a constant value of 0.669 mol/m^3 (100 sccm), while the C_3H_8 concentration was started with 0.0335 mol/m^3 (5 sccm) and increased gradually to 0.067, 0.101 and 0.134 mol/m^3 every five minutes.

- In the fourth experiment, the SiH_4 and C_3H_8 concentrations were held at a constant value of 1.304 mol/m^3 and 0.1304 mol/m^3, meanwhile H_2 was added at different concentrations of 0, 0.326, 0.647, 0.963 and 1.274 mol/m^3 that were gradually increased every five minutes.

- Finally, the seed-holder was hanged vertically (circular area parallel to the flow stream lines) allowing the possibility to be deposited on both of its sides. The temperature measured on the lower side of the seed-holder was 1950°C, the pressure was held constant at 800 mbar. The SiH_4 flow rate was held constantly at 200 sccm with a concentration of 1.318 mol/m^3, while the flow rate of C_3H_8 was initially set to zero in the first 6 minutes and then gradually increased to 5 sccm and 10 sccm leading to both concentration values of 0.0329 mol/m^3 and 0.0658 mol/m^3, respectively.

Chapter 4

HTCVD System Design and Setup

4.1 HTCVD system

The HTCVD technique can simply be described as chemical vapor deposition CVD at high temperatures, hence the name high temperature CVD: HTCVD. The growth process however, differs strongly from that of the CVD process due to the significant sublimation and etch rates at the extreme growth temperatures 1800-2300°C. In order to reach such high temperatures, inductive heating of a graphite susceptor is used. The commonly used components in CVD systems are thus required in HTCVD. Our HTCVD system is described in Figure 4.1, which is mainly comprised of hot-wall reactor (HWR)(1) with a graphite susceptor, middle frequency generator (MFG) and induction coil (2), pump and pressure regulator (3), mass flow controllers (4), gas sources (5) and pyrometer (6). The MFG is purchased from Hüttinger Elektronik GmbH and can deliver a heating power up to 50 kW at approximately 20 kHz. The induction coil is made of copper and water cooled. The MFCs are purchased from MKS Instruments Germany and have different capacities in order to control the gas flow rates. The pump

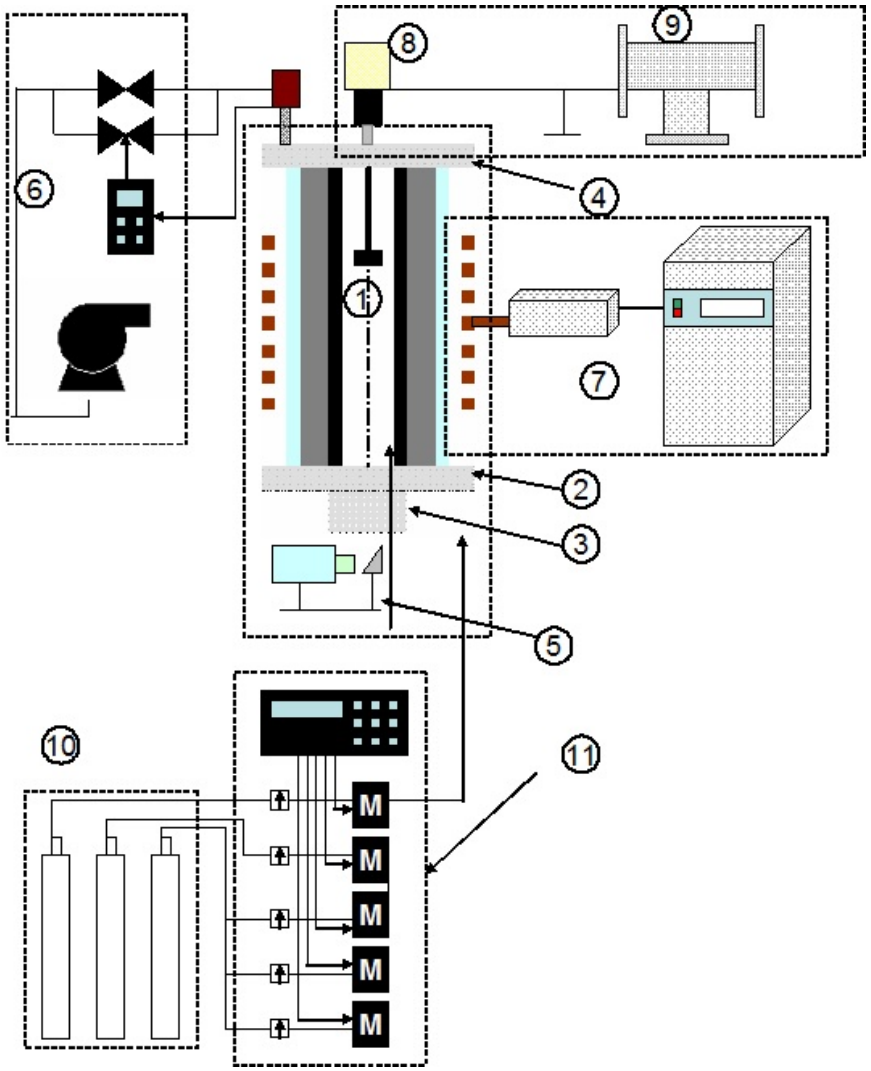

Figure 4.1: *A schematic diagram of the HTCVD system. (1) hot-wall reactor (HWR), (2) inlet flange, (3) nozzle, (4) outlet flange, (5) pyrometer, (6) pump and pressure controller, (7) middle frequency generator (MFG) and induction coil, (8) optional connection for mass spectrometry (9), (10) gases source, (11) mass flow controllers.*

was purchased from Busch GmbH and has a main pumping speed of 61 m^3/h. The pyrometer is purchased from Keller HCW and is capable to measure the temperature in a range of 1000-3000°C. The reactor is mainly comprised of inlet flange (7), outlet flange (8), nozzle (9), graphite susceptor, foam graphite and quartz tube. The design of the reactor upper flange enables the optional connection of the MSB (10) or mass spectrometer (11). Section 3.1.1 discusses the reactor design.

4.1.1 The Hot-wall Reactor

As previously introduced in section 2.3, in the HTCVD process, the precursors or the gas mixture are injected into the susceptor in upward direction, where higher temperatures are established on the inner susceotor walls. This leads to the pyrolysis of the reactants producing species or radicals that will be transported by free convection due to thermal gradients or by forced convection to the substrate or the seed-surface, where the growth mostly proceeds by diffusion. In order to thermally realize this, high temperatures in a range of (1800-2300°C) are required. Inductive heating has proofed a reliable performance of the crucible or the susceptor heating in order to reach such a high temperatures. The basic components of the induction heating are an AC power supply, induction coil, and workpiece (sample to be heated or treated). The power supply sends alternating current through the coil, generating a magnetic field. When the workpiece is placed inside the coil, the magnetic field induces eddy currents in the workpiece, generating precise amounts of localized heat without any physical contact between the coil and the workpiece. The eddy current is an electric current circulating wholly within a mass of a conductor or a semiconductor. As known, graphite was usually chosen for the susceptor material due to its high temperature resistance up to 2500°C in vacuum environments that contain no oxygen. Unlike graphite, it becomes

critical when other materials are used in the reactor, like stainless steel, which is able to withstand only temperatures up to 1200°C. Applying higher temperatures on it will increase the probability of its melting and consequentially imposing impurities into the process, which must be avoided in HTCVD of SiC. In such case, water cooling and a special welding design are very necessary for the reactor construction. One of the designs of the hot-wall reactor used for HTCVD is introduced in section 2.3, Figure 2.8. This design utilizes a crucible made of graphite, which is partially closed at its both ends. The seed-crystal is fastened on the bottom of the lid. Instead, our design deals with a susceptor made of simple graphite cylinder and a free floating seed-holder, whereon the seed-crystal can be fastened. This allows more flexibility to optimize the seed-holder position for improving the growth conditions. Thus, the temperature distribution on the inner side of the susceptor, seed-holder temperature (growth temperature) and the in-situ detection of this parameter during the growth, are important for enhancing the growth conditions and increasing the growth rate. Therefore, the design of the hot-wall reactor was carried out as a basic part of this research, which can deal with the deposition on SiC wafers with large diameters up to 75 mm.

A side view of the reactor cross section is shown in Figure 4.2. The susceptor (1) was made of a hard graphite tube of 130 mm inner diameter, 154 mm outer diameter and 600 mm length. It was purchased from SG Carbon and has a density of 1.82 g/cm^3. The outer side of the susceptor was covered by foam graphite (2) for thermal insulation. Since a vertical type reactor with an upward flow direction was desired to avoid unsymmetrical free convection, the inlet flange (3) was designed in which it is possible to be connected with a nozzle (4) by means of an ISO CF 250 flange (5). The precursors are fed into the reactor through four small holes (6) that are bored in the

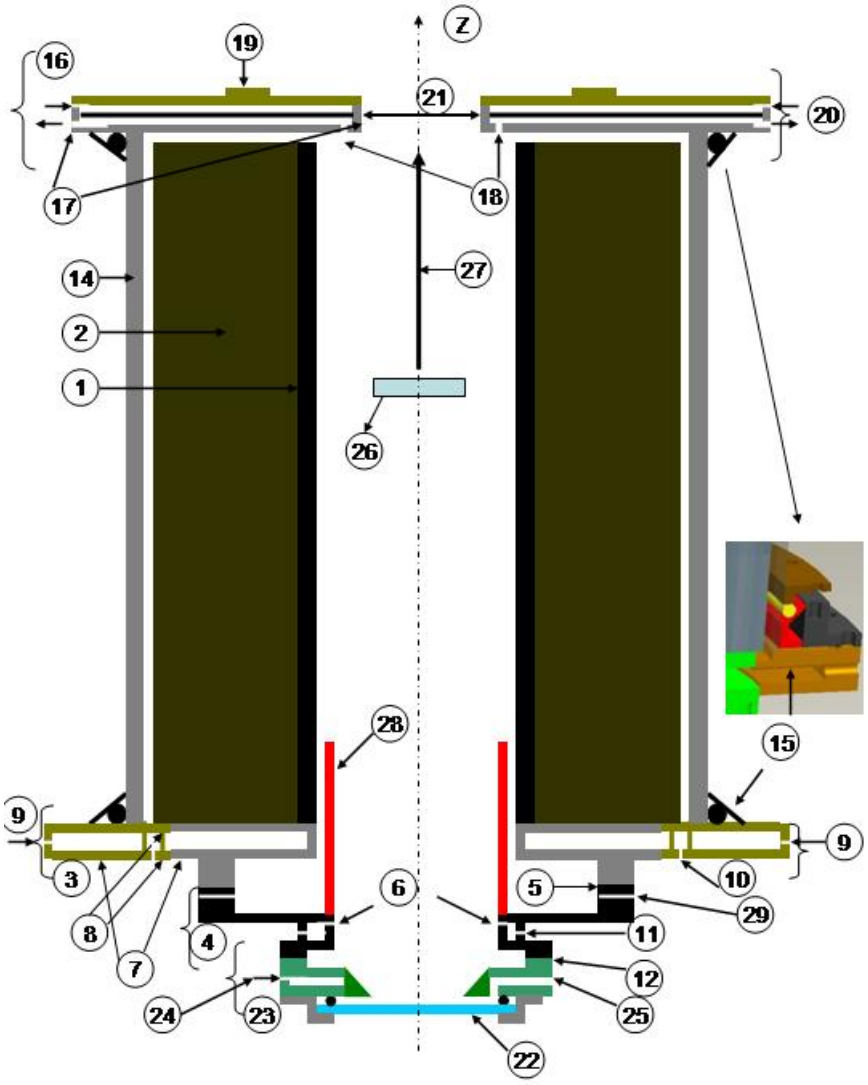

Figure 4.2: *Two dimensional view of the reactor cross section, including the inlet and outlet flanges, susceptor, graphite foam, quartz tube, nozzle and the optical access. The detailed description is given in the text.*

nozzle. The inlet flange comprises of two water cooled rings (7) that are connected to each other by welding. The flange is connected through four holes (9) with water source, further four holes (10) were allocated for purging the foam graphite. Both parts are inserted in each and welded at the perimeters (8). This design was intentionally done to shift the welding butt far enough from the thermal radiation area. The duct is water cooled at (11) and can be connected to an ISO CF 160 flange at (12). Flange (23) has an optical access and is connected to the bottom of flange (12), which comprises of four parts as shown in Figure 4.2. A transparent plate of pyrex glass (22) with a diameter of 140 mm and 8 mm thickness is sealed by means of o-ring with a cross section diameter of 5 mm to allow temperature measurement by the pyrometer. This flange is connected to the water source through one hole at (24), whereas on the other side, another hole was designed for the inlet of purging flow at (25). This flange was permanently cooled by air keeping its temperature less than 300°C.

The assembly is centered in a quartz tube (14) and sealed at its both ends by two O-Ring and the steel parts that are scaled in (15). The outlet flange is also water cooled and comprises of two plates (16) that are welded at their perimeters (17). For the removal of the gases, four canals (18) were designed passing by the water cooled area to connect the flange by the pump. An ISO CF 250 flange (19) was built on the upper side of the flange for its connection with the magnetic suspension balance or with the mass spectrometer. In the center of the flange, a relatively large hole (21) of 100 mm diameter was made to enable inserting the seed-holder downwards into the susceptor(26), which is hanged by means of a graphite cord (27). The graphite tube (28) was put on the inner side of the nozzle for separating the flow from the susceptor walls due to an external carrier gas flow, which is fed into the reactor at (29).

4.2 Gases

Chemical sources may be classified as: Inert gases such as argon and nitrogen, which are used as carrier gases of a precursor vapor. Reactant gases are required such as oxygen for oxidation or hydrogen for hydrogenation or reduction, (producing volatile hydrocarbon compounds). Precursors are the source material of the deposits, which should be thermally stable at room temperature and volatile at low temperatures. Mass flow controllers are used to control and mix the amount of gases fed into the reaction chamber during the deposition process.

4.2.1 C-Precursor: Propane

Under normal atmospheric pressure and temperature, propane is a gas. Under moderate pressure and/or lower temperatures, however, propane changes into a liquid. Propane is easily stored as a liquid in pressurized tanks. It has a vapor pressure of 7.6 bar at 21°C. The boiling point of propane is -42°C (-44°F) which makes it vaporize as soon as it is released from its pressurized container. Propane has an auto ignition temperature of 480°C. The propane used in our experiments was purchased from the company of Air Liquid.

4.2.2 Si-Precursor: Silane

Silane is a colorless, pyrophoric gas. Being pyrophoric, leaks will immediately ignite on contact with air. However, under certain conditions such as high humidity or rapid release, it may not immediately ignite and may form pockets of gas, which may cause a delayed vapor cloud explosion. This means it is self-igniting in air because it has an autoignition temperature below ambient temperatures. Leaks of silane may cause a fire or possibly form explosive mixtures in air. Some very small leaks will not give a

visible flame but may be detected by the presence of oxide powder buildup at the leak point. The chief product of combustion is silicon dioxide SiO_2. Silane fires must only be extinguished by stopping the flow of silane to the fire. The lower flammable limit is 1.37 volume percent. Silane mixtures in the 3 to 4 percent range can exhibit pyrophoric behavior. Its autoignition temperature is -50°C. It has a density of 1.35 kg/m^3 at 20°C. Its bpoiling temperature is -112°C. Silane has a very high vapor pressure; at -3°C, it has a vapor pressure of 47 bar, which possibly develops reasonable concentrations at high temperatures compared with chlorinated silanes like SiH_2Cl_2, $SiHCl_3$ and $SiHCl_4$, which have lower decomposition temperatures and higher nucleation rates in hydrogen dilutions as reported in [45]. The decomposition kinetics of silane is therefore very important for systems with fast temperature rise, where the decomposition of silane do not occur at low temperatures. Silane was purchased from Air Liquid company at two volumetric concentrations of 1.5% and 5%.

4.2.3 Carrier Gas

In such open systems, convection heat transfer reveals through forced convection and/or free convection. The velocity range in the susceptor plays a decisive role defining the convection mode. In forced convection, the internally imposed flow is generally known, whereas in natural or free convection, the flow results from an interaction of the density difference with their gravitational, or some other body force. The velocity in natural convection is supposed to be slow compared with the velocity in the case where forced convection dominates. In our case, this velocity of the process gases lies in a range less than 0.0075 m/s, which is too slow for developing a forced convection mode, which indicates a prevalence of free convection mode.

In previous works that were presented in sec.2.3, H_2, He and Ar were widely chosen as carrier gases in SiC growth systems. In order to determine the optimal heat transfer conditions in the hot-wall reactor, a convection based comparison was carried out for all three gases individually using a susceptor geometry of H = 600 mm for its length and a diameter of d = 130 mm. Firstly, the convection mode was investigated at assumed uniform temperature of T_{wall} = 2200°C on the inner susceptor walls. The gases properties were taken at an average temperature $T_f = 1400$°C as presented in Table 4.1. The values of the table are showing that Ar has much lower thermal conductivity compared with both H_2 and He, where the dynamic viscosity and density of Ar is larger than those of H_2 and He. The inlet temperature T_{in} is assumed to be 600°C, while the gas is assumed to leave the susceptor at a temperature of T_∞ = 2000°C, which is 200°C below the wall temperature.

Gas	C_p [J $kg^{-1}K^{-1}$]	$10^3 * \rho$ [kg m^{-3}]	$10^6 * \eta$ [kg $m^{-1}s^{-1}$]	10^3 * k [J m^{-1} s^{-1} K^{-1}]
H_2	15784	17.53	25.0	560.0
He	5196.6	34.8	55.0	460.0
Ar	520.7	347.9	65.0	52.6

Table 4.1: *The carrier gases properties are given at 1400°C, where C_p is the heat capacity, ρ is the density, η is the dynamic viscosity and k is the conductivity coefficient.*

The convection mode can be distinguished by applying equation 4.1. If the condition

given by this equation is observed, free convection is assumed to be dominating.

$$\frac{Gr_H}{Re_H^2} >> 1 \tag{4.1}$$

Where Reynolds number Re_H is a dimensionless number that gives a measure of the ratio of inertial forces to viscous forces and consequently quantifies the relative importance of these two types of forces for given flow conditions and Grashof's number Gr_H which is a dimensionless number used for approximating the ratio of the buoyancy to viscous force acting on a fluid. It frequently arises in the study of situations involving natural convection. Both numbers are respectively given by equations 4.2 and 4.3.

$$Re = \frac{u * D}{\nu} \tag{4.2}$$

$$Gr_H = \frac{g * \beta * (T_{wall} - T_\infty) * H^3}{\nu * k} \tag{4.3}$$

Where ν is the kinematic viscosity (calculated from η/ρ), β is 1/T_f, H is the reactor length (600 mm), D is the hydraulic diameter given by 4*area/(π*d) for cylinders and k is the thermal conductivity of the gases. The resulted values of the term Gr/Re^2, are much greater than 1 for all gases, as evaluated from the Gr and Re numbers listed in Table 4.2, which matches the condition given in Eq.4.1 proving that free convection dominates, meanwhile forced convection is accordingly assumed to be negligible. Now the heat transfer can be calculated by equation 4.4 as found in [44].

$$Q_H = \frac{Nu_H * k * \Delta T_{in,wall}}{H} \tag{4.4}$$

Where Δ $T_{in,wall}$ is the difference between the inlet gas temperature (600°C) and the susceptor temperature (2200°C) and Nu_H is Nusselt number of an upward flow in

cylinders given by equation 4.5.

$$Nu_H = 0.52 * (Ra_H)^{1/4} \tag{4.5}$$

Where Ra stands for the Rayleigh number and is given by equation 4.6 [46]. In fluid mechanics, the Rayleigh number for a fluid is a dimensionless number associated with buoyancy driven flow (also known as free convection or natural convection). When the Rayleigh number is below the critical value for that fluid, heat transfer is primarily in the form of conduction; when it exceeds the critical value, heat transfer is primarily in the form of convection. .

$$Ra = \frac{\beta * g * C_p * \rho^2 * H^3 * (T_{wall} - T_\infty)}{\eta * K} \tag{4.6}$$

The heat transfer coefficient (h) can be determined using equation 4.8. The values calculated for h are given in Table 4.3 for all three gases.

$$h = \frac{k * Nu}{D} \tag{4.7}$$

Gas	Re	Ra*10^{-5}	Gr*10^{-4}	Nu
H_2	0.68	10.5	0.38	16.64
He	0.62	7.5	0.42	15.31
Ar	5.24	558.0	30.8	44.94

Table 4.2: *Re, Ra, Gr and Nu are unit-less numbers calculated for H_2, Ar and He.*

By substituting the resulted values of the Re, Gr, Ra and Nu numbers listed in table.4.2

in the equations 4.4 and 4.7, the heat transfer and heat transfer coefficient can be calculated for *free convection* in all three gases as presented in Table 4.3. Upon those results, it was found that H_2 has the maximum heat transfer coefficient, which requests an energy of 24.85 kW to reach an outlet temperature of 2000°C, while He and Ar require less energy than H_2 in order to reach the same temperature. Although the use of Ar as carrier gas would lead to the lowest consumption rate of energy, but inhomogeneity or thermal instability could be resulted due to its very low heat capacity. Therefore, the higher thermal conductivity and heat capacity of He make it as a better alternative of Ar and also H_2, which requires higher consumption rate of energy than He. A heat transfer rate of 19 kW was obtained using He. This value seems to be quite reasonable in our case, taking into consideration that large amount of the energy will be dissipated by the water and air cooled parts of the hot-wall reactor.

Gas	h[W/m^2*K]	Q_H 10^{-3}*[W/m^2]	10^2*$Q_{H,carrier}/Q_{H,He}$ %
H_2	71.68	24.850	132.2
He	54.20	18.790	100
Ar	18.19	6.30	33.5

Table 4.3: *The heat transfer rates are calculated in He, Ar and H_2 mediums. They were compared with each other taking the heat transfer in He as datum. The maximum heat transfer coefficient was resulted in Helium medium.*

As previously explained, a flow rate of 6 slm was required for the process causing a flow velocity of 0.0075 m/s. By setting such a velocity in the susceptor, laminar flow and free convection heat transfer will be established. Higher flow rates might develop

a forced convection heat transfer or combined free and forced convection mode. In such a case, at a given instance of the flow stream there will be some delay until the temperature and velocity have reached their maximum. The distances required for an instance of the fluid to reach these two conditions are called: fully developed temperature profile H_T and fully developed velocity profile H_V. H_T and H_V that are given by the equations 4.8 and 4.9.

$$H_T = 0.28 * D * Re_D \tag{4.8}$$

$$H_V = 0.04 * D * Re_D \tag{4.9}$$

Re, H_T and H_V are calculated at three different helium flow rates of 6 slm, 24 slm and 42 slm, as presented in table 4.4. At the lowest flow rate of 6 slm (0.0075 m/s), the distances H_T and H_V remain too small, where, as previously discussed, free convection dominates. However, increasing the flow rate to 24 and 42 slm, results in increased values of Re, H_T and H_V, which shows that the flow stream will require longer distance to reach its maximum temperature and velocity in the reactor. Therefore, increasing the flow velocity to relatively high values will result in a cooler flow stream, and therefore, in lower growth temperatures. The flow stream temperature T(K) for the gas center can be calculated by equation 4.10, which can be applied in forced convection heat transfer at high flow velocities where a value of 3.66 is used for the Nusselt number. But, since increasing the velocity to a value of 0.0525 m/s results in a value of 683.8 for the term Gr/Re^2, which is still much greater than 1, therefore, it could be resolved that even at this velocity, the heat transfer mode remains dominated by free convection

and the application of equation 4.10 is not valid at this flow condition.

V· (slm)	Re	H_T (cm)	H_V(cm)
6	0.620	2.25	0.32
24	2.47	8.89	1.28
42	4.32	15.71	2.24

Table 4.4: *Different flow rates of helium were applied. The corresponding distances of the fully developed temperature and velocity are listed in this table. At a flow rate of 42 slm (velocity of 0.0525 m/s), a distance of 15.79 cm was calculated for a fully developed temperature profile, which indicates that increasing the flow velocity will significantly influence the temperature profile.*

$$\frac{(T_{wall} - T(H)_{gas,center})}{(T_{wall} - T_{gas,in})} = \exp\left(Nu_D * k * \pi * H/m^{\cdot} * C_p\right) \tag{4.10}$$

Where m· is given by equation 4.11.

$$m^{\cdot} = \rho * \pi * r^2 * u \tag{4.11}$$

4.3 Substrates

As previously introduced in this chapter, seed-crystals are necessary for the epitaxial growth of SiC using the HTCVD technique. Without a seed-crystal, amorphous or polycrystalline films will be grown on arbitrary substrates. The polytype of the grown SiC film can be determined by the polytype and the surface orientation of the seed-crystal. For the seed-crystal fixation, the use of a suitable seed-holder is necessary. In the hot-wall reactor design, it was planned to use a floating seed-holder, which can be

hanged horizontally inside the susceptor. These points are discussed in the following part of this chapter.

4.3.1 Seed-holder

In non-seeded growth experiments, SiC was directly deposited on substrates made of graphite foil, which were formed in different shapes as seen in Figure 4.3. In seeded growth experiments, the substrate holder was made of hard graphite with a density of 1.83 g/cm^3. Different versions of seed-holder were applied in the growth experiments and improved corresponding to the growth results. More details about the applied seed-holders in this work are presented in section 5.2.4.

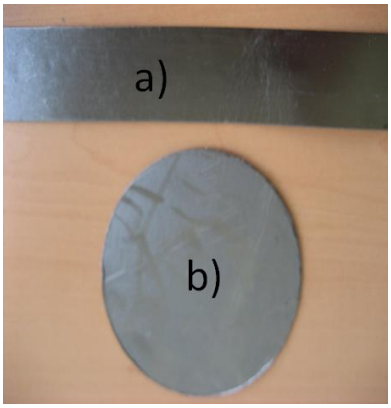

Figure 4.3: *The firstly used seed-holders were cut out of a graphite foil. a) Vertically hanged holders of long stripes. b) Horizontally hanged holders with disc shape.*

4.3.2 Substrate Polytype

On-axis, 2 inch 6H-SiC wafers with 250 μm thickness were purchased from SGL Carbon and divided manually into six pieces with triangular shapes for their initial application in the epitaxial growth experiments, where epitaxial growth of SiC is expected to result in its cubic polytype, as explained in section 2.3.3. For the homoepitaxial growth of SiC, small 3.5° and 8° off-axis surfaces crystals were purchased with the dimensions of 6×6×0.25 mm and applied for targetting the homoepitaxial growth of

6H-SiC.

4.3.3 Seed Adhering

The use of a free floating seed-holder, where the gas flow is in upward direction, requires fixing the seed-crystal on the lower side of the seed-holder. The small size of the seed-crystals and the required purity of the process make it difficult to mechanically fix the seed-crystal, especially by the use of additional parts or materials. This problem was previously solved by Kordina in [31], who fastened the seed-crystal on the seed-holder using molten glycol. This method was successfully followed in our laboratory using molten sugar. A thin layer of sugar was put between the seed-crystal and the seed-holder, which was heated for around 10 minutes at a temperature of 250°C until the sugar was completely decomposed.

4.4 Deposition Mode

4.4.1 Temperature Profile

The hot wall reactor was designed for a maximum temperature of 2500 K. The temperature was controlled by the output of the MF-generator, which is capable to produce an output power up to 50 kW. The temperature on the susceptor walls is not constant on its whole length due to the geometry of the inductive coil and the high rate of heat dissipation on both ends of the susceptor. The optical access designed at the bottom of the reactor enabled the temperature measurement along most of the susceptor inner space. A mirror made of Aluminum was manufactured and polished to be used for reflecting the rays emitted by the hot object (inner susceptor walls, seed-holder or seed-crystal) to the pyrometer. This mirror is fixed on a bench, which enables flexible adjustment of

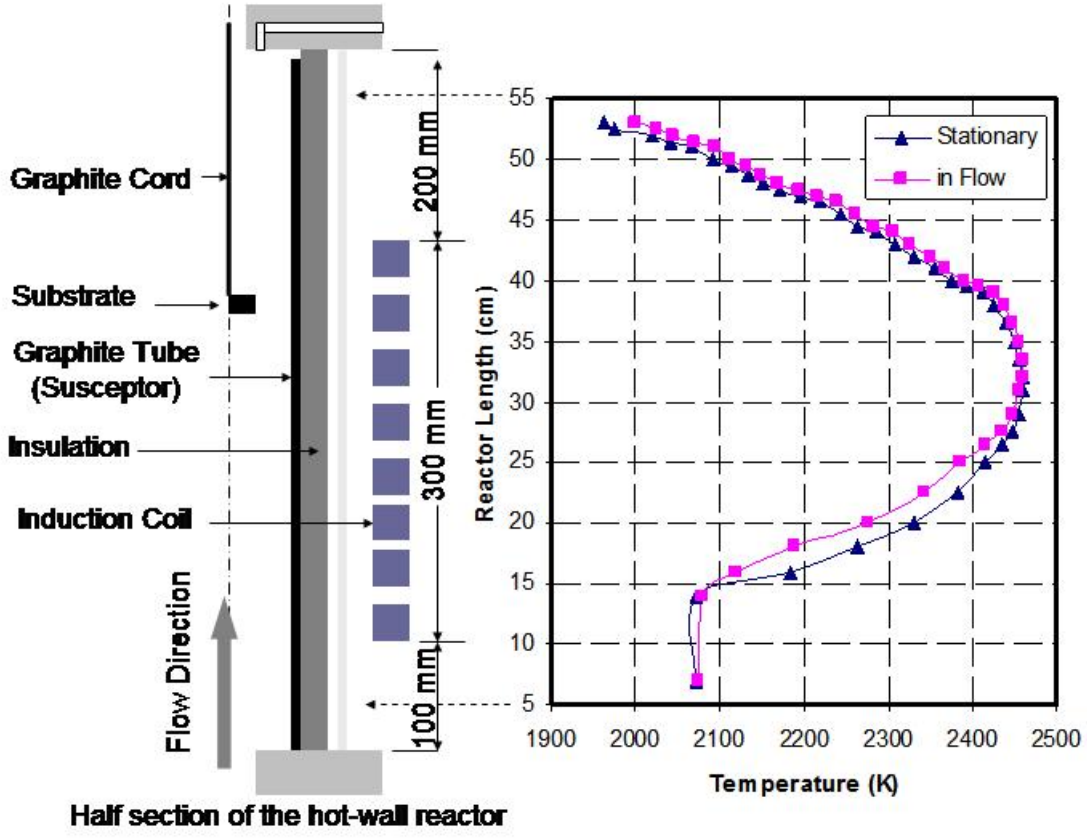

Figure 4.4: *A half view of the reactor cross section is represented on the left side, while on the right side, the temperature distribution profile is illustrated in relation with the position on the susceptor walls.*

the mirror. The application of such a design allowed the monitoring of the temperature along most area of the susceptor inner surface, which can be considered as a novel improvement of the temperature measurement in HTCVD systems, where the temperature was usually measured on small spots of the outer cylinder of the susceptor or on the upper side of the lid, where the seed-crystal is fastened on its bottom.

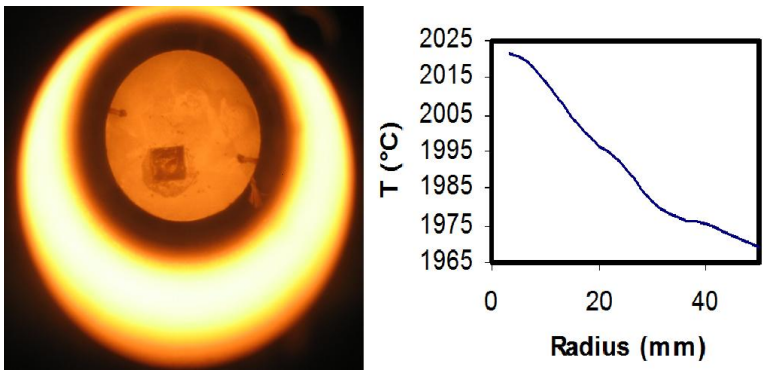

Figure 4.5: *Left: Picture taken through the optical access and shows the seed-holder (made of graphite foil) at a temperature of 2000°C. Right: Temperature profile of the seed-holder starting from the center point and ending at the maximum radius of the substrate.*

The temperature profile of the susceptor could be measured at a pressure of 300 mbar under two different flow conditions, firstly without flow, and secondly under a flow velocity of 0.0075 m/s at a Helium flow rate of 6 slm. The measured temperatures are illustrated versus their individual z-positions (60 cm length) as seen in Figure 4.4. The temperature profile has a non-constant distribution with a maximum wall temperature of 2180°C. This temperature was recorded for a point, which is coincident with the middle length of the inductive coil, which indicates that the vertical position of the inductive coil (in regard with the susceptor position) has a significant influence on the temperature profile. The helium flow was found to have a negligible effect on the tem-

perature distribution, which indicates that the applied flow velocity is still too slow for decreasing the heat transfer coefficient and consequentially changing the heat transfer mode from free to forced convection. The temperature measured at a z-position of 5 cm below the outlet flange was 1700°C, whereas a temperature of 1800°C was measured at a z-position of 46 cm below the outlet flange.

During heating, the seed-holder temperature was continuously measured by the pyrometer till the desired growth temperature is reached. Once the desired value is achieved and became stable, the precursors were then fed into the reactor. The silane SiH_4 is known for its pyrolysis at temperatures close to 1000°C. A temperature range of 800-1200°C is usually reached in the duct causing an early or preliminary pyrolysis of SiH_4 causing a dusty sight in the inner space of the susceptor, through it a continuous temperature measurement is not possible, therefore, the SiH_4 flow must be shortly stopped during the deposition until the dust disappears from the reactor space, thereafter the temperature measurement can be carried out. The temperature distribution was thus measured on a seed-holder, which is hanged 18 cm below the outlet flange, as illustrated in Figure 4.5. The pyrometer has recorded a maximum temperature of 2025°C on the center of the seed-holder, while a temperature difference of around 50°C between the center point and the substrate holder perimeter was recorded.

4.4.2 Geometrical Setup

In such a vertical flow hot-wall reactor, where the carrier gas and the precursors are injected through the duct in an upward direction towards the stagnant surface of the substrate, suitable positioning of the substrate holder is required. In non-seeded growth, long stripes made of graphite foil were initially used to indicate the vertical range

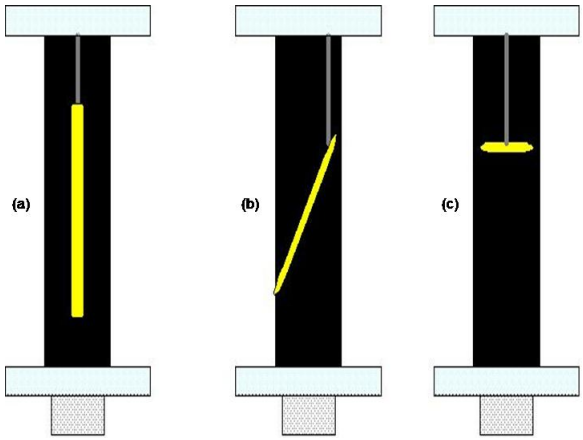

Figure 4.6: *Schematic description of different substrate positioning. a) long stripe is hanged vertically. b) long stripe is hanged with a small tilt angle to the susceptor centerline. c) Circular substrate hanged horizontally stagnating the flow.*

whereon polycrystalline SiC will deposit. This range was used as an indicative for the initial substrate position in epitaxial growth experiments. Additionally, other graphite stripes were hanged with a vertically inclined plane in order to cover a wide range of the susceptor space. Figure 4.6 illustrates three different flow geometries.

In epitaxial growth experiments, the stagnation flow geometry was further changed by adding an aperture below the substrate, whereby the flow velocity is increased and consequentially, more of the flow stream can be focused on the stagnant surface of the seed-holder. Different aperture geometries are illustrated in Figure 4.7.

4.5 Experimental Procedure

As previously mentioned, in seeded growth experiments, the seed-crystals were fixed on graphite seed-holders. The seed-holder is conducted into the HWR by means of graphite cords. Thereafter, the reactor was tightly sealed. The explosive nature of SiH_4 in air requires tight sealing of the reactor assembly to ensure safe deposition pro-

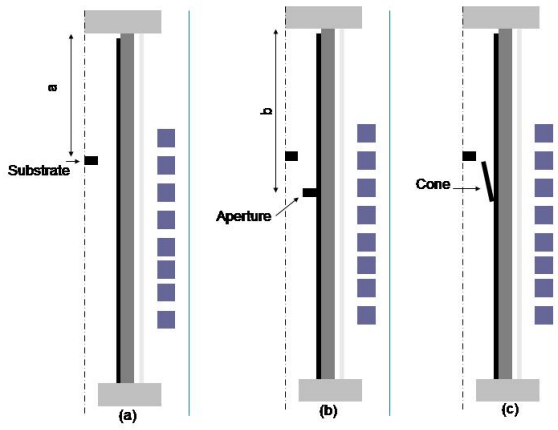

Figure 4.7: *Three different stagnation flow geometries. a) The substrate is hanged horizontally. b) An aperture is fixed a few centimeters below the substrate. c) A conical aperture is used to avoid flow turbulences.*

cess. In order to detect any leakage before starting the experiments, the reactor was pumped out to a low pressure of 10 mbar, which was kept constant at this value for testing leakage rate. Leak detection is a control method used to identify, monitor, and measure the unintentional entry or escape of fluids and gases, usually from pressurized systems or into empty enclosures. Leaks can move from the inside of a component or machine into the outside, or penetrate from the outside in, due to differences in pressure between two regions. Most leak detectors are primarily responsible for locating the leak, determining the extent or rate of leakage, and keeping track of increases or decreases in leakage. Leak detection is highly important in industrial systems that rely on sensitive components or equipment with the potential for being damaged by external contaminants. Leak testing and detection are implemented to prevent material or energy loss, improve a manufacturing systems reliability, and reduce the risk of environmental contamination. In our case, a helium leak detector was used to detect the parts or the portions that are responsible for the leak. Since, O-rings were used to seal

some parts in the reactor, so a leak rate of 10^{-9} mbar * l/s was expected. This step is followed by a heating period of around 30 minutes. Once the growth temperature required is reached on the seed-holder, the deposition can be started by feeding the reactor with the gas mixture. Once the deposition period is finished, all flow valves must be closed(except those used for cooling water) and the MF-generator is switched off. After a cooling period of 60 minutes, the seed-holder can be taken out of the reactor and the seed-crystal can then be separated from the seed-holder for its investigation.

Chapter 5

Deposition of SiC

5.1 Non-seeded Growth of SiC

Non-seeded growth of SiC can be achieved using the same concept like the one applied in the Lely method, which is presented in section 2.2.2. This method was used to observe the growth of polycrystalline SiC at high temperatures and find optimum conditions including the substrate position. Long stripes of graphite foil were hanged vertically in the reactor whereon, SiC is expected to be grow. The deposition of polycrystalline SiC was also studied on circular substrates made of graphite foil, which were hanged normally to the upward flow direction.

5.1.1 Observation of SiC Growth on Graphite Stripes

In order to observe the growth of SiC using our HTCVD system, long stripes made of graphite foil were hanged vertically in the reactor with slight inclination in order to extend the area whereon, SiC can be possibly deposited. The stripe has a length of 60 cm and a width of 5 cm. A maximum temperature of 2160°C was measured on the

susceptor walls, where the pressure was set to a value of 300 mbar. A flow rate of 4 slm of diluted SiH_4 in helium with 1.5% (60 sccm) and 30 sccm C_3H_8 have been fed into the reactor for 30 minutes. The total gas flow rate was set to 5 slm. 1 slm of this flow is used for cooling the glass disc of the optical access.

Figure 5.1: *Long stripe of graphite foil hanged vertically and deposited with SiC. A film of smooth, black powder was recognized on the lower area of the substrate, while a brilliant surface could be noticed on the upper area of the stripe.*

A film grown on the graphite foil was noticed on the top area of Figure 5.1, which is considered as the first evidence for the growth of SiC by the present HTCVD system. However, the deposition range of SiC was indicated within a vertical length of 5-10 cm starting at a position of 15 cm below the outlet flange. Unlike this area, where a bright green film is visible, a dark area was noticed on the bottom of the graphite foil. On this area, no optical evidence that proves the growth of SiC crystallites could be observed, which indicates improper growth conditions in this range.

The top area was magnified by optical microscopy as seen in Figure 5.2, where random growth of small crystallites in form of bars is visible in this image. Such non-epitaxial (polycrystalline) film growth can be described as a polycrystalline SiC.

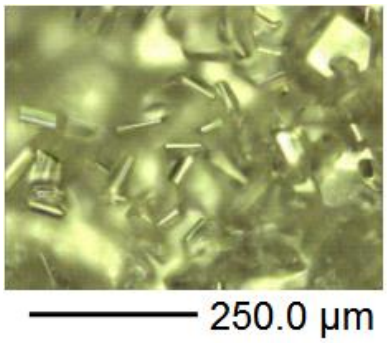

Figure 5.2: *Image taken with an optical microscope. Small crystallites in form of small bars were grown on the graphite foil. No preferred orientation of the grown crystallites is visible.*

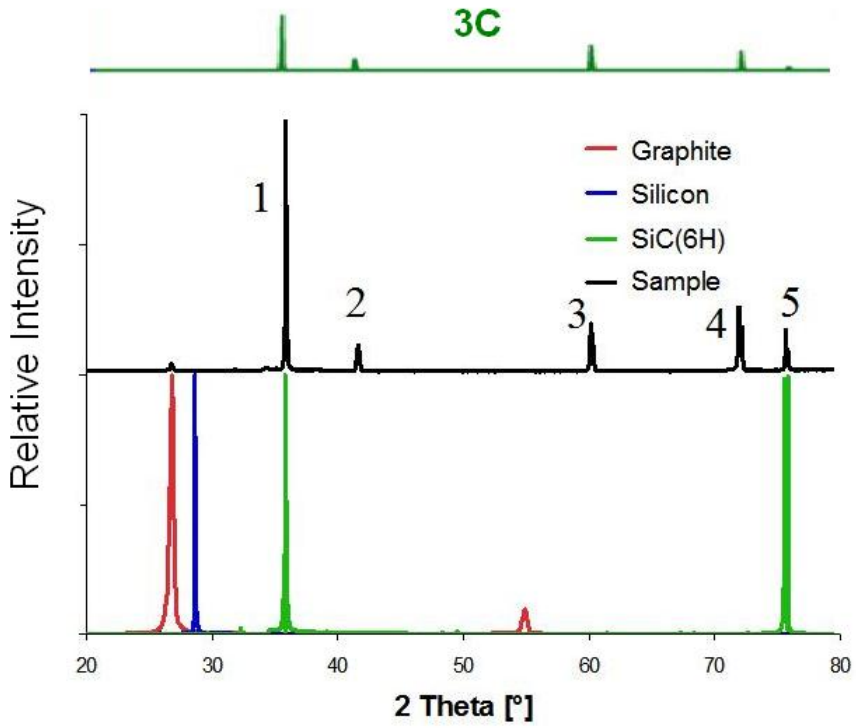

Figure 5.3: *X-ray diffractogram of the grown polycrystalline film on the graphite foil. The X-ray diffractograms of graphite, silicon and 6H-SiC are also plotted. The reflections 1,2,3,4 and 5 of the sample indicate the growth of the cubic SiC polytype. No reflections could be observed at 34.2° or 38.2°, which observes that 6H polytype was not included in the grown film.*

The film was also analyzed by XRD as seen in Figure 5.3. The positions of the Bragg reflections were compared with powder diffraction patterns of of different SiC polytypes. The most important peaks of the sample were assigned the numbers 1,2,3,4 and 5 and compared with the diffraction pattern of the diffractogram discussed by Klimenkov in [47]. The most intense peak 1 at $\theta = 35.6°$ of 6H-SiC (102) is nearly at the same position as the strongest 3C-SiC peak (111), therefore it cannot be used for identification. Thus, the reflections 2,3,4 and 5 that are observed respectively at $\theta = 41.2°$, 61° of 3C<220>, 72° of 3C<311> and 77° are overlapping in both 3C and 6H patterns, but since no reflections could be observed at $\theta = 34.2°$ or 38.2°, which are necessary for the identification of the 6H polytype, it is likely that the grown film is of the 3C-SiC polytype.

5.1.2 Stagnation Flow Geometry

The observation of polycrystalline SiC growth, was followed by finding the vertical level at which SiC intensively and optimally grows. In the previous experiment it was noticed that SiC tends to deposit within a vertical range of 5 to 10 cm length on the graphite stripe. This range starts at a distance of 15 cm below the outlet flange, therefore the substrate was placed at this level (15 cm below the outlet flange). The applied (stagnation flow) geometry was previously introduced in Figure 4.6-c.

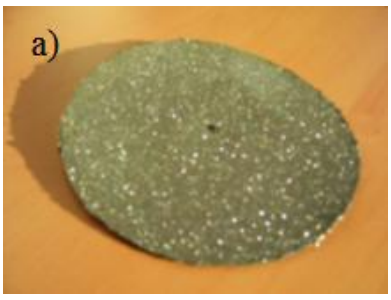

Figure 5.4: *Homogeneous film growth of brilliant, green crystallites of polycrystalline SiC.*

Figure 5.4 shows a substrate made of graphite foil with 10 cm diameter. SiC was deposited on it for 30 minutes at a pressure of 300 mbar and a maximum reactor temperature of 2160°C. Both concentrations of SiH_4 and C_3H_8 were set to both values of 0.484 and 0.121 mol/m^3 at flow rates of 60 sccm, 15 sccm, respectively, while the total flow rate was set to 5 slm with a flow velocity of 0.0063 m/s. The deposition of a green brilliant film of polycrystalline SiC was optically observed on the substrate. The homogeneity of the grown film is an indicative for reasonable growth conditions and precursor concentrations.

5.1.3 Fastening of the Seed-crystal

Fixing the seed in the HTCVD reactor is one of the problems, which had to be overcome in the early phase of this work. The substrates or the seed-crystals were fastened on the seed-holder using the method introduced in section 3.3.3. 6H-SiC wafers are expensive, therefore only small pieces of the wafers were used in the experiments to reduce the experimental cost. As seen by the picture of Figure 5.5, the seed-crystal was fastened to a seed-holder made of graphite foil with a circular shape of 9.5 cm diameter, which was hanged at a distance of 18 cm below the outlet flange. A maximum temperature of 2180°C was recorded on the reactor walls, where a temperature of 1850°C was measured on the seed-holder. Both concentrations of SiH_4 and C_3H_8 were set to 0.573 and 0.229 mol/m^3 at flow rates of 100 sccm, 40 sccm, respectively, while the total flow rate (including the carrier gas) was set to 7 slm leading to a flow velocity of 0.009 m/s at a pressure of 300 mbar.

Here, only the film grown on the non-seeded area is discussed, it was analyzed by means of SEM. A small crystallite of around 6 μm width was magnified by the SEM

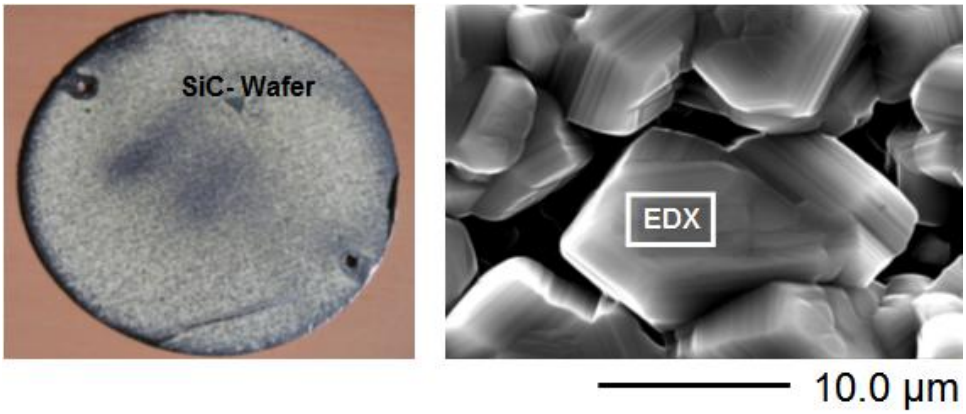

Figure 5.5: *Left, picture shows an SiC seed-crystal, which was fixed on circular graphite foil. Right, SEM image shows the surface morphology of the film grown on the non-seeded area of the seed-holder.*

image seen in Figure.5.5-b. Grooves with parallel traces could be noticed on the irregular surfaces of this crystallite, which indicates an oriented growth of the crystallite epilayers. Both elements Si and C were detected by EDX analysis as seen in the spectrum shown in Figure 5.6. A composition ratio of (C/Si: 56/44) was evaluated on the film, where an error of $\pm$0.1-0.5% can be considered for the values resulted by the EDX evaluations. This ratio differs slightly with the ratio obtained for an unused SiC wafer (C/Si: 48/52), which observes a slightly excessive carbon composition, which seems to be a result of high C_3H_8 concentration.

The picture shown in Figure 5.7 is taken from the seed-holder backside after 30 minutes of deposition, whereon yellow powder was accumulated during this period. This powder was analyzed by XRD as shown in Figure 5.8. It shows that all the reflexes obtained by the powder sample, at $\theta = 41.2°$, 61° of 3C<220>, 72° of 3C<311> and 77°, are coincident with the reflexes of cubic SiC pattern, which proves that this powder if of the 3C-SiC polytype. Thus, comparing the positions of the resulting re-

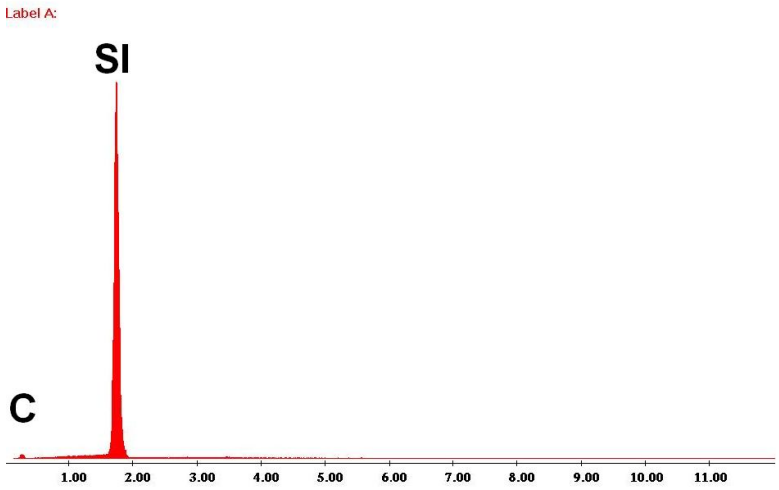

Figure 5.6: *EDX-spectrum observes a film composition of both carbon and silicon elements.*

flections by the sample X-ray diffractogram with the positions of the reflections of the 6H pattern, no further reflections could be observed at $\theta = 34.2°$, $41.2°$ or even at $65°$, which indicates that the 6H polytype was not grown.

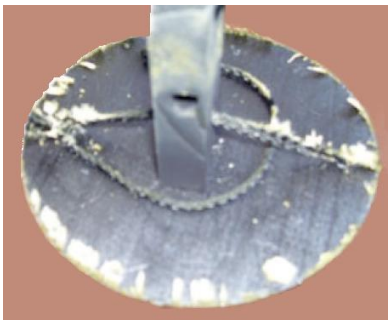

Figure 5.7: *The picture is taken from the substrate holder backside and shows a free, undesired growth of yellow SiC powder, which was accumulated in form of small bars.*

5.2 Seeded Growth of SiC

The results discussed in the previous part of this chapter have discussed the film growth on non-seeded substrates, which resulted in the growth of polycrystalline SiC. For the epitaxial growth of SiC, the use of a seed-crystal is necessary when single crystalline

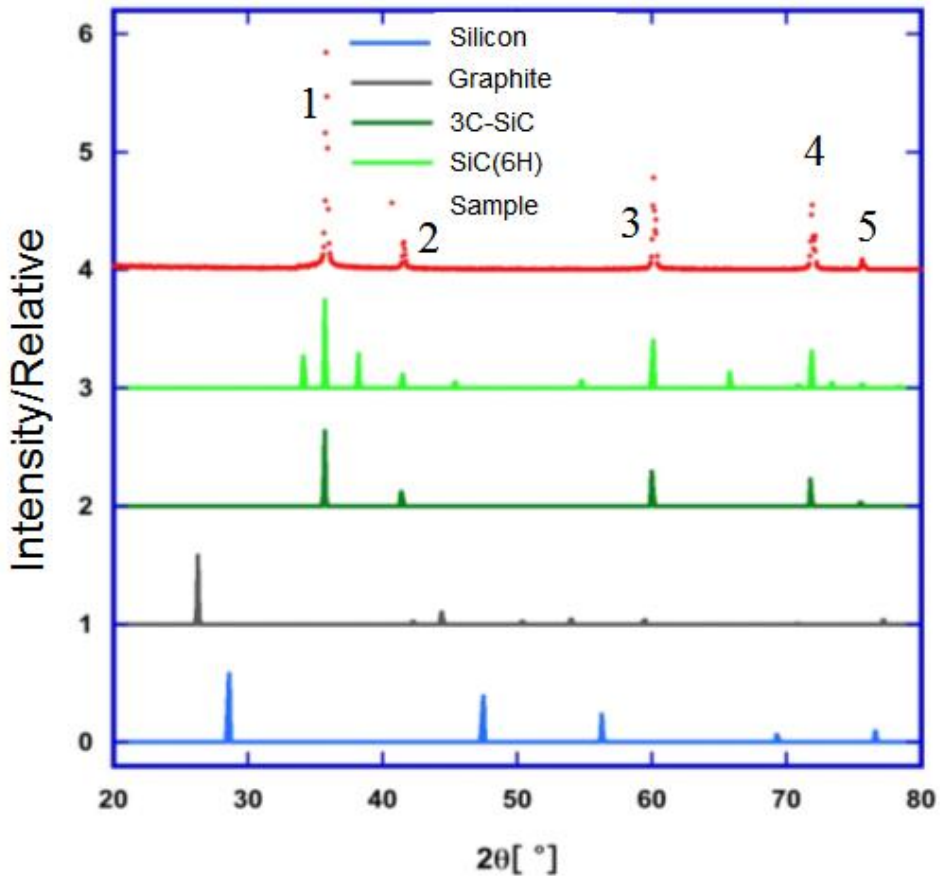

Figure 5.8: *The X-ray diffractogram of the powder sample was compared with the powder diffraction patterns of 3C and 6H-SiC. All the peaks of the sample pattern are coincident with the peaks has cubic 3C-SiC.*

growth is desired using the HTCVD technique. The results of the films grown on seed-crystals with different surface orientations are discussed.

5.2.1 Substrate Surface Treatment

Graphitization of the seed surface in the HTCVD technique is one of the known, severe problems, which is usually generated during the initial stages, especially during heating. Graphitization is caused due to the deposition of the carbon decomposed from the susceptor into the gas-phase, which later deposits on the seed-surface as by the decomposition of the substrate due to incongurrent evaporation. The quality of the epitaxial layer depends not only on the CVD growth conditions, but also on the substrate quality. The surface of commercially available substrates contain a variety of defects that will disturb the growth of the epitaxial layer reducing its quality. Such defects that originate from the substrate can not be eliminated before growth start, but good surface treatment may inhibit further defects that can be caused by carbon transport from the graphite parts to the seed surface. Surface preparation of SiC wafers was frequently carried out using hydrogen [48] or hydrogen/propane [49]. In this work, different flow procedures were applied during heating in order to reduce the transport of the carbon decomposed from the susceptor material to the seed surface. Those procedures were studied upon the SEM and EDX analysis of the surfaces of the heated seeds. In all procedures the substrates were heated for 30 minutes till a temperature of 1900°C was reached. Firstly, the substrate was heated under a pressure of 800 mbar and a helium flow of 6 slm. Secondly, only a treatment in a hydrogen flow of 200 sccm was applied at a pressure of 800 mbar. Finally, the reactor was just pumped out till a pressure less than 10 mbar was reached, thereafter heating was started without any flow. The surface morphology of the three seeds are shown in Figure 5.9. The SEM images of the three

seed surfaces could observe the growth of small deposits with random distribution.

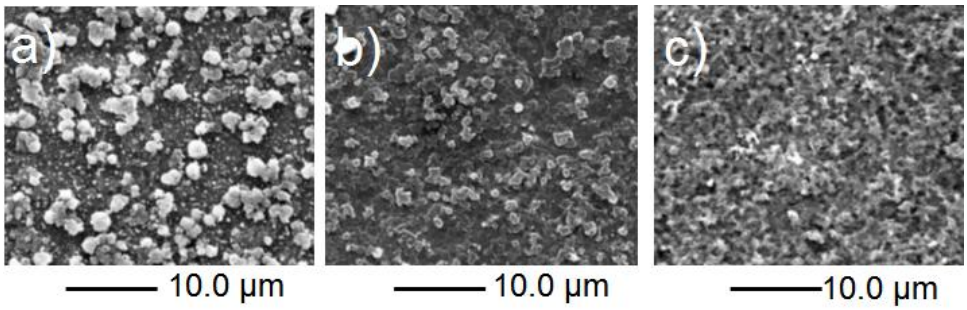

Figure 5.9: *Three SEM images taken for 3 different seed crystals that were heated up to the actual growth temperature in a period 30 minutes. Image a) shows a seed surface morphology after heating in helium atmosphere, which was continuously supplied with 6 slm at 300 mbar. Image b) shows seed surface heated under a hydrogen flow rate of 200 sccm at 300 mbar. Image c) shows the surface morphology of heated seed at low, constant pressure of 10 mbar without any addition of gases.*

The lowest carbon concentration (C/Si ratio) was evaluated on the seed surface heated using the third procedure. A composition ratio of C/Si:72/28 was evaluated for the seed surface using this procedure. The application of both other heating procedures, resulted in a carbon-rich seed surface. A composition ratio of C/Si:80/20 was evaluated for the seed heated due to the first procedure, while a ratio of C/Si:88/12 was evaluated by applying the second procedure. According to this result, it can be concluded that, firstly, heating the reactor at low pressure and zero flow rate reduces the transport of graphite from the susceptor to seed surface. Secondly, the carbon contamination of the surface can not be completely inhibited using any of those flow procedures, which requires further improvement of the flow procedure or applying further etching methods.

5.2.2 Indication of Optimum Growth Temperature

The non-constant temperature distribution recognized by the temperature profile presented in section 3.4.1, indicates a significant relation between the seed-holder position and its corresponding temperature. In other words, it could be resolved that the seed-holder temperature (growth temperature) is a function of distance (H) measured between its position and the outlet flange. Therefore, seeded growth experiments were carried out at different seed-holder positions in order to increase or to decrease the growth temperature. In this section, seeded growth results are discussed for films grown at three different seed-holder positions. Table 5.1 lists three distances of H, their corresponding temperatures and the EDX composition ratios. The concentrations of the SiH_4 and the C_3H_8 were set to 0.667 and 0.200 mol/m^3 at flow rates of 100 sccm and 30 sccm, respectively. The helium flow was set to 6 slm resulting in a flow velocity of 0.0075 m/min at a pressure of 300 mbar. The deposition was carried out for 20 minutes.

Experiment	H (cm)	$T_{substrate}$ (°C)	Composition Ratio (C/Si)
a)	14	1850	47/53
b)	16	1950	47/53
c)	18	2035	-

Table 5.1: *Table listing three different substrate positions and the corresponding temperatures and composition ratios of the film's surfaces.*

The surface morphologies of the resulting films were firstly compared with each other based on optical microscopy, see Figure 5.10. A film of small crystallites was grown

on the seed-crystal of experiment (a). The increased temperature caused by shifting the seed-holder 2 cm towards the hot zone in experiment (b), resulted in the growth of crystallites with hexagonal boundaries on a large area of the substrate. The same surface morphology found on the film obtained in (a), was also recognized inside the boundaries of the hexagonal areas obtained by experiment (b). The hexagonal shapes obtained in (b) denote a relative enhancement of the film morphology towards epitaxy, which is a result of the increased growth temperature. Further increase of the temperature due to lower positioning of the seed-holder, as in experiment (c), resulted in the growth of large crystallites with plain surfaces. The morphology resulted in (a) and (b), where small crystallites were compactly grown, was completely disappeared in the film obtained in (c). Upon those results, it could be concluded that a growth temperature of approximately than 1950°C is required to advance the growth conditions. Indeed, lower positioning of the substrate towards the hot zone results in higher temperature of the seed-holder, which consequentially leads to improving the epitaxial growth conditions.

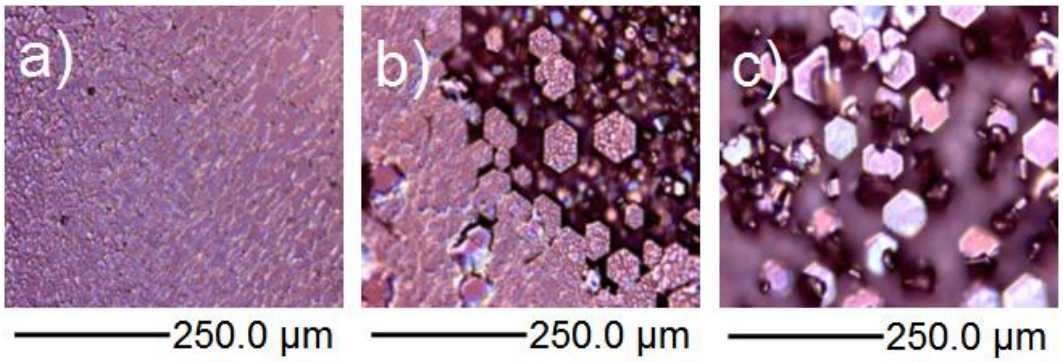

Figure 5.10: *Images taken with optical microscope and show the surface morphology of three films grown at different growth conditions. Those conditions are presented in table 5.1 and explained in the text.*

For further investigation of the surface morphology and the composition of the grown films, SEM and EDX analysis were carried out for both films obtained by experiments (a) and (b). A composition ratio of (C/Si: 47/53) was evaluated for the film obtained in experiment (a), which indicates a reasonable precursor concentrations. The growth of polycrystalline SiC could be observed by analyzing the surface morphology of both SEM images shown in Figure 5.11.

The film obtained in experiment (b) was thus analyzed by means of SEM. A small area of 250 μm width, was magnified to clearly show its morphology details, see Figure 5.11-b1. One hexagonal structure is clearly seen in the SEM image of Figure 5.11-b2, which has a width of 8-9 μm. The appearance of such a new structure within the surface morphology could be considered as an indication for a relative advance of the growth conditions, whatever that the resulting film is optically recognized as a polycrystalline film, as seen by the image of Figure 5.12-b3. This image observes the growth of compact film composed of small SiC crystallites. The EDX analysis evaluated a composition ratio of (C/Si:47/53) for this film, which is approximately equal to the composition ratio evaluated for an unused 6H-SiC seed-crystal of C/Si: 48/52. This result indicates an appropriate gas-phase composition that is established at the applied precursor concentrations. Generally, it could be concluded that increasing the temperature to a value of 1950°C, leads to enhancing the growth conditions that are necessary for achieving an epitaxial growth mechanism.

5.2.3 Improved Flow Geometry

In the previous experiments, it was noticed that large amount of SiH_4 decomposes in the low temperature zone, which leads to particle building that later fall on the glass

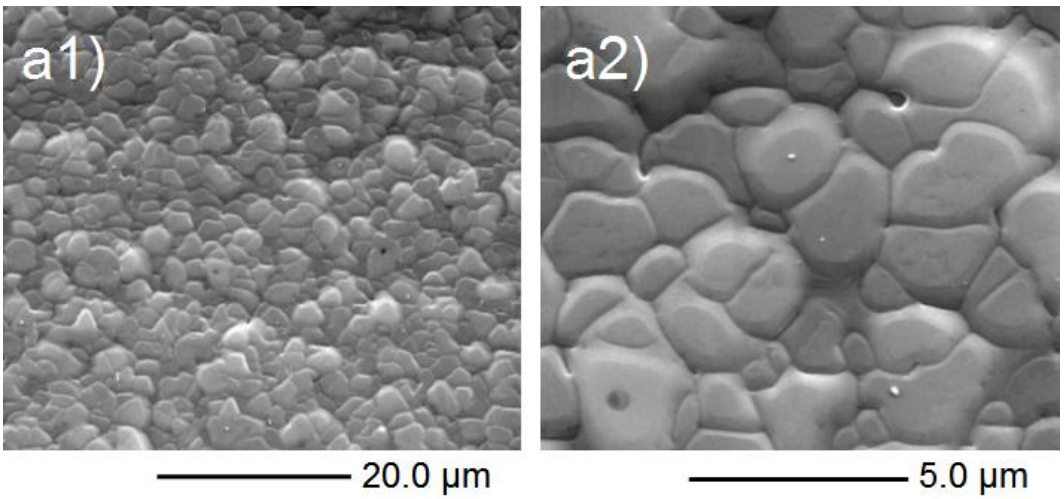

Figure 5.11: *Two SEM images of the film grown in experiment (a). Image (b) is a magnified area of image (a). The film is composed of compactly grown crystallites.*

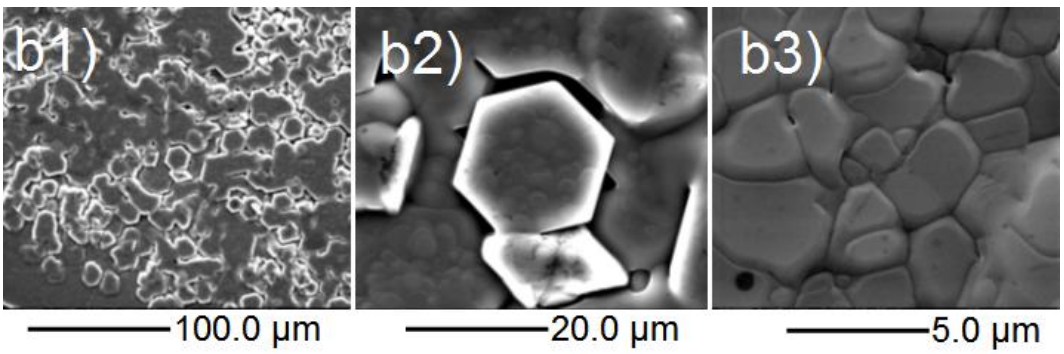

Figure 5.12: *SEM images of the film obtained in experiment (b). Image (a) shows the substrate surface, where hexagonal structures are visible. (b) Magnification of one hexagonal structure. (c) Shows the internal morphology of the hexagonal structure shown in image (b). Compact growth of small, individual crystallites are observed by this image.*

plate of the optical access. The installation of an aperture below the seed-holder, as presented in section 3.4.2, was suggested as an alternative flow geometry that can be used to force the most amount of the flow stream to be stagnated by the seed-holder. The use of the aperture is involved in this section only. An aperture made of graphite foil, which has an inner diameter of 50 mm and an outer diameter, which is equal to the susceptor inner diameter of 130 mm, was installed inside the susceptor at a distance of 28 cm below the outlet flange. The seed-crystal was fixed on a seed-holder made of graphite foil and placed 24 cm below the outlet flange. A temperature of 1800°C was measured on the seed-holder, where the aperture temperature exceeded 2100°C. The concentration of both precursors of SiH_4 and C_3H_8 were set to 0.573 and 0.229 mol/m^3 at flow rates of 100 sccm and 40 sccm, respectively. A total flow rate including the helium carrier gas was set to 7 slm leading to a flow velocity of 0.6 m/min. The deposition was carried out for 20 minutes at a pressure of 300 mbar.

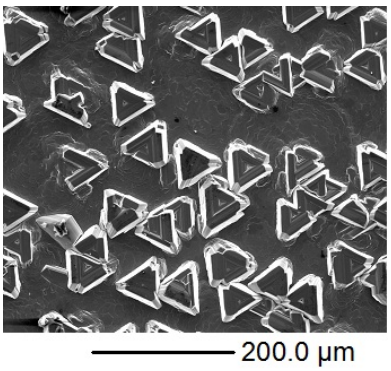

Figure 5.13: *Triangular shaped crystallites were grown on an on-axis seed surface. The edges of the crystallites are shown to be grown towards three certain directions, which reveals the influence of the seed surface orientation on the growth mechanism.*

The surface morphology of the grown film is shown by the SEM image of Figure 5.13. Several crystallites with triangular shape were grown on an on-axis 6H-SiC seed. The crystallite edges were grown into three parallel directions. Such a mor-

phology is of great importance, since it showsthe possibility of growing SiC epilayers by our HTCVD system. The EDX-analysis evaluated a composition ratio of (C/Si: 51/49), which observes a slight excess of carbon concentration comparing it with the composition of C/Si: 48/52, which was evaluated for a non-used 6H-SiC wafer. This indicates a relatively high concentration of the C_3H_8 added to the process.

5.2.4 Seed-holder Improvement

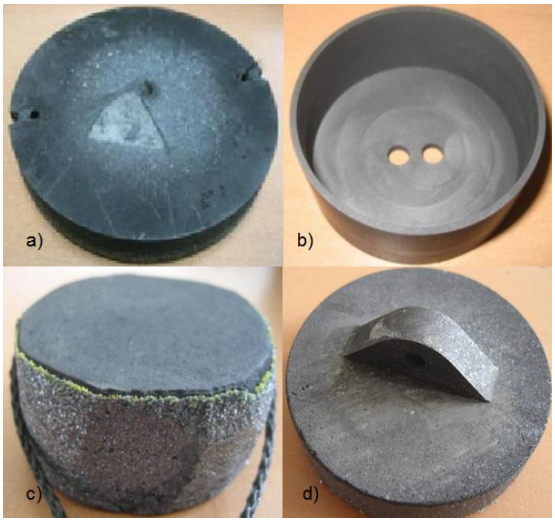

Figure 5.14: *Four different geometries of the seed-holder (SH). a) SH has a diameter of 10 cm, b) Hollow SH with 5 cm diameter and 25 mm hight. The graphite cord is normally tied through both holes shown. c) SH with 5 cm diameter and 25 mm hight. d) Improved version of SH with 5 cm diameter and 12 mm hight. This SH can be hanged via a hole drilled through its ridge.*

Graphite foils did not show a promising performance using it as a material for the seed-holder, since the seed-crystals were strongly bonded to the holder surface or damaged at their adhered side, which usually resulted in some mass reduction of the seed-crystal. Hard, dense graphite was used instead of graphite foil in order to solve this problem.

Four geometries to the seed-holder design were studied and gradually improved upon the growth results. The four seed-holder types a,b,c and d are shown in Figure 5.14.

Firstly, applying seed-holder a), which has a relatively large diameter of 10 cm led to hardly bonded seed and holder, which consequentially caused the damage of the seed-crystal while detaching it. Additionally, only the central area of the seed-holder was coated, meanwhile the outer area near the perimeter remained free of deposition. This problem was later eliminated by the use of smaller seed-holders with a diameter of 50 mm, which indicates that the seed-holder size seems to have a significant effect on the diffusion layer near the substrate surface. However, in order to solve the bonding problem, the seed-holder geometry was improved in such a way, where the contact area between the seed and the holder is minimized. Accordingly, the seed-holder b) was made in beaker shape, as seen in Figure 5.14-b. In this case, a complete wafer with a diameter of 50 mm must be adhered on its cylindrical walls, which have a thickness of 2 mm. Such a type of seed-holder was applied in one experiment, where a 2-inch diameter SiC wafer with on-oriented surface was deposited for 2 hours. The seed-holder was hanged by means of a graphite cord 18 cm below the outlet flange and heated till a growth temperature of 1900°C was reached. The precursor concentrations of SiH_4 and C_3H_8 were set to 0.5736 and 0.172 mol/m^3 at a flow rates of 100 sccm and 30 sccm, respectively. The total flow including the carrier flow rate was set to 7 slm leading to a flow velocity of 0.0088 m/s.

A rough, green film was found in the middle area of the substrate shown in Figure 5.15, while a smooth, tapered area was noticed near the perimeter, which observes the decomposition of the seed material in this region. However, the growth of a polycrystalline film could be observed by means of the SEM image shown in Figure 5.16-a.

Figure 5.15: *2-inch wafer fastened on the hollow seed-holder. The circumferential area looks flat, while a rough growth morphology could be noticed in the middle of the wafer after deposition.*

The grown crystallites are shown to be oriented towards three certain directions, which resembles a remarkable influence of the surface orientation of the seed polytype (6H, on-axis) on the growth mechanism. The seed-crystal was broken into relatively large pieces while detaching it from the substrate holder. The cross section area of one of the broken pieces is shown in the SEM image seen in Figure 5.16-b. A trace distinguishing the film from the original seed-surface was recognized on this image, which was used for measuring the film thickness. By measuring the distance between this trace and the film surface, a relatively thick film of 40 μm could be observed corresponding to a growth rate of 20 μm/h. Although this seed-holder type simplified the detachment of the seed-crystal in order to measure the film thickness for the growth rate determination, the damage of the substrate on its backside could not be inhibited as observed on the SEM image shown in Figure 5.16-b.

A further disadvantage of the hollow seed-holder type was noticed during the temperature measurement, since the pyrometer has recorded instable values for the temperature during heating. This problem could be suppressed using another seed-holder of type (c), which has a simple shape of a can, diameter of 50 mm and a thickness of 25 mm. This type of seed-holder was further optimized to the type (d), which is approximately 50% lighter than the (c) type providing an attractive weight that enables its connection

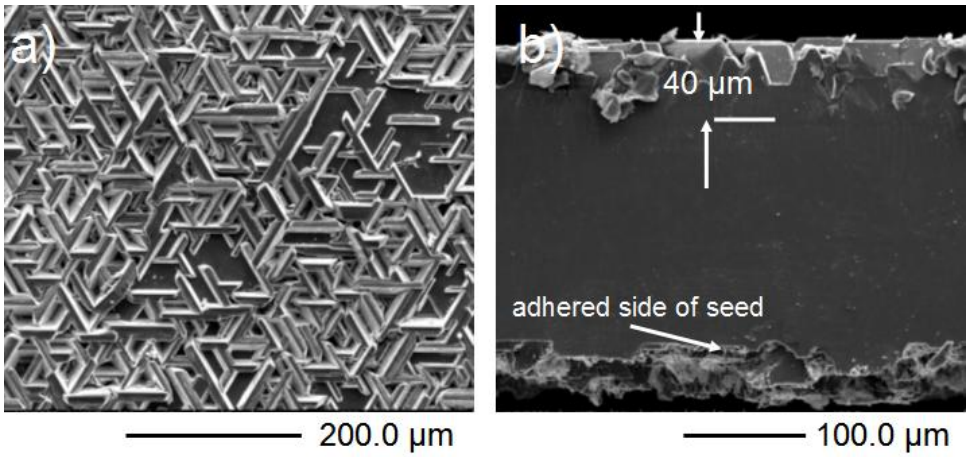

Figure 5.16: *a) SEM image taken of a small portion of the middle area of the seed surface, where the growth of small longitudinal crystallites in three growth directions is visible. b) SEM image showing the side view of the cross section area of the deposited seed-crystal. A film thickness of 40 µm could be observed on this image. The adhered side of the wafer looks damaged.*

with the magnetic suspension balance, which has a maximum measuring capacity of 80 g.

5.2.5 Improvement of Growth Conditions for Epitaxy

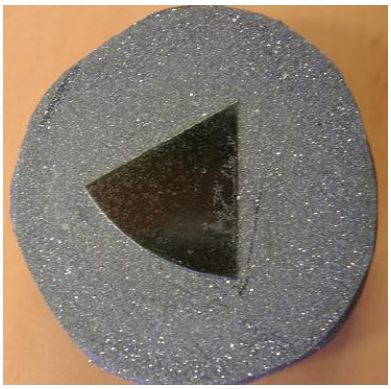

Figure 5.17: *On-Axis SiC substrate fixed on a graphite seed-holder of 50 mm diameter. A plain, transparent surface morphology is visible. Growth defects can be recognized within a small area on the right of the seed surface.*

The results introduced in section 4.2.2 have shown a significant enhancement of the

film quality due to shifting the seed-holder position towards the hot zone and consequentially increasing its temperature. This result resolves the importance of the growth temperatures applied in relation with the vertical position of the seed-holder. Accordingly, the seed-crystal was fastened on a graphite seed holder, as seen in Figure 5.17, and hanged at a distance of 30 cm below the outlet flange. The seed-crystal has a triangular surface and is a part of an on-axis 6H-SiC wafer. A temperature of 1995°C was measured on the seed-holder at this position. A maximum temperature of 2050°C was recorded at a point, which is 35 cm below the outlet flange. The SiH_4 concentration was set to 0.996 mol/m^3 at a flow rate of 150 sccm, while the concentration of C_3H_8´was set to a relatively low concentration of 0.066 mol/m^3 at a flow rate of 10 sccm, because a very low ratio of (C_3H_8/SiH_4:1/8) was established by O.Kordina [22], who recommended to start with such low concentrations of C_3H_8. The carrier gas flow rate was set to 6 slm providing a total flow velocity of 0.0075 m/s. The epitaxial growth of SiC by HTCVD was achieved by Elisson in [32] at high growth rates of 1 mm/h at an established pressure, which is close to atmospheric pressure. Therefore, the pressure was also set to a value of 800 mbar, which is relatively lower than the atmospheric pressure in order to avoid sudden pressure increase above the atmospheric pressure, which might lead to the explosion of the quartz tube. The deposition was then carried out for two hours.

By the optical inspection of the seed-crystal, the appearance of the unused seed-crystal remained partially unchanged. The seed surface has kept its original green color and transparency. However, on the right side of the seed surface, a small portion with rough morphology was recognized the image a1 shown in Figure 5.18. An area of 1 mm^2 is magnified by the SEM image shown in Figure 5.18-a1. Growth defects

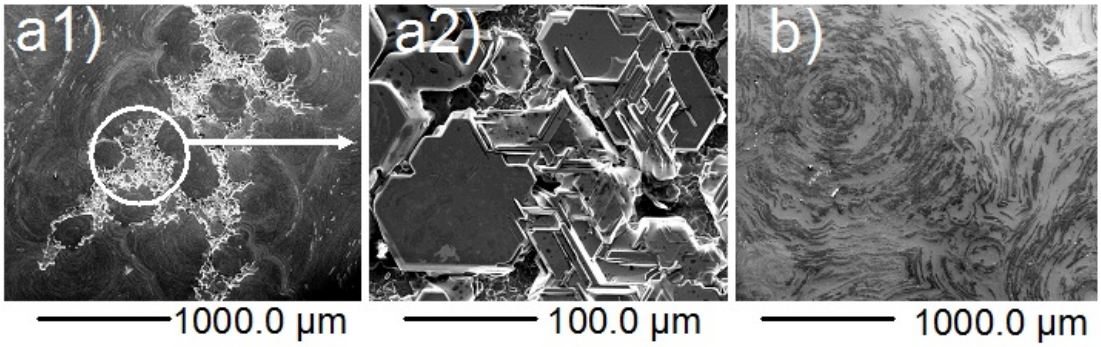

Figure 5.18: *SEM images of two films grown at different propane concentrations. Image (a1) shows growth defects grown in an area of 1 mm. The defects are magnified in image (a2), which observes an oriented defect growth. Image b) shows a plain surface morphology of film deposited at higher propane concentration.*

are visible on a large area of the film, which seems to be caused due to improper precursor concentrations. An oriented defect growth could be observed by further magnification of the surface morphology, as seen by the image a2 of Figure 5.18, where the edges of the defect areas are seen to be orientated towards three certain directions. Such an oriented morphology of the grown defects reflects the effect of the original seed polytype on the grown film structure, which indicates that the process is pushed towards epitaxy. In fact, different reasons can be responsible for such a growth defect. Seed surface contamination with carbon during heating, unsymmetrical temperature gradients on the seed crystal or even the low concentration of C_3H_8 are suspected to be the reason that is responsible for obtaining such a result. Therefore, the surface morphology and the growth rate was further investigated by SEM and EDX at higher concentrations of C_3H_8.

The C_3H_8 concentration was increased to a value of 0.099 mol/m^3 (15 sccm), which resulted in a remarkable improvement of the surface morphology as seen on the SEM

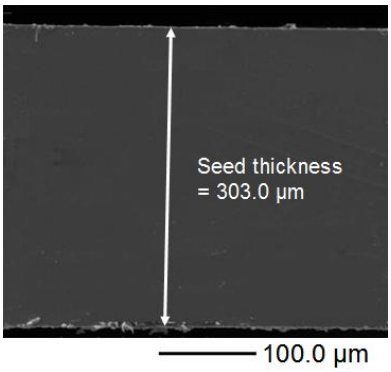

Figure 5.19: *SEM image of a vertical cut in the substrate. The total substrate thickness after deposition is 303μm, which corresponds to a growth rate of 26$\mu m/h$.*

image shown in Figure 5.18-b. This shows a defect free, plain surface morphology. The growth rate was initially evaluated by subtracting the seed weights after and before the growth experiment, which was thus validated by means of the optical microscopy or SEM analysis. A growth rate of 17 μm/h (see table 5.2) was achieved in the first experiment, where low concentration of C_3H_8 (0.066 mol/m^3) was used, while in the second experiment, a growth rate of 24 μm/h resulted by increasing the C_3H_8 concentration to 0.099 mol/m^3. The latter growth rate was evaluated by the weight subtraction, while a total seed thickness of 303 μm could be measured using the SEM image of Figure 5.19, which makes a growth rate of 26.5 μm/h. A deviation of 7% was calculated for both evaluated growth rate values in the second experiment. Indeed, increasing the C_3H_8 concentration in the second experiment enhanced the growth rate by 56%. Thus, the growth defects observed at very low C_3H_8 concentration of 0.066 mol/m^3, disappeared of the film obtained by the second experiment (see Figure 5.18-b), where the concentration of C_3H_8 was slightly increased by 50% to 0.099 mol/m^3.

The crystallography of the film grown by the second experiment was further analyzed by means of Low Energy Electron Diffraction (LEED) at the Institute of Experimental Physics. Figure 5.20 shows two known patterns of hexagonal SiC with (3×3) and (2×2) reconstructions. Despite of the unclear or bad appearance of atom spots, which

is mostly caused due to non-planer film surface, both patterns are observed for both 3C and 6H polytypes of crystalline SiC as reported in [50] and [51]. This result resolves the success of the epitaxial growth of crystalline SiC.

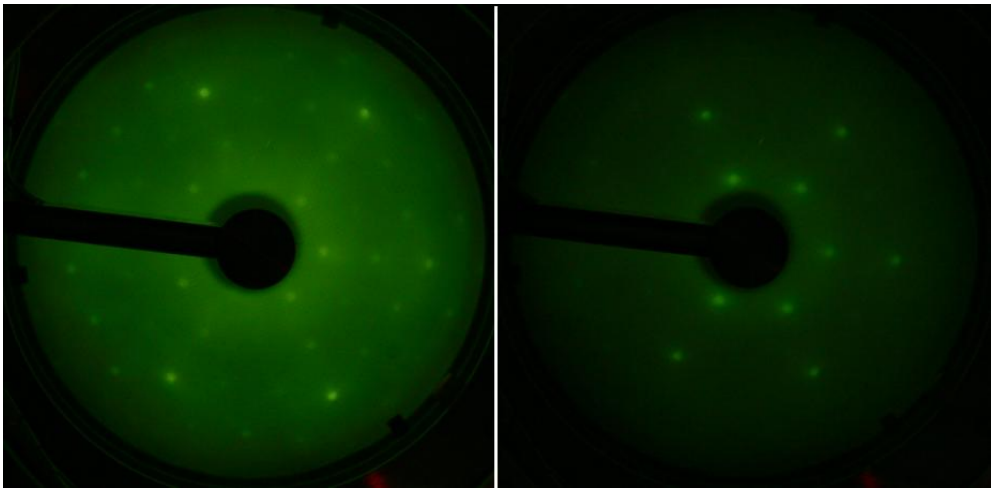

Figure 5.20: *Left: LEED pattern of (3×3)obtained at 564 eV. Right: LEED pattern of (2×2) obtained at 364 eV.*

The film prepared by the second experiment was further analyzed by means of XRD, see Figure 5.21. The substrate sides were covered by an aluminum foil to exclude the diffraction of the entire layers of the original substrate depth within the resulting film. Since these layers might belong to the original layers of the seed-crystal and not to the grown layers. The reflections of the aluminum were observed at $\theta = 38°$, $45°$ and $65°$. The X-ray diffractogram obtained for the film surface has shown that sharp peaks were resulted at the reflection angles $37°$ and $76°$ with high intensities. Comparing this result with the diffractogram obtained by the XRD analysis of an unused on-axis 6H-SiC seed-crystal, it can be found that all its reflections are also obtained by the film pattern. Only the reflex observed at $\theta = 42°$, indicates the growth of 3C polytype. Although

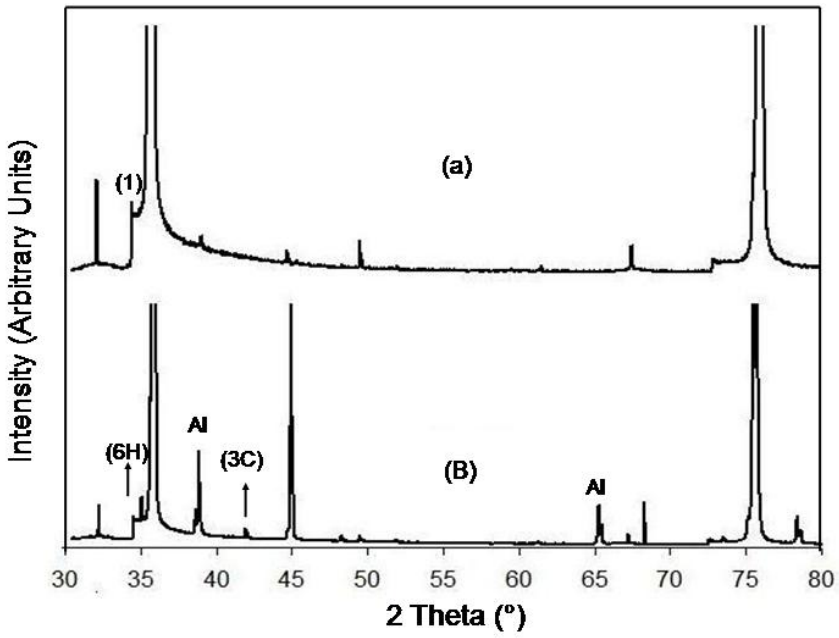

Figure 5.21: *Two X-ray diffractograms of (a): unused 6H-SiC seed-crystal with on-axis surface, and (b) Deposited seed-crystal on on-axis seed surface. The seed edge was covered at its side with Al (its reflection at 38°). Further reflection at 42.2° identifies the growth of 3C-SiC. The reflection observed at 34.2° indicates the growth of 6H polytype.*

this reflex is supposed to be observed by both polytypes 3C and 6H as reported in [47], it is here more expected to stand for a 3C reflection, since such a reflection was not observed in the X-ray diffractogram of the original 6H-SiC seed-crystal. This result meets the known theory of the heteroepitaxial growth of 3C polytype on on-oriented surfaces of SiC.

Sample	C_3H_8 (mol/m^3)	Growth Rate (μm/h)	Composition Ratio (C/Si)
Unused seed	-	-	48/52
a	0.066	17	48/52
b	0.099	28	46/54
c	0.132	31	53/47
d	0.165	29	51/49
e	0.198	27	49/51
f	0.231	-	60/40

Table 5.2: *The table lists the growth rates and the corresponding composition ratios of films resulted in six experiments at different propane concentrations.*

5.2.5.1 Effect of Propane Concentration on Growth Rate

A series of three complimentary experiments to both previous ones, were carried out for investigating the effect of further increase of the C_3H_8 concentration on the growth rate as well as on the film composition. The C_3H_8 concentration was increased in steps from 0.066 to 0.099, 0.132, 0.165, 0.198 and 0.231 mol/m^3. The SiH_4 concentration was kept constant at a value of 0.996 mol/m^3 at a flow rate of 150 sccm. The growth temperature and the pressure were kept at similar conditions to those that were established in the first two experiments (T = 1955°C, P = 800 mbar). The depositions were

carried out for 2 hours.

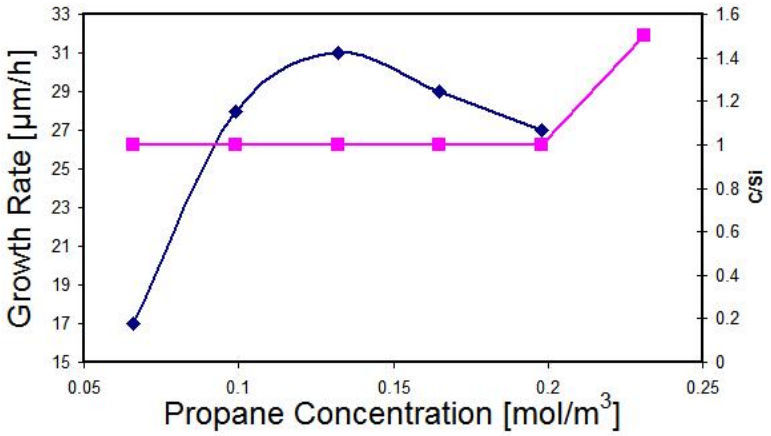

Figure 5.22: *Diagram shows the effect of propane concentration on growth rate (Blue) and film composition C/Si (Pink). The optimum growth rate was reached at a propane concentration of 0.132 mol/m^3. High propane concentration that exceeding a certain limit, result in high (C/Si) ratio, which hence, lead to lower growth rates.*

The growth rates of the films could be evaluated by means of SEM analysis, where the composition ratios (C/Si) of the films were evaluated by EDX. The resulting growth rates and the corresponding composition ratios are presented in table 5.2. The effect of the C_3H_8 concentration on both, the growth rate and the film composition ratios (C/Si) are shown in Figure 5.22. The gradual increase of C_3H_8 concentration to 0.132 mol/m^3, enhanced the growth rate to 31 μm/h, while further increase of C_3H_8 concentration to 0.165 mol/m^3 and 0.198 mol/m^3, resulted in slower growth rates of 29 μm/h and 27 μm/h, respectively. Further increase of C_3H_8 concentration to 0.231 mol/m^3 led to bad growth conditions, which resulted in the growth of polycrystalline film. In the SEM image shown in Figure 5.23, the growth of relatively large, individual crystallites with hexaonal surfaces could be observed.

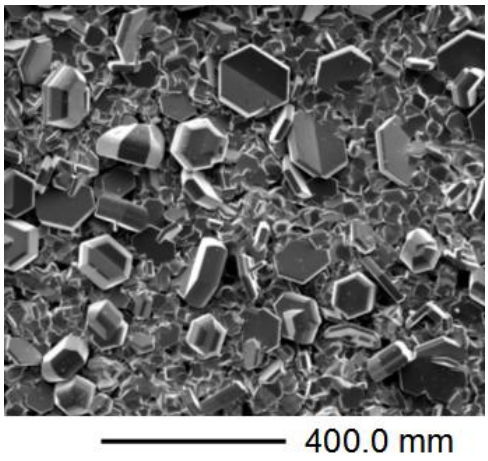

Figure 5.23: *SEM image shows the growth of polycrystalline film as a result of excessive carbon concentration caused due to increased doses of propane.*

A composition ratio of approximately C/Si:50%/50% was obtained for all the films grown at C_3H_8 concentrations, which are $\leq$ 0.198 mol/m^3, while increasing its concentration to 0.231 mol/m^3, resulted in a higher percentage of C atoms inducing a ratio of (C/Si:60%/40%). According to this, it can be concluded that the addition of high C_3H_8 concentration is shown to have a negative effect on the growth conditions, which limits the growth rate and leads to low Si-content. However, very low flow rates of C_3H_8 are required for achieving epitaxial growth conditions and high growth rates of SiC. This is commitment with the results of Sumakeris in [22], where low flow rate ratio of approximately 1/8:C_3H_8/SiH_4 was applied.

5.2.6 Growth Morphology on On/Off-oriented Surfaces

As introduced in section 2.3.3, in order to grow SiC with 4H or 6H polytypes, which have better properties than 3C, the growth of SiC must be carried out on off-oriented seed surfaces. This process proceeds due to the step flow nucleation mechanism leading to the homoepitaxial growth of the same seed polytype. Accordingly, the growth of SiC was investigated on 6H-SiC seed-crystals with three different surface orientations (on-axis, 3.5° off-axis and 8° off-axis). Three seed-crystals with those surface orientations and the dimensions of 6×6×0.25 mm, were simultaneously fastened on one

seed-holder and hanged 30 cm below the outlet flange. The deposition was carried out for two hours at a growth temperature of 1955°C. The precursor flow was established at C_3H_8 and SiH_4 concentrations of 0.132 mol/m^3 and 0.995 mol/m^3 at flow rates of 20 sccm and 150 sccm, respectively.

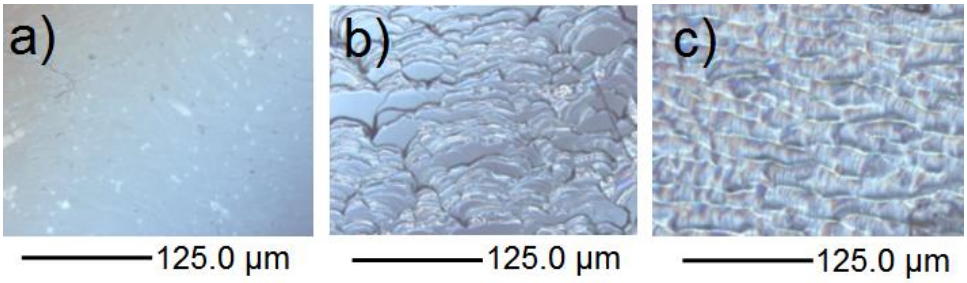

Figure 5.24: *Optical microscopic images for SiC growth on three different seed orientations of: (a) on-axis substrate, (b) 3.5°-off-axis, (c) 8°-off-axis. On (b) and c) substrates, large terraces or wavy surface morphology are visible, which reveals homo-epitaxial growth of SiC through step-flow nucleation mechanism, while on (a), plain surface morphology is visible, which resolves hetero-epitaxial growth of SiC through two dimensional nucleation mechanism.*

The surface morphology was investigated by means of optical microscopy as seen in Figure 5.24, which shows the different surface morphologies of the films grown on all seed-crystals. Image a) was taken for the film grown on the on-oriented seed surface, where a plain surface with a flat morphology could be observed on this image. In this case, the film growth mechanism is supposed to proceed due to *two dimensional nucleation*, which, as previously introduced, leads to heteroepitaxial growth of 3C SiC. Image b) shows the surface morphology of the film grown on 3.5° off-axis surface, which observes the growth of flat terraces ending with sharp steps. Image c) observes the growth of a wavy surface morphology. The growth on both off-axis surfaces is

controlled by *step-flow nucleation* epitaxy. The image shown in Figure 5.25, which was taken from a vertical cut in the 3.5° off-axis substrate, observes the crystal growth of 62 μm, resulting in a growth rate of 31 μm/h. The boundary between the film and the original seed surface is marked by a thin line as seen in this image, which seems to be due to surface contamination with carbon during heating, since, as previously mentioned, at high temperatures the susceptor material decomposes to carbon, which could be later transported by the flow and coats the seed surface. The portions contaminated of the seed surface causes the growth of small pipes along the film depth.

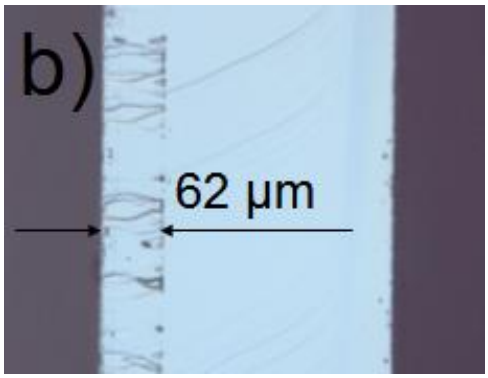

Figure 5.25: *Optical microscopic image of the seed side view of the film deposited on 3.5° off-axis seed. The film thickness could be evaluated by this image to result in a value of 62 μm. The boundary between the grown film and the original seed surface is visible in this image, which resolves a seed surface contamination with carbon.*

XRD analysis was carried out for all films shown in Figure 5.24. Their resulting diffractograms are shown in Figure 5.26. Aluminum foil was used to cover the substrate side during XRD analysis in order to only analyze the film surface without the original seed surface. The resulting X-ray diffractograms of both films grown on the on-axis and 8° off-axis seeds are shown to have large similarity, except that the diffractogram of the film grown on the on-axis seed included an additional reflex at $\theta = 42°$,

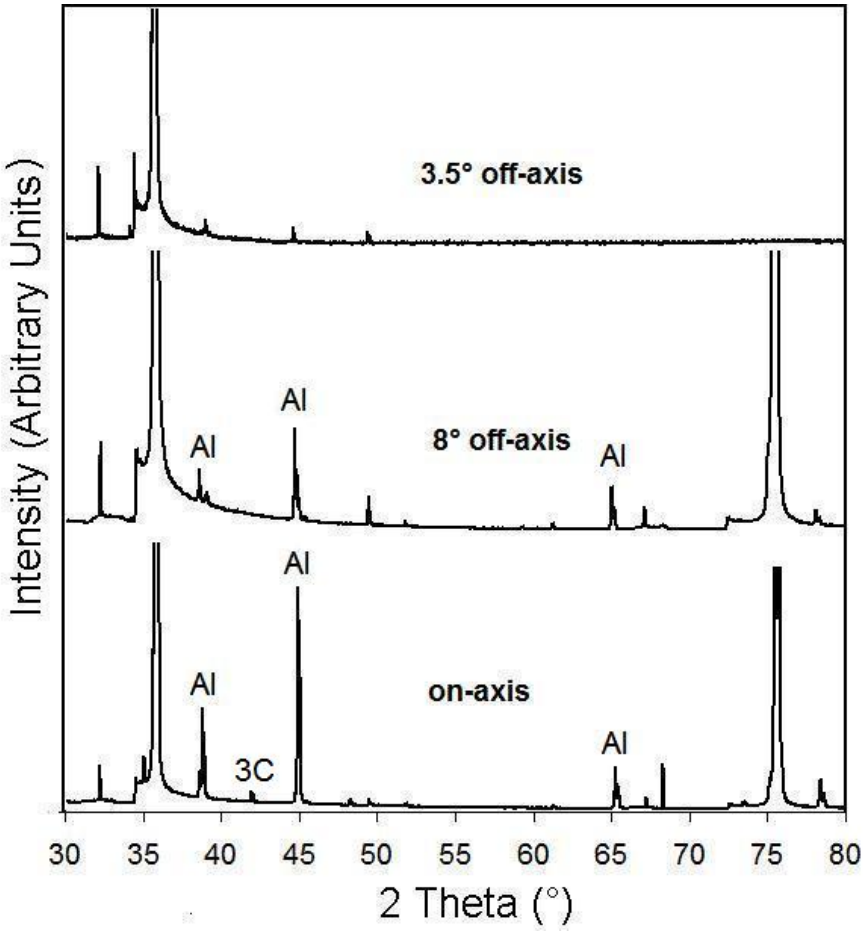

Figure 5.26: *Three X-ray diffractograms of the films deposited on 6H-SiC seeds with different surface orientations. On-axis: reflection observed at 42.2° observes the growth of 3C polytype. This reflection was not observed in both other patterns (3.5° and 8° off-axis), which resolve that on off-axis seeds, only 6H was grown. The reflection observed at 76° on both on-axis and the 8° off-axis seeds could not be observed on the 3.5° off-axis seed.*

which indicates the growth of polytypic structure of 3C-SiC. Due to the small size of the analyzed 3.5° off-axis seed and covering its side with the aluminum foil led to improper scanning of its diffractogram, therefore, the XRD analysis was carried out for this substrate without covering its side. The resulting diffractogram of the film grown on the 3.5° off-axis seed included no reflections at $\theta > 50°$. But the reflections obtained at θ = 34.2°, 35.6°, 38° and 45° were also obtained by the diffractogram obtained for an original 6H-SiC seed as presented in section 4.2.5. Furthermore, no reflection was found at θ = 42°, which normally stand for observing the growth of 3C polytype. According to this result, it could be concluded that the deposition on the 3.5° off-axis seed resulted in the homoepitaxial growth of 6H-SiC, while on on-axis surfaces the growth of 3C-SiC will result.

5.2.7 Effect of Silane Concentration on Growth Rate.

A maximum growth rate of 31 μm/h was observed by the results presented in section 4.2.4. This growth rate was achieved at SiH_4 and C_3H_8 concentrations of 0.994 mol/m^3 and 0.132 mol/m^3 at flow rates of 150 sccm and 20 sccm, respectively. Since further increase of the growth rate was required, the SiH_4 concentration was increased by adding 50 sccm in steps to its flow rate. Although the concentration of SiH_4 was increased, the growth rate remained limited to a value of 31 μm/h at a growth temperature of 1995°C. Increasing the SiH_4 concentration to a value of 2.240 mol/m^3 at a flow rate of 350 sccm, resulted in Si-rich film as observed by the EDX analysis.

The surface morphology of the film obtained at the highest SiH_4 concentration of 2.240 mol/m^3 is shown by by the image a of Figure 5.27, which observes the growth of white Si-rich droplets with circular shapes. EDX analysis was done on on the white

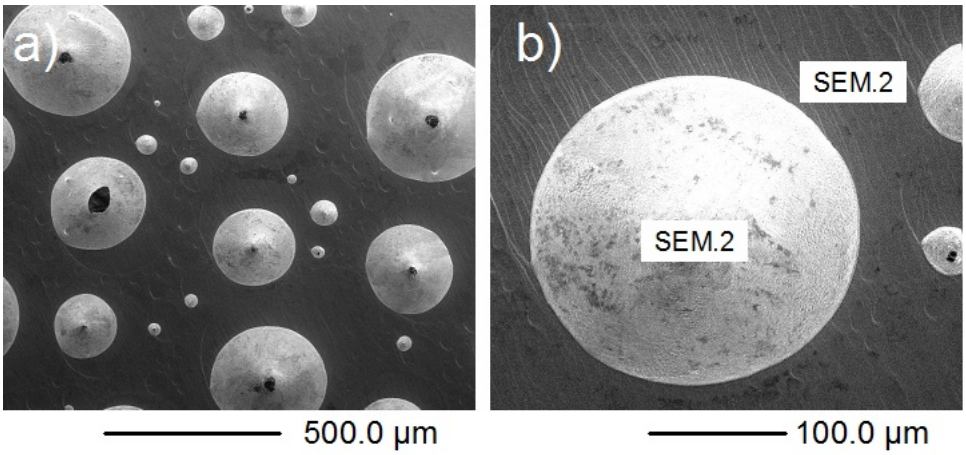

Figure 5.27: *(a): In this SEM image, the growth of white deposits on the film surface is observed. (b): SEM image shows the location of EDX analysis, which observed that droplets rich with Si are grown as a result of high silane concentration or low growth temperatures.*

droplets and on the area around it. A composition ratio of (C/Si:18/82%) was found for the white deposits (EDX-1), which reveals about excessive concentration of SiH_4, while on the rest of the film, a resonable composition ratio of (C/Si:52/48%) with low percentage of Si was evaluated by (EDX-2). According to this result, it could be considered that increasing the SiH_4 concentration at this growth temperature (1955°C) will not result in higher growth rate, which leads to the conclusion that the growth process is limited by the surface kinetics at such a growth temperature. Further increase of the growth temperature seems to be necessary for increasing the surface nucleation and consequentially consume a larger amount of the Si clusters formed in the gas-phase.

5.2.8 Dependence of Growth Rate on Temperature

Temperature is one of the most important parameters, which plays a dominant role in HTCVD of SiC. Increasing the reactor temperature results usually in a higher seed-

holder temperature (growth temperature). In HTCVD, the growth temperature plays an important role of increasing the growth rate. Thus, as introduced in the second chapter, the surface orientation and the polytype of the seed-crystal are decisive factors of defining the grown polytype. For example, at a high growth temperature of approximately 2000°C, some polytypes like, 3C-SiC or 2H-SiC are not stable and tend therefore to transform to the 6H polytype, while 4H and 6H can be grown on off-oriented surfaces showing high stability at temperatures exceeding 2000°C. This result was discussed in [52]. In this section, the influence of higher growth temperatures than 1955°C on the growth rate and the film quality will be investigated.

A series of three experiments were carried out at different growth temperatures of 1985°C, 2030°C and 2060°C. In the first experiment (at 1985°C), three seeds with three different orientations (on-axis, 3.5°-off-axis and 8°-off-axis) were simultaneously fastened on the seed-holder and deposited. In both other experiments, the growth was carried out on a 3.5°-off-axis seed. The carrier gas flow rate was kept constant at 6 slm, while the concentrations of SiH_4 and C_3H_8 were set to 2.240 mol/m^3 and 0.256 mol/m^3 at flow rates of 350 sccm and 40 sccm, respectively. The seed-holder was placed at the usual position, which is 30 cm below the outlet flange (5 cm above the ultimate temperature point). The pressure was kept constant at 800 mbar. The depositions were carried out for one hour in each experiment.

In the first experiment, where a growth temperature of 1985°C was set to the seed-holder, a maximum growth rate of 45 μm/h was obtained on the 3.5° off-axis seed, while the minimal growth rate was obtained on on-axis seed, which is expected to be caused due to the growth of the thermally instable 3C-SiC that usually results when seeds such a surface orientation are applied at this growth temperature range. The

growth rate obtained on 8° off-axis is also less than the one obtained on the 3.5° off-axis seed. According to this result, it could be concluded that the application of seeds with 3.5° off-oriented surface has led to achieving the fastest growth rates at growth temperatures above 1995°C. Therefore, the usage of both other surface orientations (on-axis and 8° off-axis) in further experiments at higher temperatures is not useful.

Tsubstrate °C	On-Axis m/h	3.5° Off-Axis	8° Off-Axis
1955	31	31	31
1985	24	45	39
2030		74	
2060		100	

Table 5.3: *The values of the growth rates evaluated for three films grown on different seed orientations are listed in this table in correspondence with their growth temperature.*

Further increase of the temperature to 2030°C resulted in a growth rate enhancement to a value of 74 μm/h, while a maximum growth rate of 100 μm/h was achieved at a growth temperature of 2060°C, which could be evaluated from the SEM image shown in Figure 5.28-b. The image shows the side view of a through cut in the deposited seed-crystal. In Figure 5.28-a, an inhomogeneous surface morphology is visible on the substrate surface. The usual surface morphology involving terraces and steps appears on around 60% of this image, while plain portions are visible on random areas of the film. These areas are mostly expected to be amorphous, which seems to be caused due to excessive concentrations of the gas-phase hydrocarbons or graphitized seed surface. EDX analysis observed a composition ratio of (C/Si:62/38) and (C/Si:76/24) on both seeds deposited at 2030°C and 2060°C, respectively. According to this, it could be con-

cluded that the growth temperature is strongly related with the carbon percentage of the films. Increasing the temperature of the susceptor might lead to carbon decomposition of its material, which leads to exceeding its concentration beyond the nucleation ratio and consequentially results in unreasonable growth conditions. This problem can be propably solved by reducing the concentration of C_3H_8.

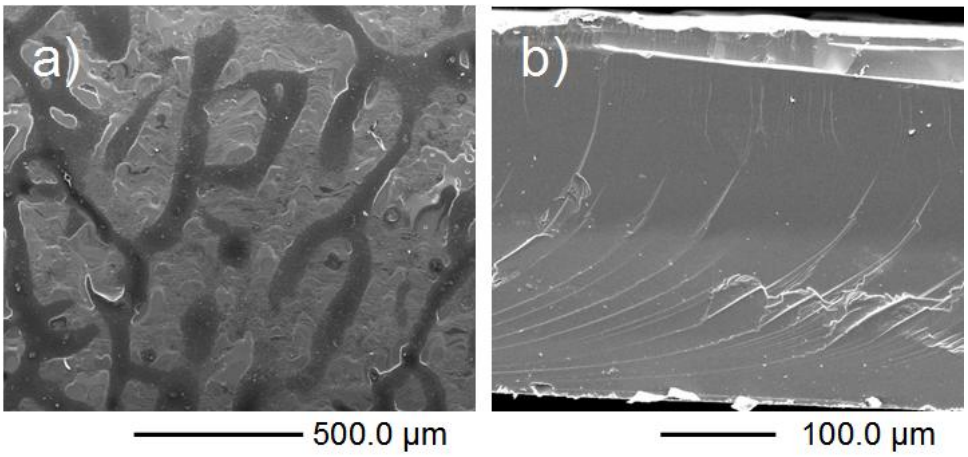

Figure 5.28: *(a): SEM image shows the surface morphology of the film after one hour deposition at a temperature of 2060°C. (b): SEM image of the seed side view. A total crystal thickness of 350 μm was measured on this image.*

In order to evaluate the total activation energy of the HTCVD process, an Arrhenius diagram, as seen in Figure 5.29, was plotted with the results listed in Table 5.3. The growth results obtained by Elisson in [34], are also included in the same diagram in order to compare it with the present results. The green and the pink curves stand for the results obtained by Elisson, whereby an activation energy of 500 kJ/mol was evaluated. Meanwhile, an activation energy of 600 kJ/mol was evaluated for the present study, which showed a deviation of $\approx 20\%$ comparing it with the value obtained by Ellison. Such a deviation seems to be caused due to geometrical or setup differences

between both HTCVD systems. Thus, high growth rates up to 150 μm/h were achieved by Elisson at growth temperatures above 2150°C as shown in the diagram, while the maximum growth temperature achieved with our system is 2060°C. According to both results, it could be concluded that further increase of the growth temperature to a range of 2060-2250°C is necessary for achieving higher growth rates. Thus, the resulting growth rates of the present study must not be limited by surface kinetics, but may be due to low formation rate of the major species that require temperatures beyond 2050°C or by the sublimation rate of the gas-phase nucleated particles.

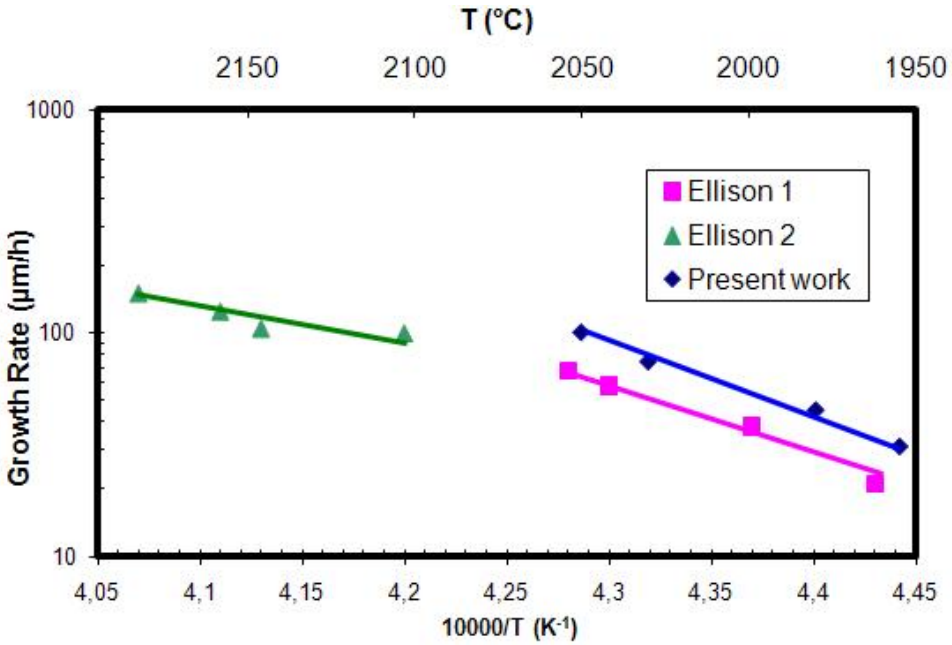

Figure 5.29: *Arrhenius plot shows the growth results obtained at different growth temperatures and compared with the results obtained at the University of Linköping at a close temperature range as discussed in [34].*

5.2.9 Deposition of Thick SiC Film

In this experiment, the deposition was carried out on off-oriented seed with a tilt angle of 3.5° for a period of 3 hours in order to grow thick epilayers of SiC. A growth temperature of 1985°C was applied. The carrier gas (helium) flow rate was set to 6 slm, while SiH_4 and C_3H_8 concentrations were set to 2.240 mol/m^3 and 0.256 mol/m^3 at flow rates of 350 sccm and 40 sccm, respectively.

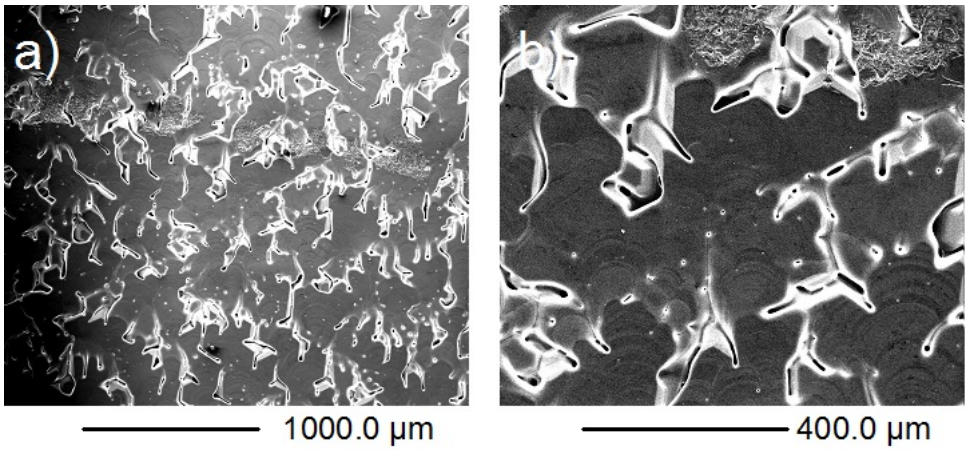

Figure 5.30: *Two SEM images. (a): SEM image taken for the surface morphology of the grown film after three hours of deposition deposition. (b) Magnifies the growth defects shown in (a). Holes could be noticed on the film surface.*

As shown by the SEM image of Figure 5.30, growth defects in form of holes or cracks are visible. Such defects seem to be mainly caused by graphitization of the seed surface during heating, particle nucleation or excessive carbon concentration in the gas-phase. Since a ratio of (C/Si:55/45) was evaluated by means of EDX analysis on the whole area shown by the image a) of Figure 5.30, which observes a relatively reasonable carbon content of the film. According to this result, it could be resolved that the concen-

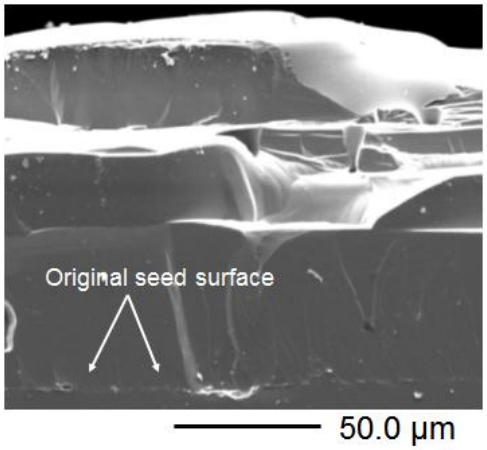

Figure 5.31: *SEM image taken for the seed crystal fracture. A trace distinguishing the original seed surface is visible in the image. Such a defected layer is expected to be caused due to seed graphitization during heating.*

tration of C_3H_8 was set to a proper value. The growth temperature applied is 1985°C, which be too low for inhibiting the particle building in the gas-phase and/or forming the species required for the high rate of surface nucleation. Therefore, for doing such a long experiment in future work, higher growth temperatures above 2060°C might reduce the particle building, which consequentially leads to enhancing the growth conditions. Thus, the absence of reasonable surface treatment during heating might result in the surface contamination with carbon causing growth defects in the initially grown layers of the film. These defects are assumed to be enlarged during the growth of few hundreds of micrometers. However, the film thickness could be measured using SEM analysis. The side view of the deposited seed is shown by the SEM image of Figure 5.31, which observes a total film thickness of 150 μm that was achieved at a growth rate of 50 μm/h. The original seed surface is still distinguished by a thin line as seen by this image observing that the seed surface was contaminated with carbon during heating. Such a problem could be solved by further improvements of the flow geometry, or by applying other procedures for the surface preparation during heating.

Individual crystallites with large sizes of around 1 mm width were noticed on the seed-holder surface as seen in Figure 5.32. Such crystallites can be used as seeds for the

growth of single crystals. Therefore, such experiments with long deposition periods, where non-seeded growth is applied, could be exploited for achieving the growth of large crystals that can be used as seeds for the growth of SiC by PVT or HTCVD.

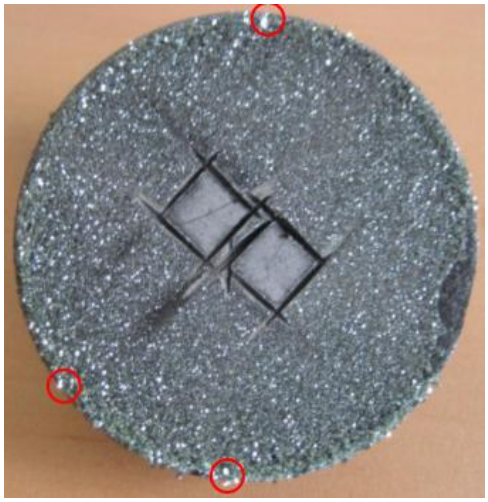

Figure 5.32: *The picture shows a polycrystalline film, which was grown on the non-seeded area of the seed-holder. The growth of large, individual crystallites was noticed (marked with red circles).*

5.3 Summary

The objective of this chapter was to successfully achieve homo-epitaxial growth of 6H-SiC with high growth rates and good crystal quality. In order to examine the initial parameters of the growth process and to investigate the growth of SiC at high temperatures using the HTCVD method, the non-seeded growth technique was used. Secondly, the epitaxial growth of SiC was studied at different precursor concentrations, different temperatures and with different orientations of the seed-crystal surface.

The vertical regions where SiC proceeds to grow, were investigated firstly. Long stripes of graphite foil were conducted vertically in the reactor in order to indicate the vertical range, where the growth of SiC occurs. The growth of polycrystalline SiC was observed at a maximum reactor temperature of 2160°C in a vertical region of 15-25 cm below the outlet flange. The XRD analysis proved the growth of SiC in its cubic

polytype (3C). The deposition of polycrystalline SiC was further investigated applying a stagnant flow geometry using horizontally placed, circular seed-holders. A homogeneous growth of a polycrystalline SiC film could be achieved at a seed-holder position of 15 cm below the outlet flange. Fixing the seed-crystal on a seed-holder made of graphite foil led to a particular seed damage through a few micrometers of its adhered side, consequentially, no mass change could be measured. Therefore, the graphite foil was later replaced by hard, dense graphite.

In the seeded-growth experiments, 6H-SiC seeds with on-oriented surface were initially used. The growth was investigated at different growth temperatures of 1850°C, 1950°C and 2035°C. Both temperatures were achieved at the same output of the MF-Generator, while different seed-holder positions were applied. The films grown at both growth temperatures of 1950°C and 2035°C included crystallites with hexagonal or plain areas on its surface morphology, while no certain structure could be observed within the surface morphology of the film grown at 1850°C. This result shows the importance of applying growth temperatures above 1900°C, which is necessary for improving the growth conditions targeting the epitaxial growth of SiC.

A hollow seed-holder was developed in order to reduce the contact area between the seed and the holder. The application of such a type of seed-holder could not suppress the usual damage of the wafer backside. Therefore in later experiments, the seed-crystals were directly fastened on seed-holders made of dense graphite. However, the use of a hollow seed-holder simplified the separation of the seed, which enabled the measurement of the total seed thickness that was used for evaluating the growth rate. A growth rate of 20 μm/h was observed by means of SEM analysis to a section of the total seed thickness. The growth of a polycrystalline film was observed by the SEM

analysis of the film surface morphology. According to this, it could be resolved that such a non-epitaxial growth of this film is a result of a low growth temperature or due to excessive concentration of propane. Those two aspects could lead to unreasonable gas-phase composition, slower formation rate of the species required for the epitaxial surface nucleation or even to the building of SiC particles in the gas-phase.

In order to improve the growth parameters for achieving epitaxially grown layers of SiC, a further increase of the temperature was carried out by shifting the seed-crystal to lower positions towards the hot zone. A seed-holder temperature of 1995°C was achieved at a position of 30 cm below the outlet flange. A plain surface morphology was observed and a maximum growth rate of 31 μm/h was achieved using an on-axis 6H-SiC seed. The influence of the propane concentration on the growth rate was investigated within a range of 10-40 sccm of it its flow rate, which led to the conclusion that increasing the propane concentration beyond the nucleation value limits the growth rate and sometimes result in the growth of polycrystalline film.

The growth on off-axis seeds was investigated in order to achieve homoepitaxial growth of 6H-SiC. Three 6H-SiC seed-crystals with different tilt angles of 0°, 3.5° and 8° to the basal plane (0001) were simultaneously deposited. The grown epilayers were compared with regard to their surface morphologies and growth rates. On the 3.5° off-axis seed, irregular growth of wide terraces with sharp steps were observed, while on the 8° off-axis seed, a wavy surface morphology was observed. A growth rate of 31 μm/h was achieved on all surfaces. A thin line distinguishing the film from the original seed surface was observed by means of SEM analysis. This line seems to be caused due to the transport of the carbon decomposed of the graphite susceptor to the seed surface.

For achieving higher growth rates of the SiC epilayers, further growth experiments were carried out at higher concentrations of silane and higher growth temperatures. The silane concentration was increased in steps by increasing its flow rate by 50 sccm till a concentration of 2.24 mol/m^3 was reached at a flow rate of 350 sccm, which resulted in the deposition of Si-rich deposits at a growth temperature of 1995°C. Thus, the growth rate could not be enhanced by increasing the concentration of silane at this temperature. However, increasing the growth temperature at this concentration of Silane (2.24 mol/m^3) resulted in growth rate enhancement. A maximum growth temperature of 2060°C could be achieved by our hot-wall reactor, whereat a growth rate of 150 μm/h was reached. Indeed, the growth rate could be measured at four different growth temperatures (1955°C, 1980°, 2030°C), whereby the activation energy of the growth process could be calculated. The resulted growth rates and the activation energy were compared with the growth results obtained in [34] using Arrhenius diagram.

Chapter 6

In-situ Growth Rate Measurement

6.1 In-situ Growth Rate Measurement of Polycrystalline SiC

The growth rate was recorded by the MSB over a period of 20 minutes after an initial heating period of 17 minutes as shown in Figure 6.1 In the initial period, the temperature was increased at constant pressure of 800 mbar, which leads to lower helium density and reduced buoyancy force. Therefore, a slight decrease of the mass was recorded by the MSB in this period. After this period, both gaseous precursors SiH_4 and C_3H_8 were fed into the reactor to start the SiC deposition. A constant increase of the mass versus time was recorded in this period with a growth rate of 1.36 g/h due to the deposition of polycrystalline SiC. The measuring technique requires a free floating substrate (except for the link to the MSB), where the deposition of SiC, do not only proceed on the stagnant side of the seed-holder, but (as ovserved in sec.4.1.3) also on its back side and circumferential area. Such an undesired deposition can not be inhib-

ited applying such a flow geometry. For this reason the conversion of the growth from mass per time into thickness per time is not appropriate. After 10 minutes of deposition, all flows were stopped for 6 minutes to check the response of the MSB, which led to small fluctuations in the mass measurement during the first two minutes due to the pressure fluctuation caused once the flows are stopped. After these two minutes, the pressure stabilizes and no further change of the mass was recorded. Afterwards, the deposition was continued for additional 10 minutes. As can be seen in Figure 6.1, the increase of the mass is again linear and the growth rate is equal to the one of the first deposition period.

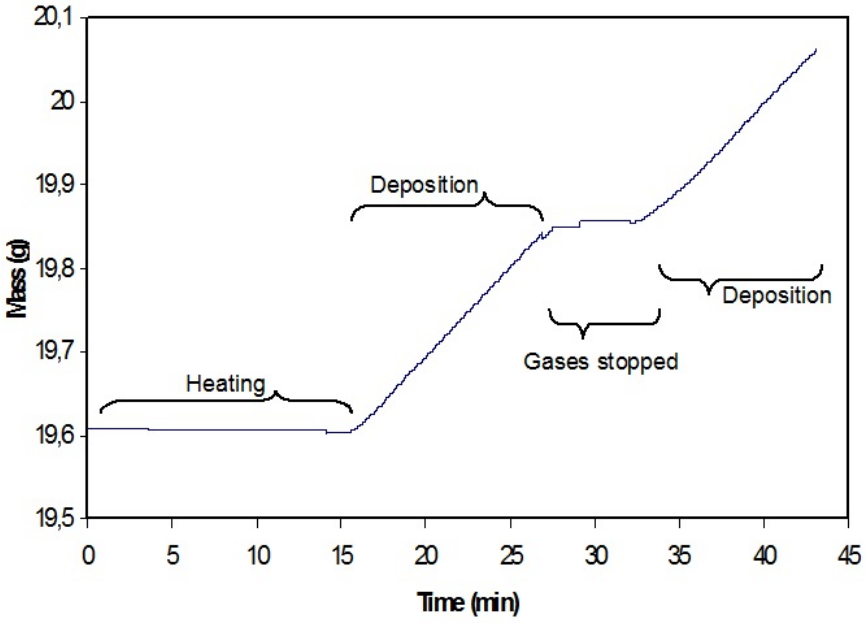

Figure 6.1: *The mass change is recorded versus the time over four growth periods. A heating period is followed by a deposition period observing a growth rate of 1.38 g/h. Thereafter, the precursor's flow was stopped to assure a zero mass change. The deposition was continued in the fourth interval observing an equal growth rate to the one evaluated by the first deposition period.*

6.2 Effect of Silane Concentration on Growth Rate

The growth rate dependence on precursor concentrations has been investigated. The SiH_4 concentration was gradually changed during the experiment, as seen in Figure 6.2-a. In this experiment, the pressure, the growth temperature and the flow velocity were kept constant at 800 mbar and 1950 °C and 0.0075 m/s, respectively. The SiH_4 concentration was initially set to 0.6683 mol/m^3 (100 sccm), while the C_3H_8 concentration was held constant at a value of 0.134 mol/m^3 (20 sccm). At this concentration of SiH_4, a growth rate of 0.48 g/h was achieved, as seen in Figure 6.2-b. A further increase of SiH_4 concentration to 0.994 mol/m^3 and 1.315 mol/m^3, increased the growth rate to 0.86 g/h and 0.94 g/h, respectively. Once the SiH_4 concentration was increased to a value of 1.631 mol/m^3, the growth rate was nearly doubled to 1.92 g/h. Inversely, increasing the SiH_4 concentration to a value of 1.9414 mol/m^3, resulted in lower growth rate of 1.37 g/h, which probably resolves that the growth of polycrystalline SiC at high SiH_4 concentration could be kinetically limited within this temperature range. Thus, the gradual increase of SiH_4 concentration must not always result in a proportional increase of the growth rate. The stoichiometric gas-phase composition of SiH_4 and C_3H_8 can be calculated due to the following reaction:

$$3SiH_4 + C_3H_8 = 3SiC + 16H_2$$

According to this equation, 3 moles of SiH_4 and 1 mole of C_3H_8 are required to produce 3 moles of SiC. Converting this on a volumetric basis, only a SiH_4 flow rate of 60 sccm will be required at C_3H_8 flow rate of 20 sccm to fulfill the stoichiometry condition, meanwhile in our case, as can be seen from the values obtained at the highest growth rate, the concentration of SiH_4 is more than 12 time the concentration of C_3H_8.

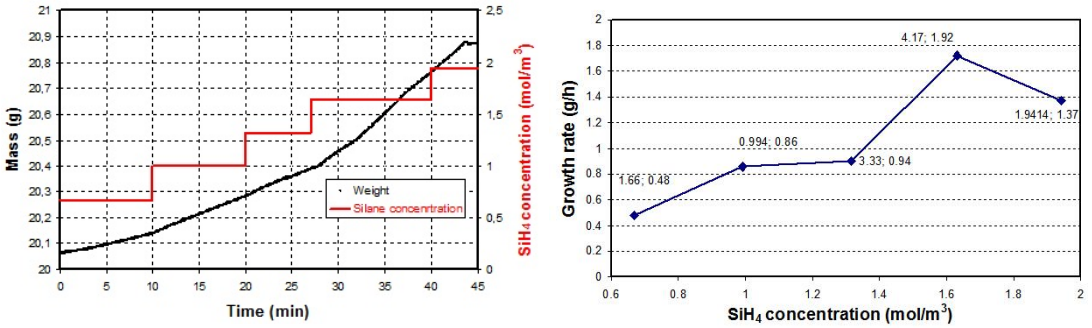

Figure 6.2: *Left: recorded mass at different silane concentrations are plotted versus time. Right: the evaluated growth rates are plotted in correspondence with their silane concentrations. The growth rate can be increased by increasing the silane concentration within a certain range. Increasing the silane concentration beyond a certain limit results in lower growth rates.*

This fact indicates the existence of a secondary carbon source in the process, which is supposed to be supplied by the amount of carbon produced due to the evaporation of the graphite susceptor at high temperatures.

6.3 Effect of Propane Concentration on Growth Rate

In this experiment, the SiH_4 flow was held at a constant value of 100 sccm corresponding to a concentration of 0.665 mol/m^3, while the C_3H_8 concentration was gradually changed during the experiment by increasing its flow rate in steps of 5 sccm every 10 minutes resulting in the following concentrations: 0.0335, 0.0669, 0.100 and 0.1336 mol/m^3. The mass change recorded was plotted versus time as illustrated in Figure 6.3-a, where no large change in the growth rate could be observed at different C_3H_8 concentrations. By plotting the growth rate versus the concentration of C_3H_8 in the diagram of Figure 6.3-b, a growth rate reduction was noticed at both concentrations of C_3H_8 at 0.0669 and 0.100 mol/m^3. However, a further increase of the C_3H_8 concentration from 0.1 mol/m^3 to 0.1336 mol/m^3, enhanced the growth rate from 0.31g/h to 0.34

g/h. According to this result, it could be observed that increasing the concentration of C_3H_8 could have a negative effect on the growth rate. Indeed, a further increase of the C_3H_8 concentration to a value of 0.1336 mol/m^3, is shown to have a better effect on the growth rate. Thus, the highest growth rate was obtained at very low concentration of C_3H_8, which is in a good agreement with the epitaxial growth results obtained in sec.4.2.5.

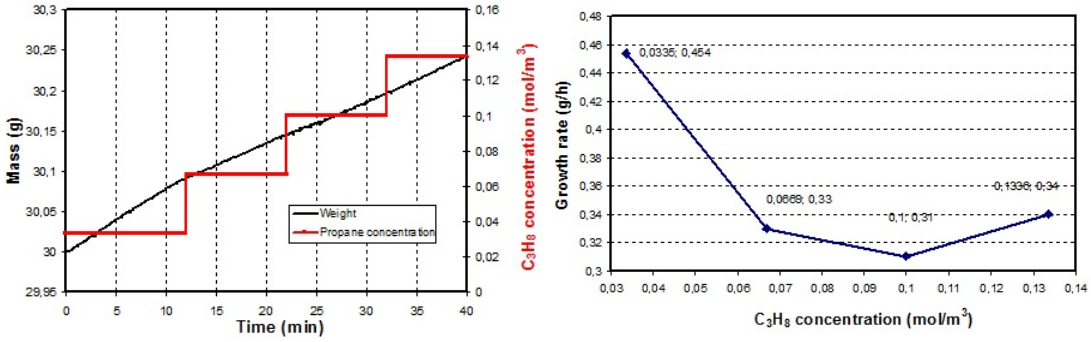

Figure 6.3: *Left: recorded mass at different propane concentrations are plotted versus time. Right: the evaluated growth rates are plotted in correspondence with their propane concentrations. Increasing the propane concentration within a certain range has a negative effect on the growth rate, but a further increase of its concentration fairly enhances the growth rate.*

6.4 Effect of Hydrogen Concentration on Growth Rate

The diagram illustrated in Figure 6.4 shows some similarity with the one shown in Figure 6.3, where the growth rate decreases with increasing the concentration of C_3H_8. At low concentrations of C_3H_8, the growth rate was measured in the first 10 minutes without any addition of H_2. A growth rate of 1.23 g/h was found for this period of time. Afterwards, the concentration of H_2 was increased from 0 to 0.3261 mol/m^3 by increasing its flow rate to 50 sccm, which caused a considerable reduction of the growth

rate, as seen in Figure 6.4. Descending growth rates of 0.9 g/h, 0.77 g/h and 0.65 g/h were recorded at H_2 concentrations of 0.336, 0.6471 and 0.9630 mol/m^3, respectively. By converting the growth rate of the value 0.9 g/h to thickness/time, assuming that no deposition of SiC powder will take place on the seed-holder backside, a growth rate of 150 μm/h will result. However, a further increase of H_2 concentration to 1.274 mol/m^3, resulted in a slightly enhanced growth rate, which seems to be a relatively an obvious result due to the increased etching rates caused by adding more H_2 to the process, which decreases the hydrocarbon species in the gas-phase. However, low concentrations of H_2 seem to have a different etching effect resulting in the formation of volatile hydrocarbons, which negatively influences the growth rate of SiC.

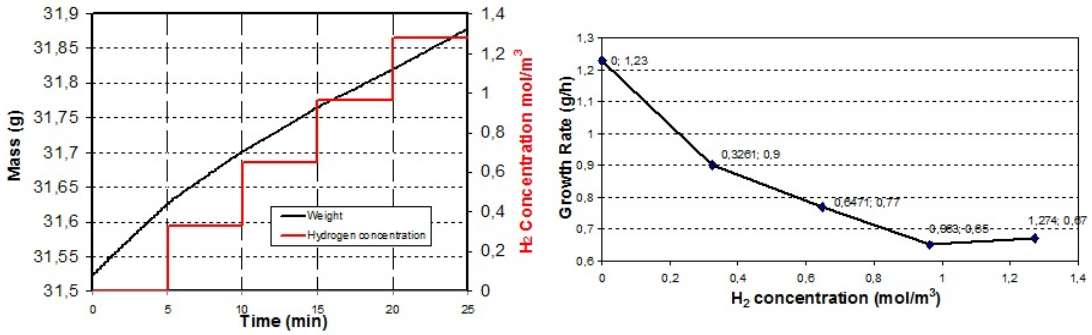

Figure 6.4: *Left: recorded mass at different hydrogen concentrations are plotted versus time. Right: the evaluated growth rates are plotted in correspondence with their hydrogen concentrations. Increasing the hydrogen concentration within a certain range has a negative effect on the growth rate, but further increase of its concentration fairly enhances the growth rate. Such an effect seem to be similar to the result obtained at increased propane concentrations.*

6.5 Vertical Placement of the Substrate

As mentioned in the experimental part, the seed-holder was placed vertically, parallel to the flow stream lines to enable the deposition on its both sides. In this case, ho-

mogeneous films are expected to be grown on both sides of the séed-holder, which is necessary for measuring the growth rate in thickness per time. The C_3H_8 concentration was varied during deposition at constant concentration of SiH_4 (1.319 mol/m^3). The seed-holder mass was measured in-situ versus the time as illustrated in the diagram presented in Figure 6.5. An oscillating mass was noticed during deposition, which seems to be the result to the new flow geometry that was established by the vertical placement of the substrate holder. The resulting growth rates at different concentrations of C_3H_8 are three or four times smaller than the growth rates obtained at similar process conditions where a horizontal placement of the seed-holder was applied. Due to this result it could be concluded that placing the substrate holder in a vertical position might increase the etching rate of the deposited SiC or however decreases its adsorption and consequentially results in a slower growth rates. Indeed, the flow geometry established by the horizontal placement of the substrate has shown a better effect on the growth rate.

6.6 Summary

The main target of this work focused on the in-situ measurement of the growth rate of non-seeded growth of SiC on a seed-holder. For this purpose, a MSB was successfully integrated to the HTCVD reactor. The mass change of the deposited polycrystalline films were accurately recorded in-situ, under different concentrations of the precursors and for the first time at such a high growth temperature of 1950°C. The application of this measuring technique enabled the growth rate measurement at wide range of the precursor concentrations that can be varied to different values in one experiment, which saved a lot of time and experimental costs. The growth rates measured, showed

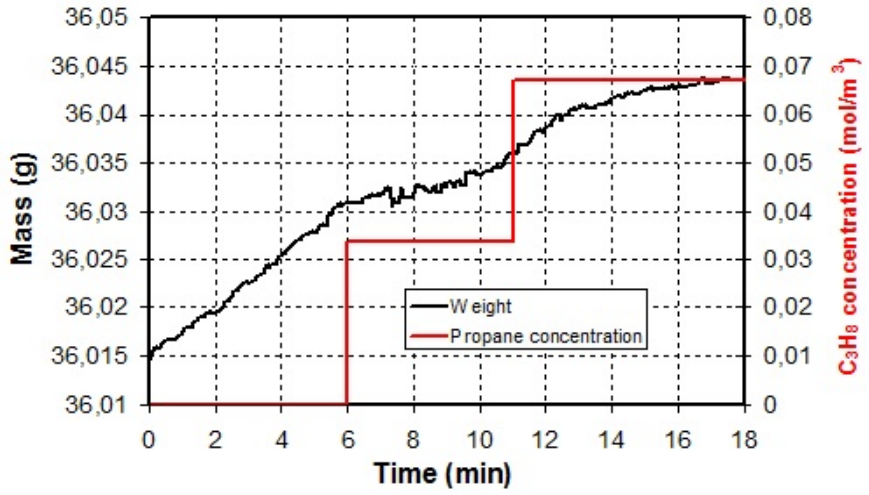

Figure 6.5: *The growth rate is plotted versus the propane concentration, while propane and silane concentrations are kept constant. The stepwise increase of propane concentration seems to have a significant, negative effect on the deposition rate.*

a significant dependency on the precursor concentration. Increasing the propane and hydrogen concentrations is shown to have a negative effect on the growth rate, while high silane concentration enhances the growth rate within a certain range.

Due to the deposition of SiC on the back and side area of the seed-holder, it was not possible to convert the mass recorded from the mass-change/time to thickness/time. The vertical placement of the seed-holder resulted in a growth rate reduction. Therefore, in order to use such a system for the in-situ growth rate measurement of a seed-crystal in an epitaxial growth process, a complete wafer of 2-inch diameter must be fastened on the seed-holder and the internal flow geometry around the seed-holder must be improved to inhibit the random growth of SiC powder on the seed-holder backside. However, the successful integration of the MSB into the HTCVD system is considered as an important step in using the gravimetric technique to study the kinetics of the seeded growth of SiC.

Chapter 7

Conclusions

A vertical hot-wall reactor was constructed and successfully used for the epitaxial deposition of SiC at very high growth temperatures. The concept of inductive heating was applied, whereby a maximum growth temperature of 2060°C could be achieved. The growth temperature could be measured via an optical access using a two color pyrometer, but only during heating where the silane concentration is still zero and the reactor space contains no particles are usually generated when silane flows. Due to the positioning of the inductive coil at the middle of the reactor, a low temperature zone is established at the bottom of the susceptor and the inlet nozzle. This and the slow flow velocity of the precursors (0.0075 m/s) prepare good conditions leading to SiC particle generation in the gas-phase that later fall on the glass window of the optical access and complicate the temperature measurement.

The reactor setup targeted the epitaxial growth of SiC using SiC substrates, which were located horizontally (normal to the flow direction) in the reactor. In order to indicate reasonable precursor concentrations and an optimal seed-holder position, a non-seeded

growth technique was initially performed on substrates made of graphite foil. A resulting film of polycrystalline SiC was observed. The experimental setup (seed-holder position and precursor concentrations) used in these experiments was then approximately applied in seeded growth experiments. Accordingly, the resulting films grown on the SiC seeds were also polycrystalline, which indicates a significant difference in the growth kinetics between both non-seeded and seeded growth techniques. The use of on-axis substrates at a vertical range of 14-18 cm below the outlet flange and a precursor flow ratio of 1/3: Propane/Silane addressed some enhancement of the surface morphology at the lowest position of the seed-holder (18 cm) where a higher growth temperature is achieved. This leads to the conclusion that for the epitaxial growth of SiC, a minimal growth temperature of 1950°C is required at such reactor design and precursor concentrations.

The use of seed-holders made of graphite foil led to the damage of the adhered side of the seed-crystal through a depth of few micrometers. This problem was partially solved using seed-holders made of dense, hard graphite. The use of small seed-holders with a diameter of 50 mm was shown to have a positive effect on the flow geometry leading to reasonable growth conditions than using seed-holders with larger diameters, which might be caused due to that the use of large diameter seed-holders results in parallel, long flow streams to the outer area, which is close to the perimeter of the seed-holder surface, the flow velocity of those streams are too fast, which leads to the conclusion that such parallel flow streams to the seed-holder surface would probably influence the diffusion rate negatively. Thus, the use of hollow seed-holders could not inhibit the damage of the seed-crystal (SiC wafer) backside.

The epitaxial growth of SiC on on-axis 6H-SiC seeds could be achieved at a distance of 30 cm below the outlet flange. This position is 5 cm above the ultimate temperature of the susceptor walls. Upon this result, it could be resolved that such a distance (5 cm) between the seed-holder and the ultimate reactor temperature is of great importance to achieve the optimal supersaturation conditions. At a temperature of 1955°C, a maximum growth rate of 31 μm/h could be achieved at low concentrations of propane, approximately 1/8:propane/silane. Increasing the concentration of the propane beyond this ratio was observed to have a significant influence on reducing the growth rate and leads to the growth of polycrystalline SiC at higher concentrations. According to this result, the concentration of the hydrocarbons is considered to be playing a decisive role of the growth kinetics of the HTCVD of SiC.

The SEM analysis of a vertical cut in the grown epilayers on on-axis SiC substrates observed a trace separating both of the film and the original seed surface. This result indicates that the seed surface was smudged before the growth starts, which might be caused due to coating the seed surface with a thin film of carbon, which is expected to be produced due to the decomposition of the graphite tube (susceptor). Such a contamination was investigated performing different flow procedures during heating. The lowest carbon contamination of the substrate resulted at very low pressure and zero flow rates of the precursors and the carrier gas, where the highest contamination resulted at helium or hydrogen flow. In order to improve the quality of the grown epilayers, the contamination of the seed surface must be inhibited or at least minimized. Therefore, the research on the surface treatment must be further proceeded.

Increasing the silane concentration to values of as high as 2.24 mol/m^3 at a temperature of 1955°C did not result in advancing the growth rate. Si droplets were recognized by EDX on the substrate surface. Due to this result, it could be resolved that the process is limited by the surface kinetics, the low formation rate of the major species or by particle formation in the gas phase at this temperature. A further increase of the temperature to 2060°C resulted in a significant enhancement of the growth rate to a value of 100 μm/h on off-axis surfaces. The limited growth rates achieved on on-axis surfaces at higher temperatures than 1955°C, indicate the growth of 3C-SiC, which is known for its lower stability at a temperature of 2000°C compared with both 4H and 6H polytypes that are more stable even at higher temperatures and can be grown homoepitaxially on off-axis substrates. However, it was shown that for achieving higher growth rates up to a value of 1 mm/h, a further increase of the temperature than 2060°C is necessary.

The production of SiC crystal by HTCVD requires long deposition times up to 10 hours at high growth rates of up to 1 mm/h. In order to achieve optimal growth conditions for obtaining such growth rates, the growth parameters involved in this process must be optimized. The techniques used for the in-situ growth rate measurements offer the possibility of investigating the influence of the different growth parameters on the growth rate and saves much of preparation and experimental time. Several variations of the growth parameters can be performed in one experiment within a short period of time to investigate their effect on the growth rate. Therefore, a magnetic suspension balance (MSB) was integrated to the hot-wall reactor and successfully used for the in-

situ measurement of the growth rate. The mass change of polycrystalline films grown directly on a seed-holder of 50 mm diameter was recorded while the precursor concentrations were varied over small periods of time without stopping the experiments. The in-situ recorded mass change observed a significant dependency on the precursor concentrations. The growth rate was reduced by increasing one of both concentrations of hydrogen or propane, while increasing the silane concentration resulted in high growth rates until the concentration reached a certain limit of silane, thereafter, the growth rate decreased at higher silane concentrations. The successful application of this technique in such high temperatures can be considered as an important step for its application in the epitaxial growth process of SiC using the HTCVD method.

Chapter 8

Appendix a: Technical Drawings

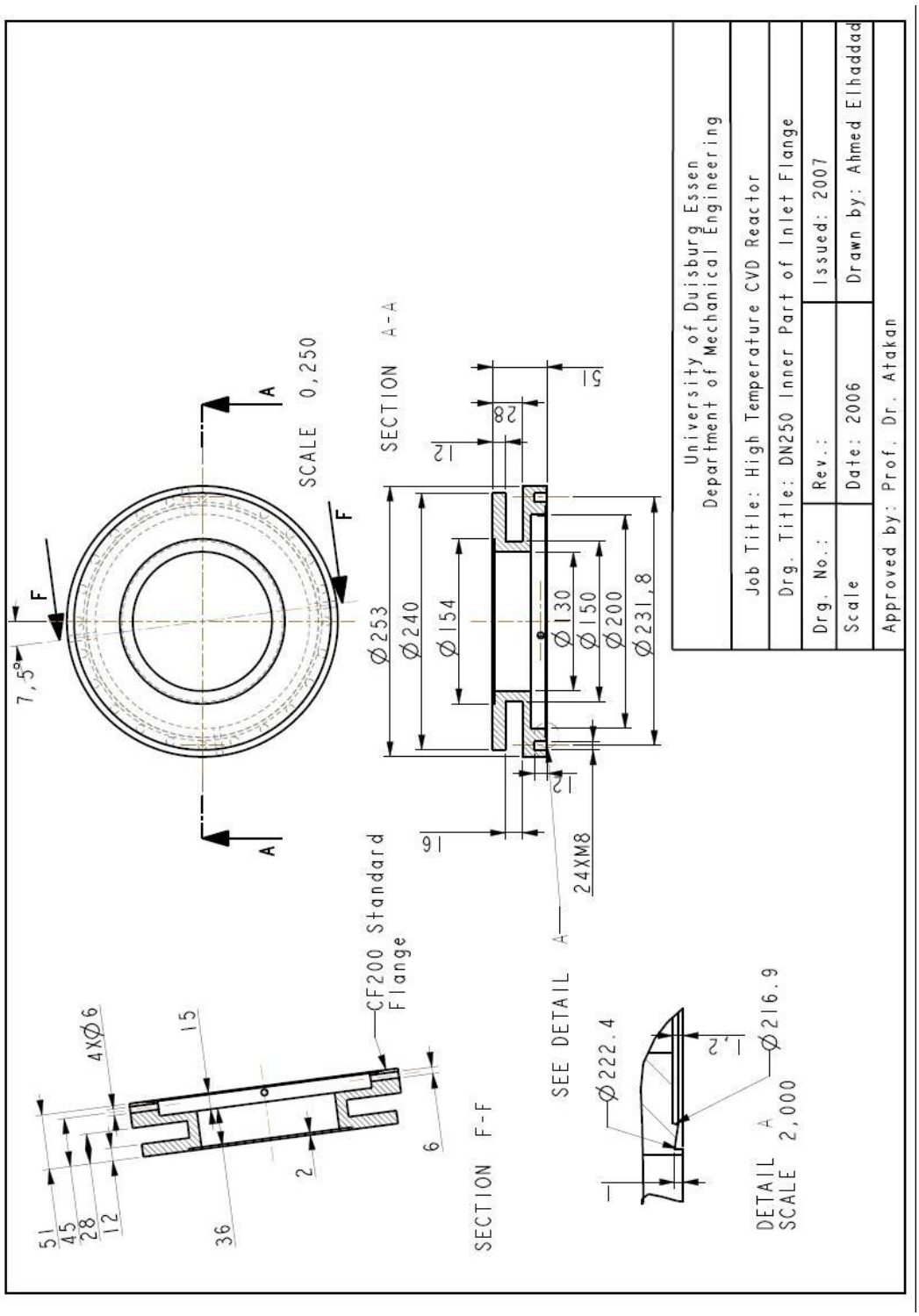
SCALE 0,250
SECTION A-A
SECTION F-F
SEE DETAIL A
DETAIL A
SCALE 2,000
7,5°
Ø253
Ø240
Ø154
Ø130
Ø150
Ø200
Ø231,8
24XM8
CF200 Standard Flange
4XØ6
Ø222.4
Ø216.9
University of Duisburg Essen
Department of Mechanical Engineering
Job Title: High Temperature CVD Reactor
Drg. Title: DN250 Inner Part of Inlet Flange
Drg. No.:
Rev.:
Issued: 2007
Scale
Date: 2006
Drawn by: Ahmed Elhaddad
Approved by: Prof. Dr. Atakan

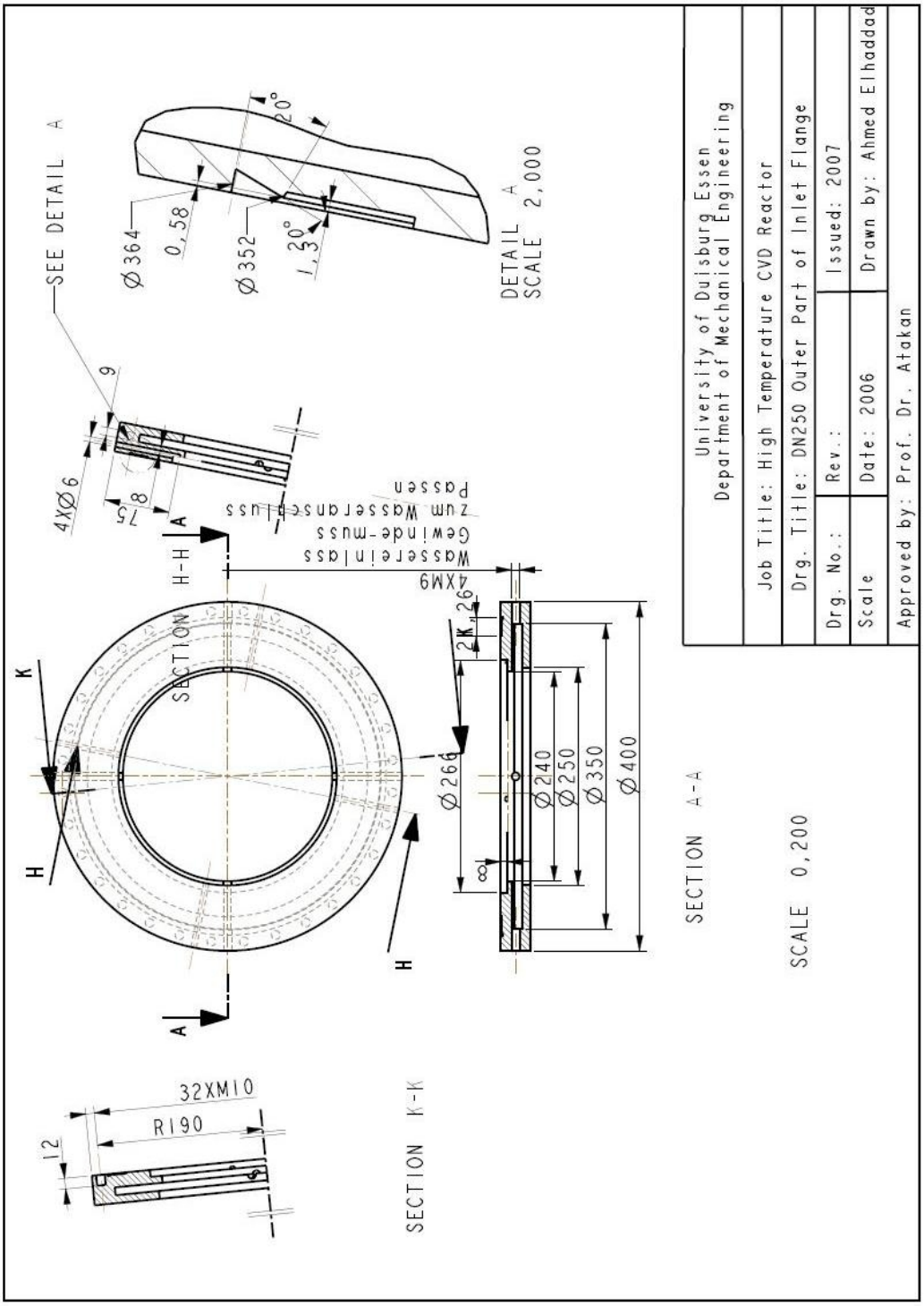
SEE DETAIL A
Ø364
0,58
Ø352
1,30
20°
DETAIL A
SCALE 2,000
4XØ6
9
7,5
8
A
H-H
Wasserleitung
Gewinde-muss
zum Wasserabschluss
Passen
4XM9
26
2K
Ø269
Ø240
Ø250
Ø350
Ø400
8
K
H
SECTION
A
SECTION A-A
SCALE 0,200
32XM10
R190
12
SECTION K-K
University of Duisburg Essen
Department of Mechanical Engineering
Job Title: High Temperature CVD Reactor
Drg. Title: DN250 Outer Part of Inlet Flange
Drg. No.:
Rev.:
Issued: 2007
Scale
Date: 2006
Drawn by: Ahmed Elhaddad
Approved by: Prof. Dr. Atakan

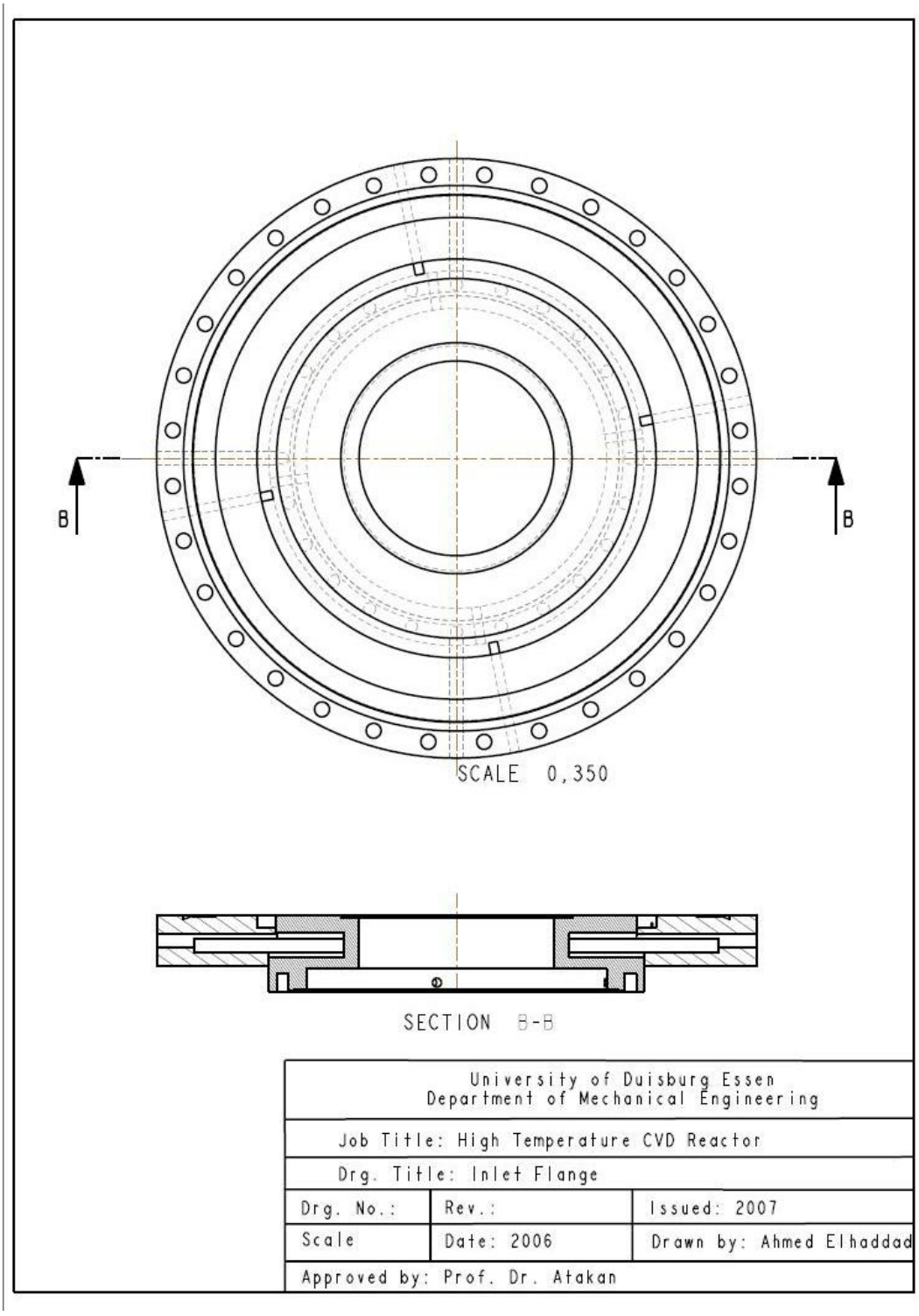
B
B
SCALE 0,350
SECTION B-B
University of Duisburg Essen
Department of Mechanical Engineering
Job Title: High Temperature CVD Reactor
Drg. Title: Inlet Flange
Drg. No.:
Rev.:
Issued: 2007
Scale
Date: 2006
Drawn by: Ahmed Elhaddad
Approved by: Prof. Dr. Atakan

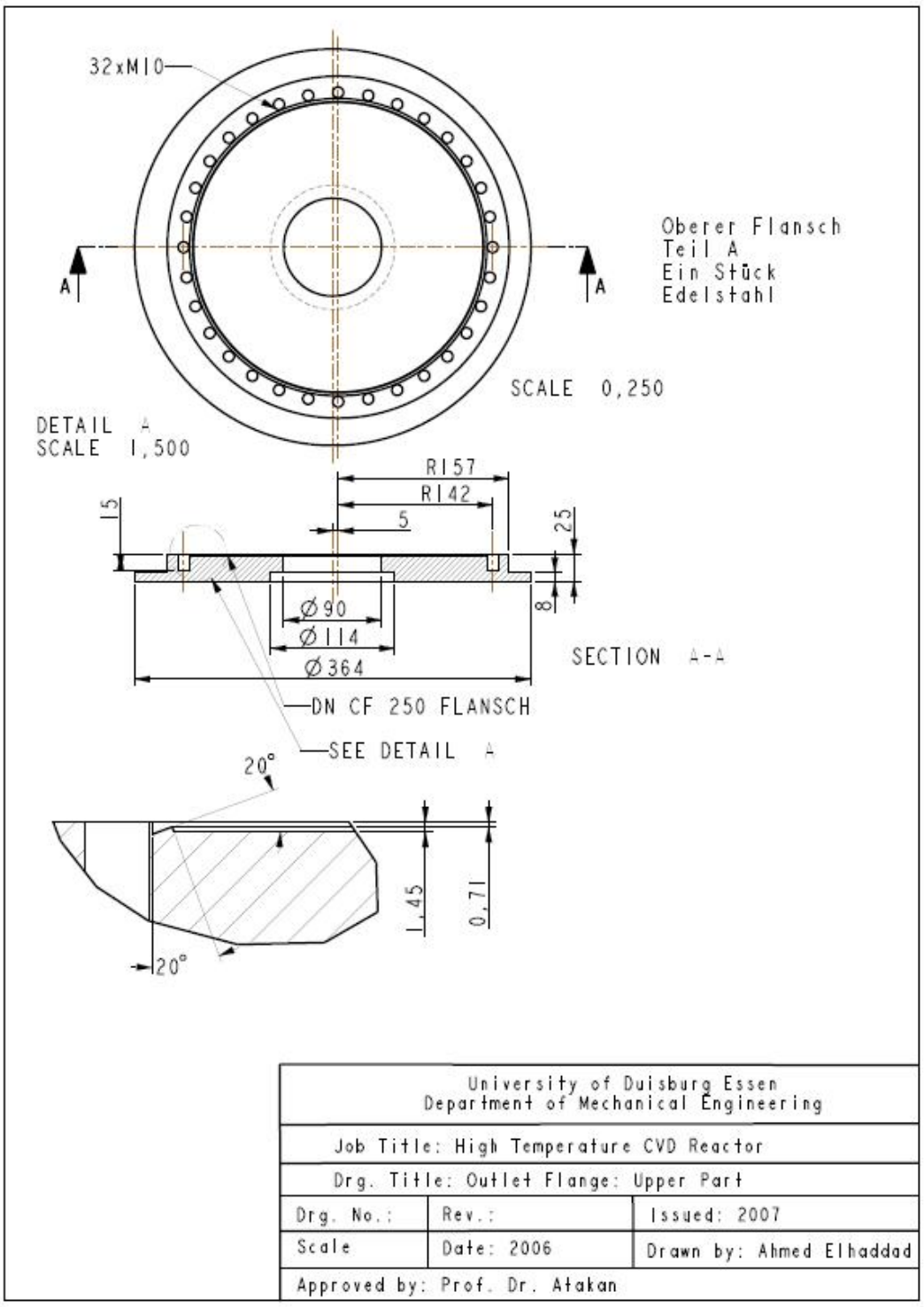
32xM10
A
A
Oberer Flansch
Teil A
Ein Stück
Edelstahl
SCALE 0,250
DETAIL A
SCALE 1,500
R157
R142
5
15
25
8
Ø90
Ø114
Ø364
SECTION A-A
DN CF 250 FLANSCH
SEE DETAIL A
20°
20°
1,45
0,71
University of Duisburg Essen
Department of Mechanical Engineering
Job Title: High Temperature CVD Reactor
Drg. Title: Outlet Flange: Upper Part
Drg. No.:
Rev.:
Issued: 2007
Scale
Date: 2006
Drawn by: Ahmed Elhaddad
Approved by: Prof. Dr. Atakan

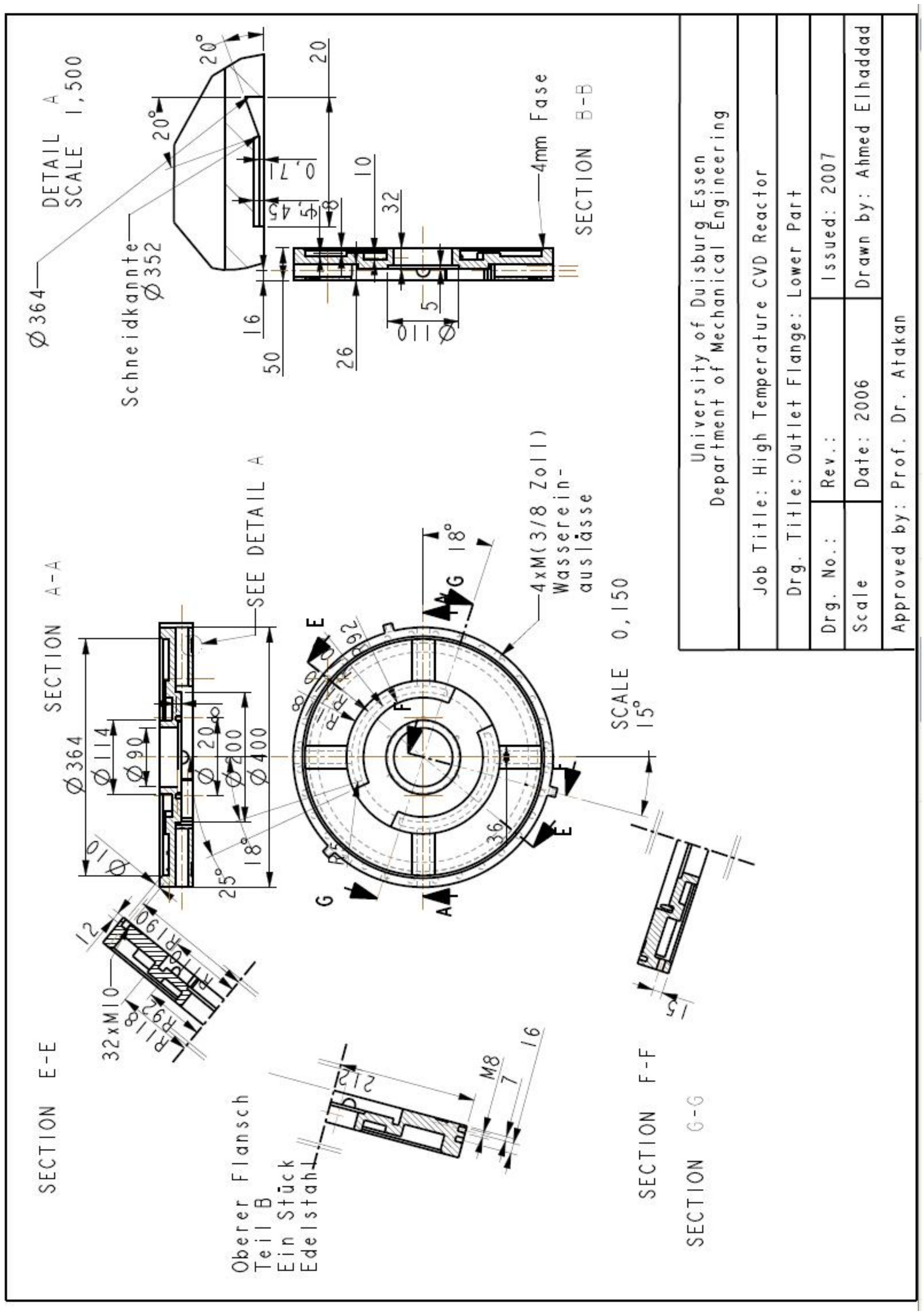
University of Duisburg Essen
Department of Mechanical Engineering
Job Title: High Temperature CVD Reactor
Drg. Title: Outlet Flange: Lower Part
Drg. No.:
Rev.:
Issued: 2007
Scale
Date: 2006
Drawn by: Ahmed Elhaddad
Approved by: Prof. Dr. Atakan
SECTION A-A
SEE DETAIL A
DETAIL A
SCALE 1,500
SECTION B-B
4mm Fase
Schneidkante
4xM(3/8 Zoll)
Wasserein-
auslässe
SCALE 0,150
SECTION E-E
32xM10
SECTION F-F
SECTION G-G
Oberer Flansch
Teil B
Ein Stück
Edelstahl

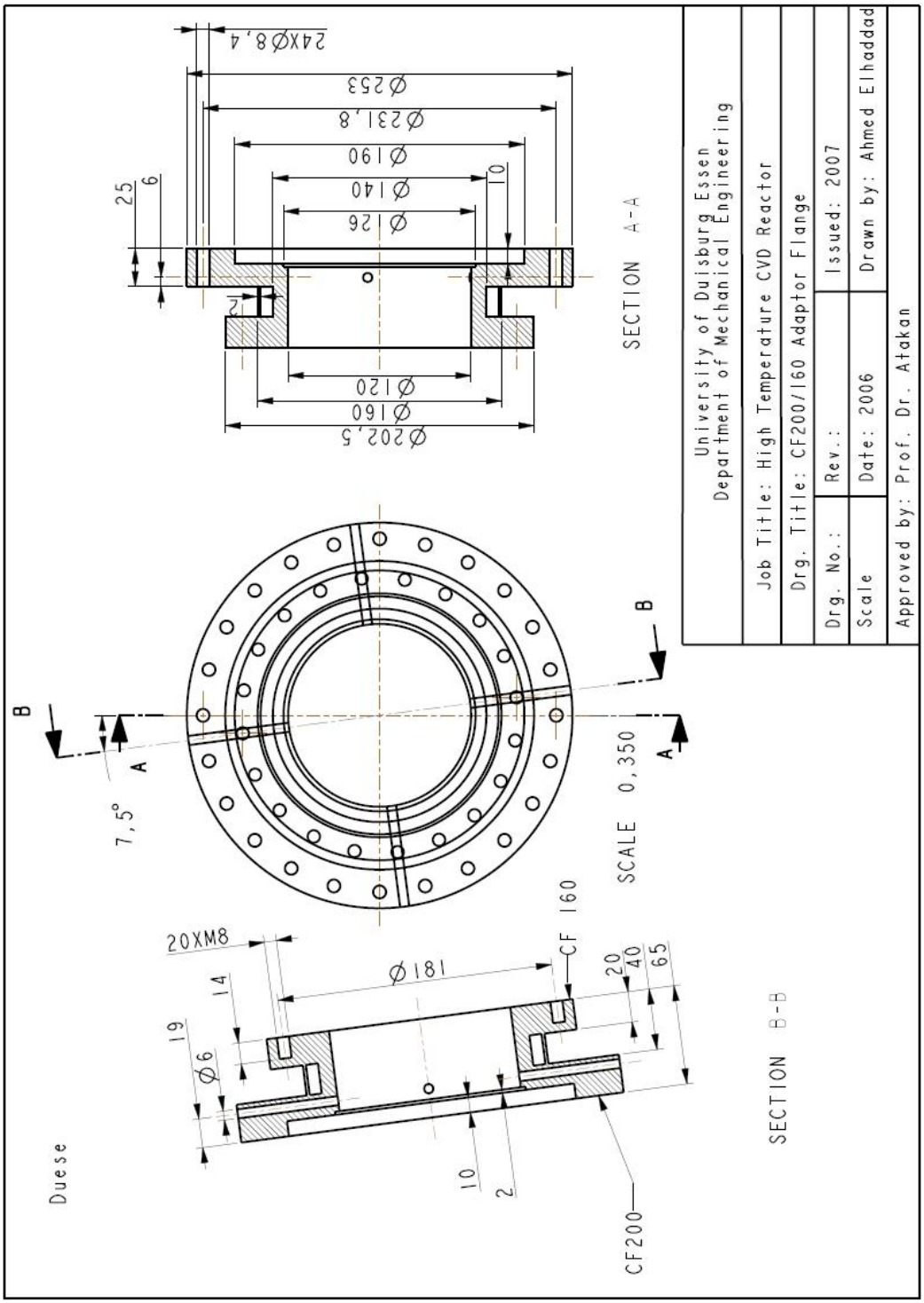
24XØ8,4
Ø253
Ø231,8
Ø190
Ø140
Ø26
25
6
9
10
2
Ø120
Ø160
Ø202,5
SECTION A-A
B
A
7,5°
SCALE 0,350
20XM8
Ø181
CF 160
14
19
Ø6
20
40
65
10
2
CF200
SECTION B-B
Duese
University of Duisburg Essen
Department of Mechanical Engineering
Job Title: High Temperature CVD Reactor
Drg. Title: CF200/160 Adaptor Flange
Drg. No.:
Rev.:
Issued: 2007
Scale
Date: 2006
Drawn by: Ahmed Elhaddad
Approved by: Prof. Dr. Atakan

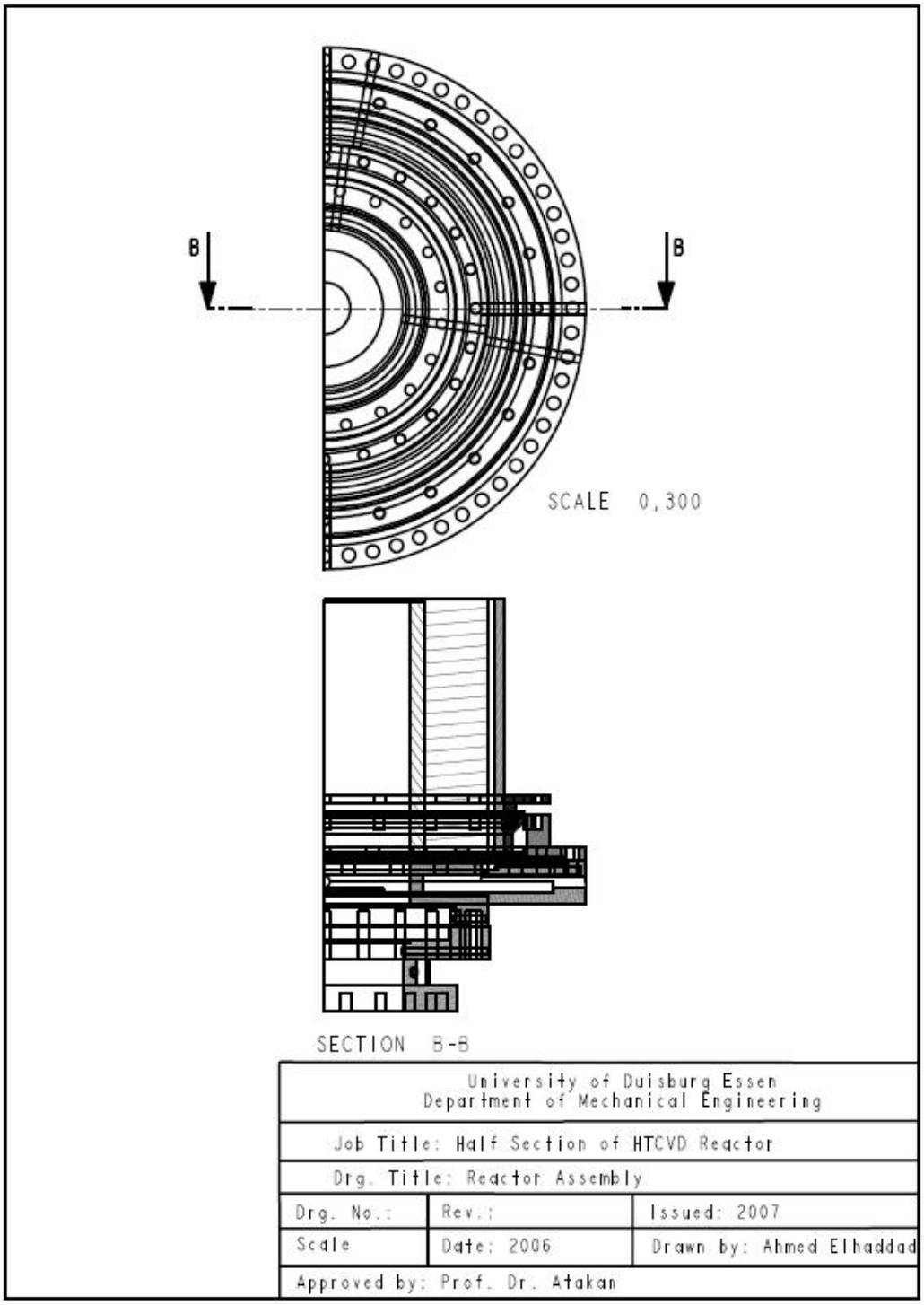
B
B
SCALE 0,300
SECTION B-B
University of Duisburg Essen
Department of Mechanical Engineering
Job Title: Half Section of HTCVD Reactor
Drg. Title: Reactor Assembly
Drg. No.:
Rev.:
Issued: 2007
Scale
Date: 2006
Drawn by: Ahmed Elhaddad
Approved by: Prof. Dr. Atakan

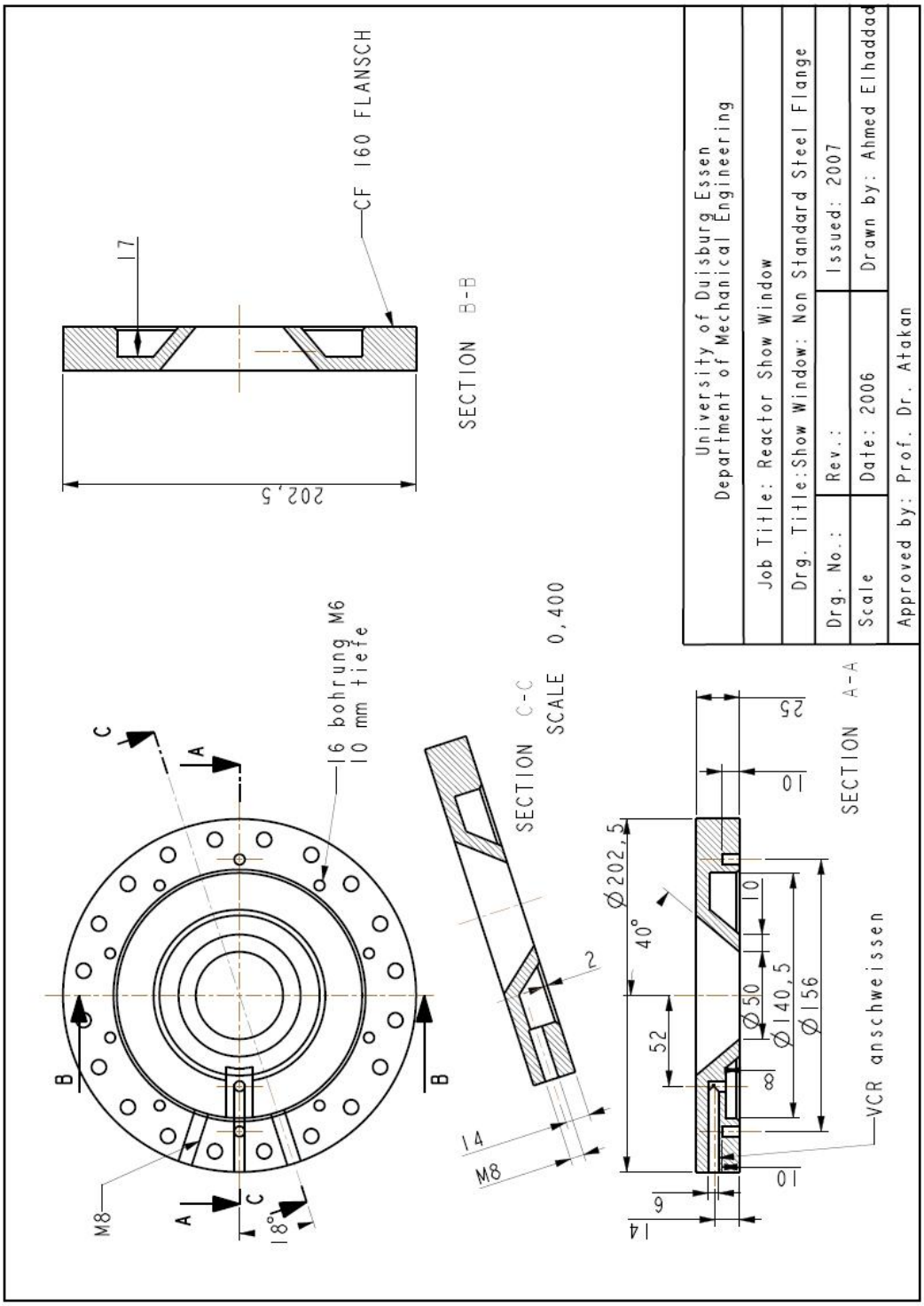
CF 160 FLANSCH
17
202,5
SECTION B-B
16 bohrung M6
10 mm tiefe
SECTION C-C
SCALE 0,400
SECTION A-A
VCR anschweissen
M8
18°
14
2
40°
Ø202,5
Ø140,5
Ø156
Ø50
52
25
10
8
6
4
University of Duisburg Essen
Department of Mechanical Engineering
Job Title: Reactor Show Window
Drg. Title:Show Window: Non Standard Steel Flange
Drg. No.:
Rev.:
Issued: 2007
Scale
Date: 2006
Drawn by: Ahmed Elhaddad
Approved by: Prof. Dr. Atakan

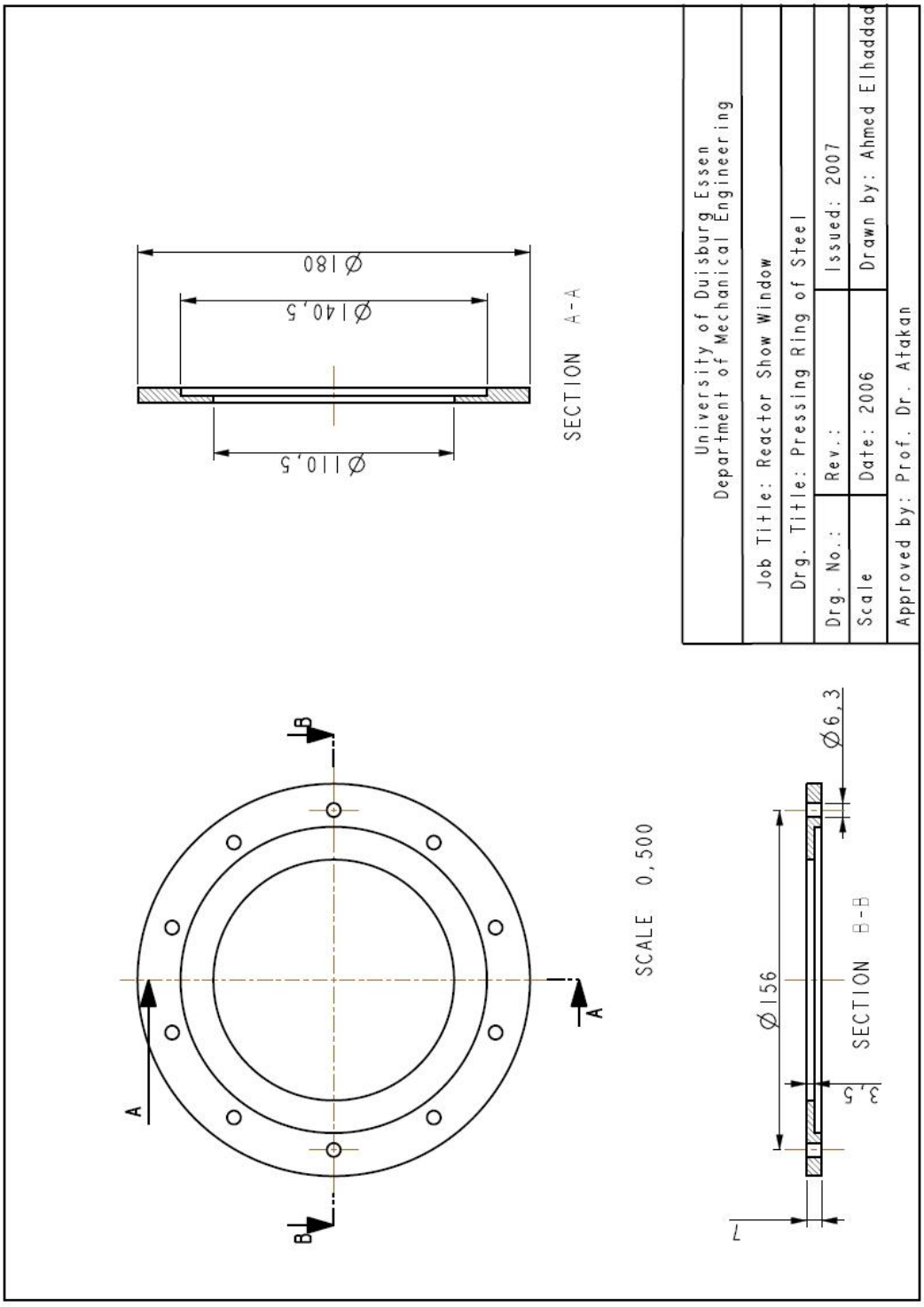
University of Duisburg Essen
Department of Mechanical Engineering
Job Title: Reactor Show Window
Drg. Title: Pressing Ring of Steel
Drg. No.:
Rev.:
Issued: 2007
Scale
Date: 2006
Drawn by: Ahmed Elhaddad
Approved by: Prof. Dr. Atakan
Ø180
Ø140,5
Ø110,5
SECTION A-A
SCALE 0,500
Ø6,3
Ø156
SECTION B-B
A
B
L

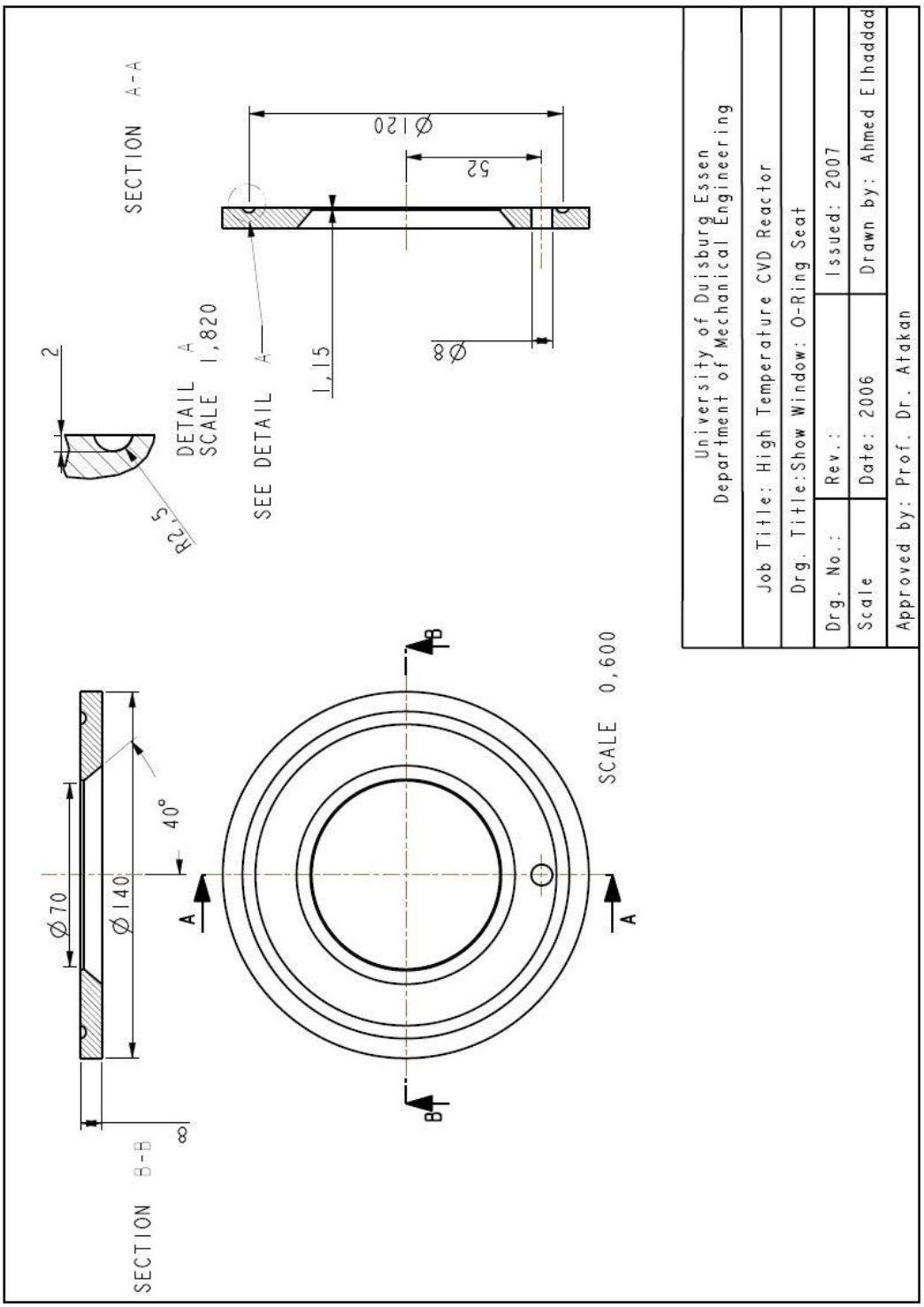
SECTION A-A
Ø120
52
8Ø
1,15
DETAIL A
SCALE 1,820
SEE DETAIL A
2
R2,5
SCALE 0,600
A
A
B
B
40°
Ø70
Ø140
8
SECTION B-B
University of Duisburg Essen
Department of Mechanical Engineering
Job Title: High Temperature CVD Reactor
Drg. Title:Show Window: O-Ring Seat
Drg. No.:
Rev.:
Issued: 2007
Scale
Date: 2006
Drawn by: Ahmed Elhaddad
Approved by: Prof. Dr. Atakan

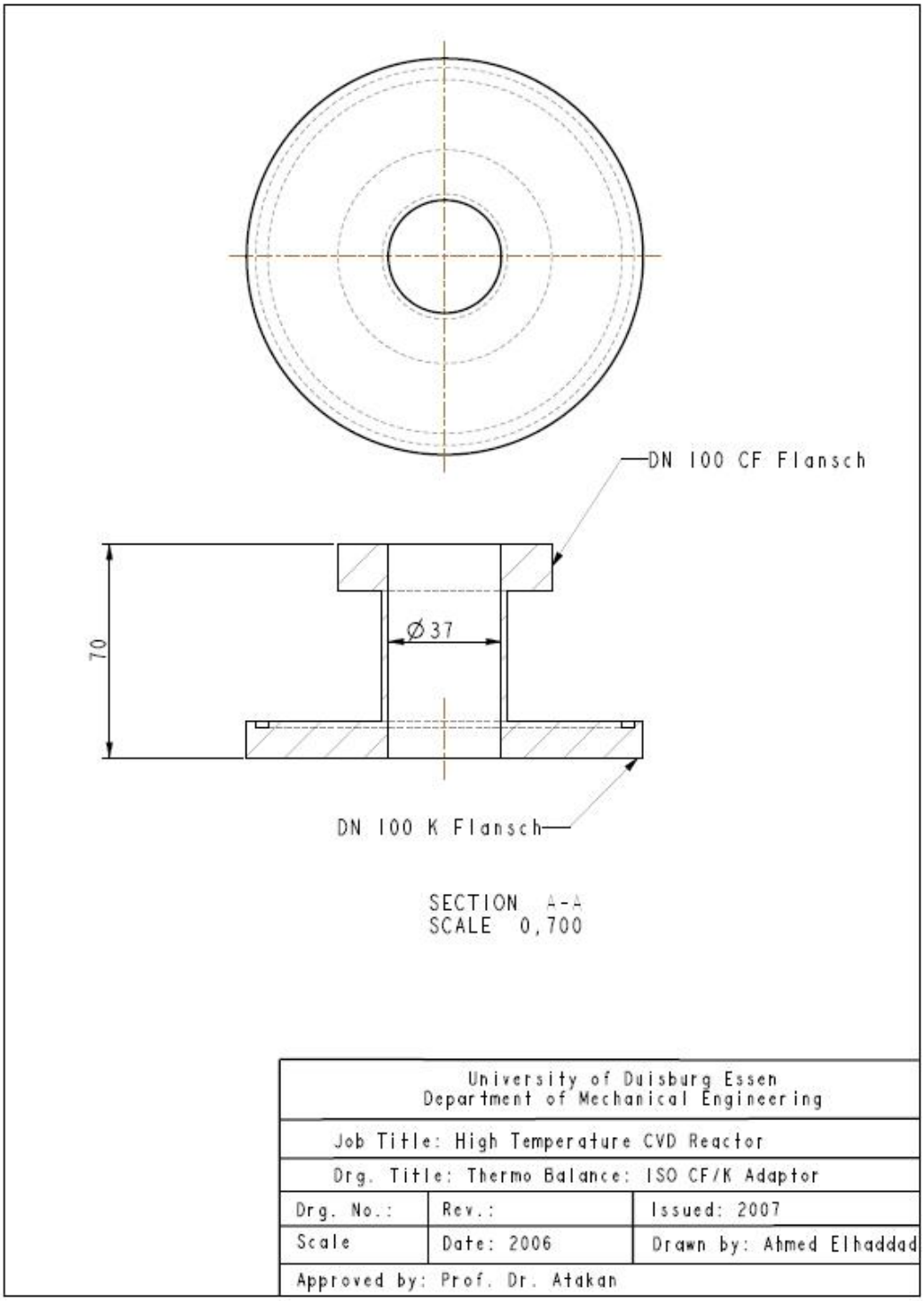
DN 100 CF Flansch
70
Ø37
DN 100 K Flansch
SECTION A-A
SCALE 0,700
University of Duisburg Essen
Department of Mechanical Engineering
Job Title: High Temperature CVD Reactor
Drg. Title: Thermo Balance: ISO CF/K Adaptor
Drg. No.:
Rev.:
Issued: 2007
Scale
Date: 2006
Drawn by: Ahmed Elhaddad
Approved by: Prof. Dr. Atakan

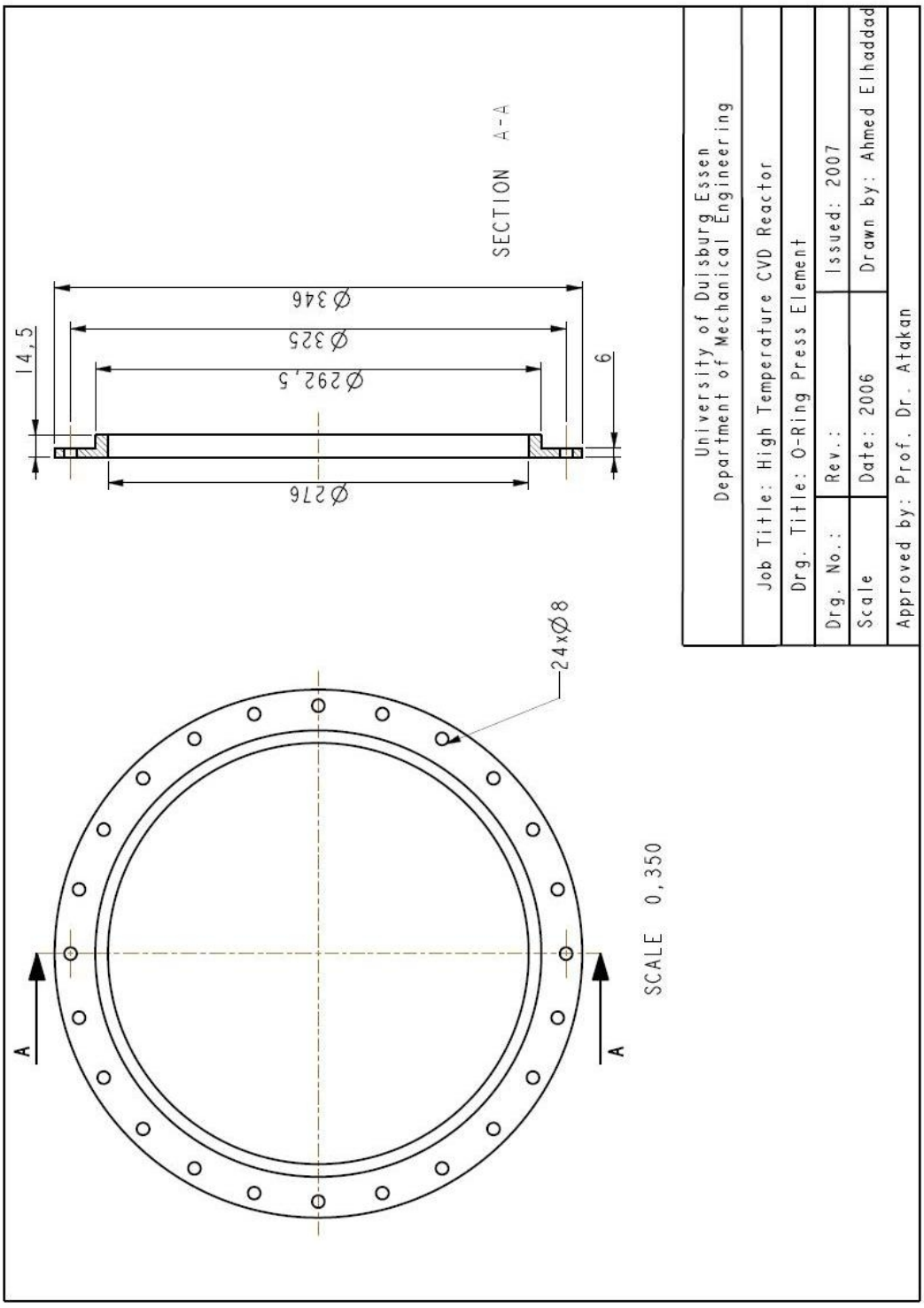
SECTION A-A
Ø346
Ø325
Ø292,5
Ø276
14,5
6
24xØ8
A
A
SCALE 0,350
University of Duisburg Essen
Department of Mechanical Engineering
Job Title: High Temperature CVD Reactor
Drg. Title: O-Ring Press Element
Drg. No.:
Rev.:
Issued: 2007
Scale
Date: 2006
Drawn by: Ahmed Elhaddad
Approved by: Prof. Dr. Atakan

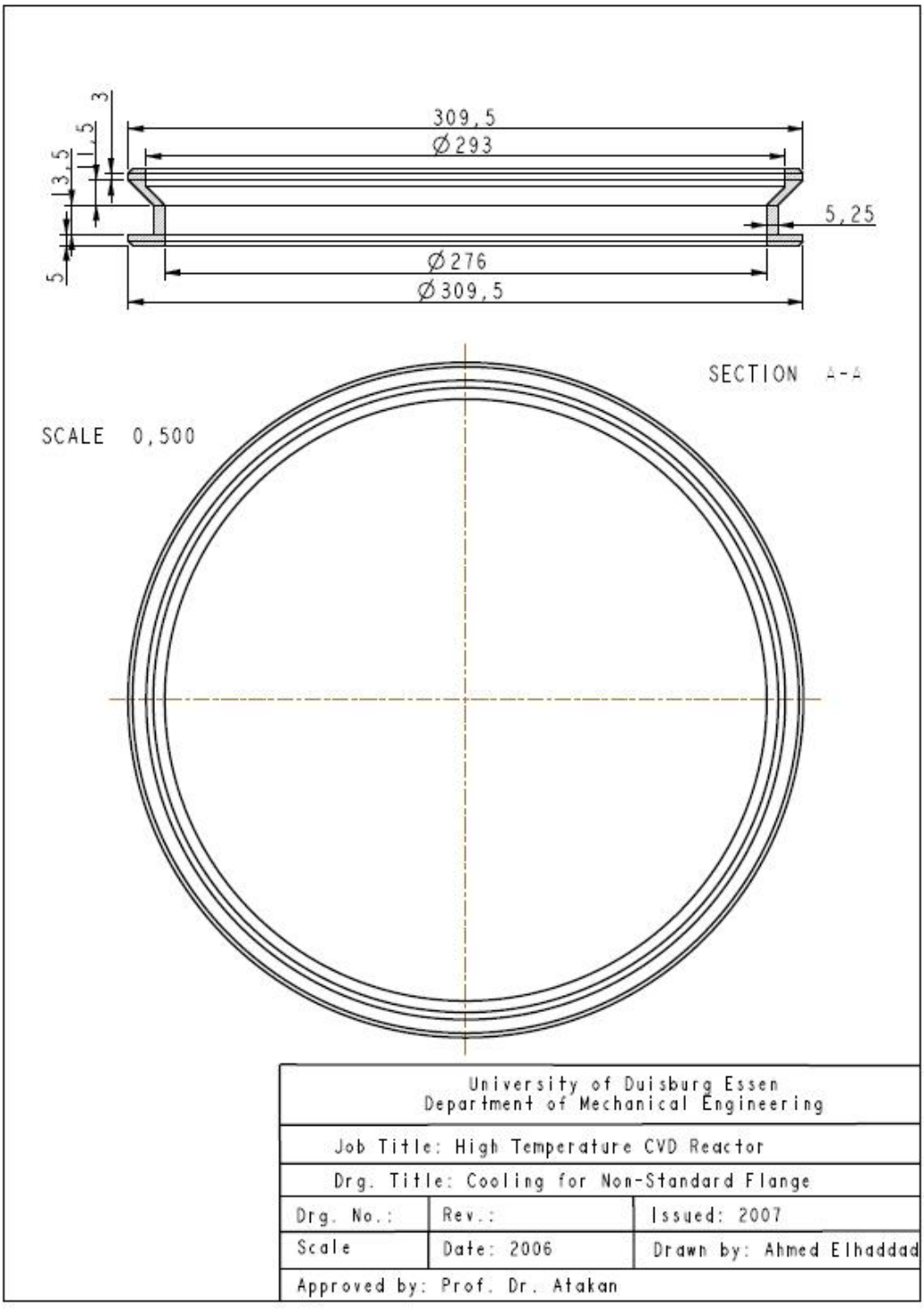
309,5
Ø293
3
1,5
3,5
5,25
5
Ø276
Ø309,5
SECTION A-A
SCALE 0,500
University of Duisburg Essen
Department of Mechanical Engineering
Job Title: High Temperature CVD Reactor
Drg. Title: Cooling for Non-Standard Flange
Drg. No.:
Rev.:
Issued: 2007
Scale
Date: 2006
Drawn by: Ahmed Elhaddad
Approved by: Prof. Dr. Atakan

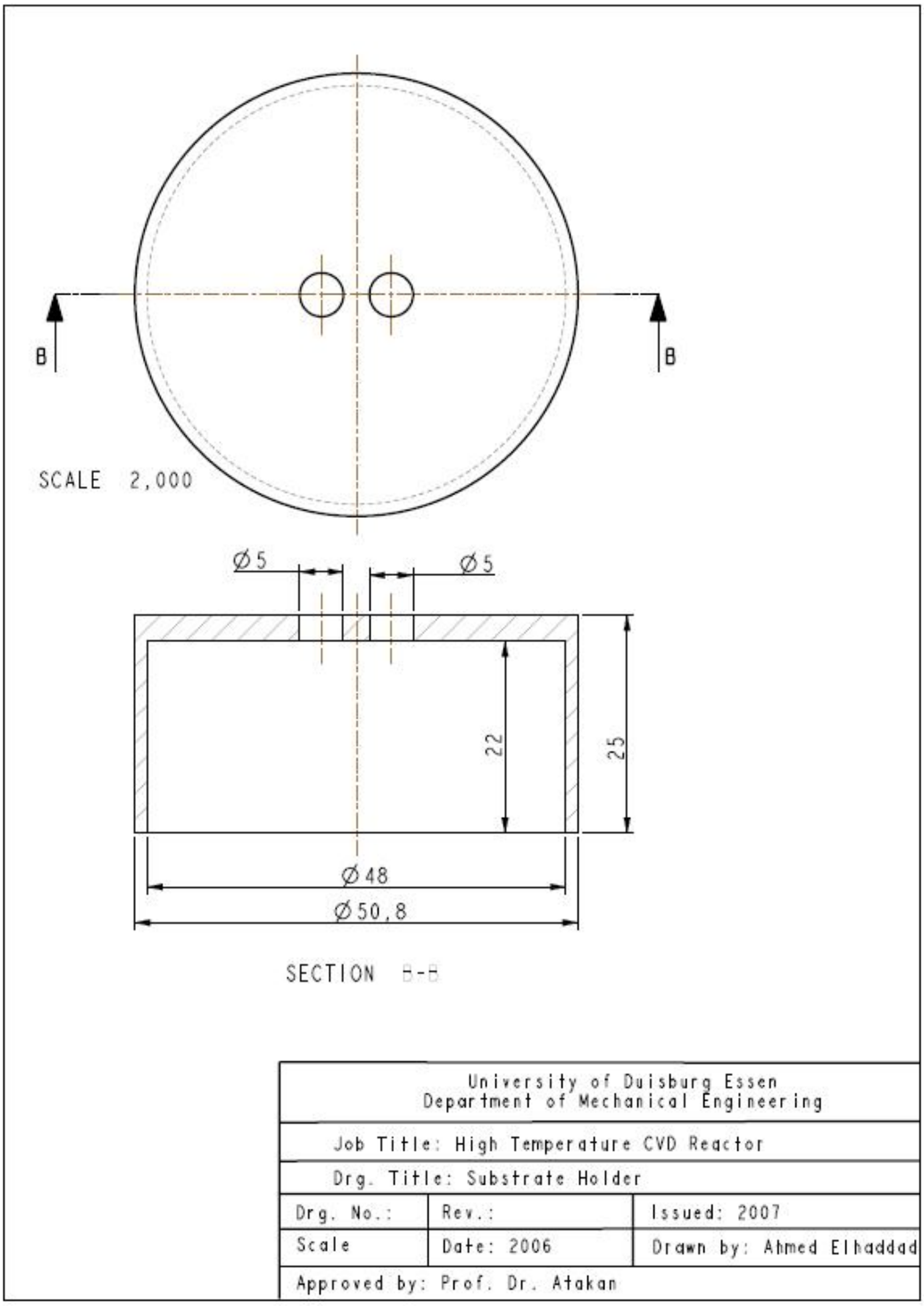
B
B
SCALE 2,000
Ø5
Ø5
22
25
Ø48
Ø50,8
SECTION B-B
University of Duisburg Essen
Department of Mechanical Engineering
Job Title: High Temperature CVD Reactor
Drg. Title: Substrate Holder
Drg. No.:
Rev.:
Issued: 2007
Scale
Date: 2006
Drawn by: Ahmed Elhaddad
Approved by: Prof. Dr. Atakan

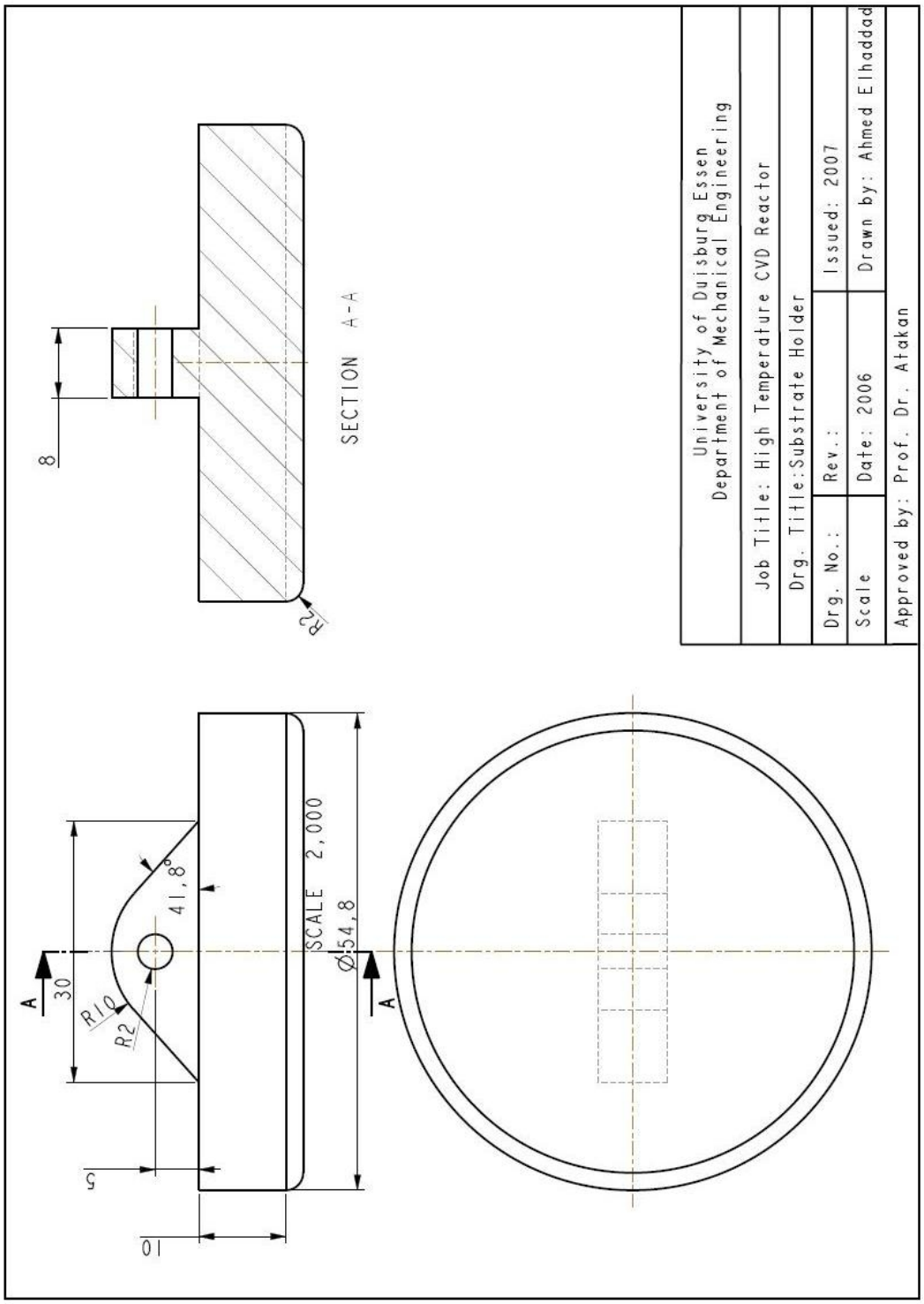
SECTION A-A
8
R2
SCALE 2,000
Ø54,8
41,8°
30
R10
R2
A
A
5
10
University of Duisburg Essen
Department of Mechanical Engineering
Job Title: High Temperature CVD Reactor
Drg. Title:Substrate Holder
Drg. No.:
Rev.:
Issued: 2007
Scale
Date: 2006
Drawn by: Ahmed Elhaddad
Approved by: Prof. Dr. Atakan

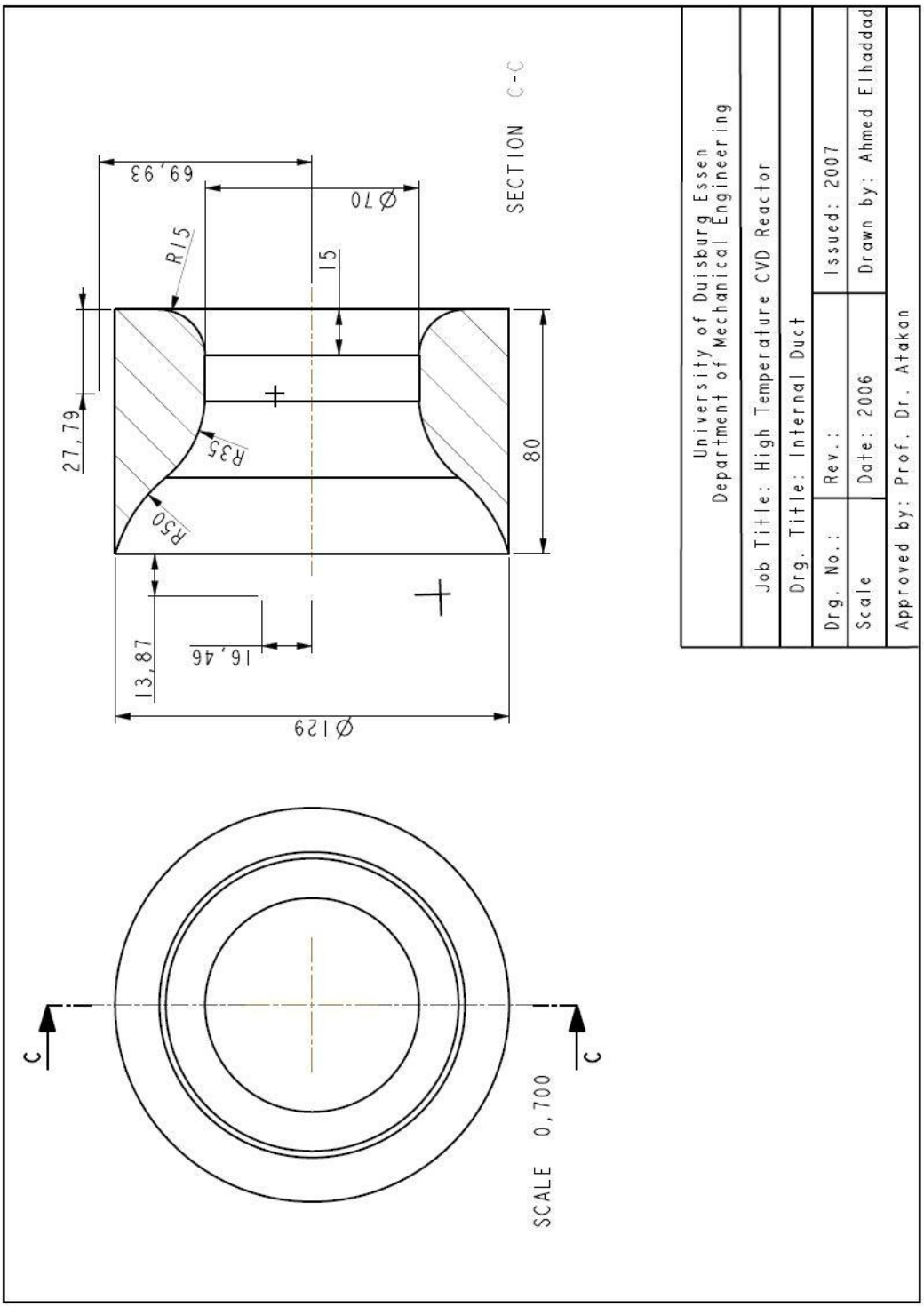
SECTION C-C
69,93
Ø70
R15
15
27,79
R35
R50
80
13,87
16,46
Ø129
C
C
SCALE 0,700
University of Duisburg Essen
Department of Mechanical Engineering
Job Title: High Temperature CVD Reactor
Drg. Title: Internal Duct
Drg. No.:
Rev.:
Issued: 2007
Scale
Date: 2006
Drawn by: Ahmed Elhaddad
Approved by: Prof. Dr. Atakan

Chapter 9

Appendix b: Pictures of the Hot-wall Reactor

Figure 9.1: *Water cooled outlet flange with four symmetrical outlet openings, which can be connected to small standard flanges of CF 40.*

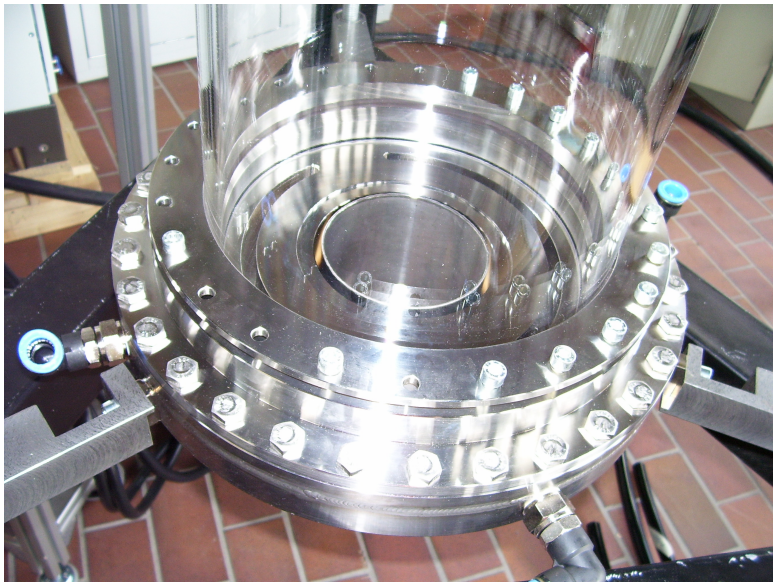

Figure 9.2: *Inlet flange sealed with the quarts tube.*

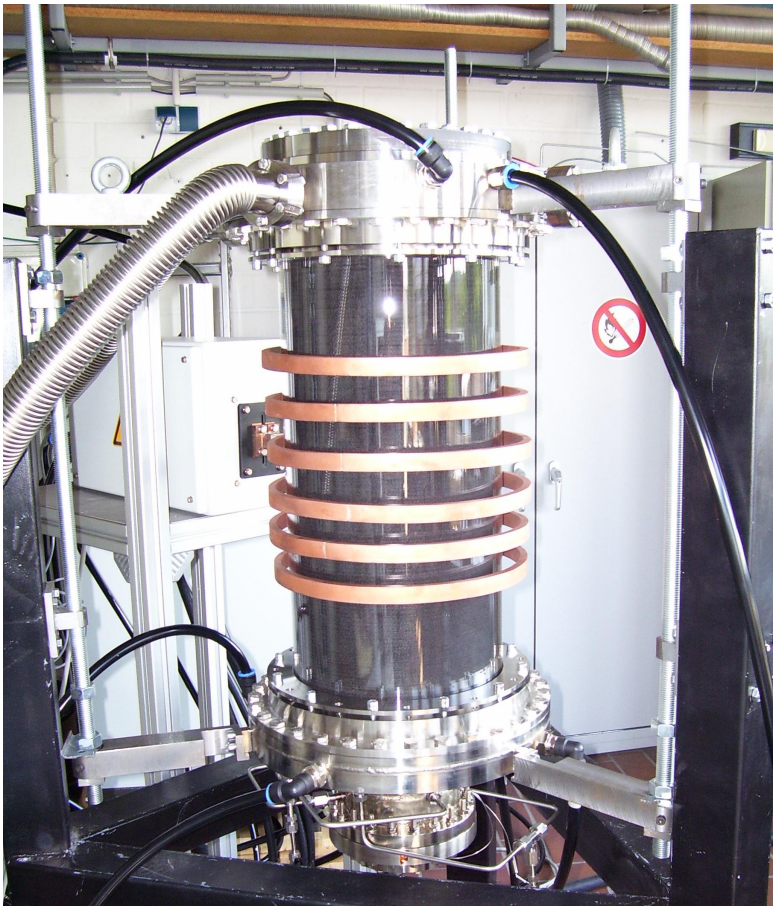

Figure 9.3: *The hot-wall reactor is shown in this figure. The induction coil is fixed around the quartz tube. The reactor connected to inlet and outlet water cooled flanges at its both ends.*

Bibliography

[1] Peter Råback. *Modeling of the sublimation growth of silicon carbide crystals*. PhD thesis, Department of Engineering Physics and Mathematics Helsinki University of Technology, 1999.

[2] J.A. Lely. Ber. deutsch. keram. ges. *Deutsch. Keram. Ges.*, 32:229–231, 1955.

[3] S. N. Rashkeev W. R. L. Lambrecht, S. Limpijumnong and B. Segall. Electronic band structure of sic polytypes: A discussion of theory. *Physica Status Solidi (b)*, 202(1):5–33, 1977.

[4] A. Zywietz K. Karch B. Adolph K. Tenelsen F. Bechstedt, P. Käckell and J. Furthmüller. Polytypism and properties of silicon carbide. *Physica Status Solidi (b)*, 202(1):35–62, 1997.

[5] Hina Ashraf. *Investigation of symmetries of phonons in 4H and 6H-SiC by infrared absorption and raman spectroscopy*. PhD thesis, Linköpings Universität, Department of Physics and Measurement Technology, 2005.

[6] Christian Janzen. *Untersuchungen zur Synthese von Eisenoxid-Nanopartikeln in der Gasphase*. PhD thesis, Duisburg Uni, 9. April 2002.

[7] frank.filser@mat.ethz.ch F. Filser & L.J. Gauckler. Materialwirtschaft 1, keramische werkstoffe. ETH-Zürich, Departement Materials.

[8] V. F. Tsvetkov R. C. Glass, D. Henshall and C. H. Carter. Sic seeded crystal growth. *Physica Status Solidi (b)*, 202(1):147–162, 1997.

[9] I. G. Ivanov M. Syväjärvi, R. Yakimova and E. Janzén. Growth of 4h-sic from liquid phase. *Materials Science and Engineering*, B46:329–332, 1997.

[10] V. E. Chelnokov M. P. Scheglov A. A. Lebedev, A. S. Tregubova and A. A. Glagovskii. Growth and investigation of the big area lely-grown substrates. *Materials Science and Engineering*, B46:291–295, 1997.

[11] Yu. M. Tairov and V. F. Tsvetkov. Investigation of growth processes of ingots of silicon carbide single crystals. *Journal of Crystal Growth*, 43:209–212, 1978.

[12] V. F. Tsvetkov Yu. M.Tairov. General principles of growing large-size single crystals of various silicon carbide polytypes. *J.Cryst.Growth*, 52:146–150, 1981.

[13] V. F. Tsvetkov Yu. M. Tairov. Crystal growth and characterization of polytype structures. *Pergamon Press, London*, page 111, 1983.

[14] D. Theis C. Weyrich G. Ziegler, P. Lang. Single crystal growth of sic substrate material for blue light emitting diodes. *Transactions on ED*, ED-30(4):277–281, 1983.

[15] C. H. Carter R. F. Davis and C. E. Hunter. *U.S. Patent*, Re. 34,861, 1995.

[16] R.A. Stein and P.Lanig. Influence of surface energy on the growth of 6h- and 4h-sic polytypes by sublimation. *Mat. Sci. Eng*, B11:69, 1992.

[17] Yu. M. Tairov and V. F. Tsvetkov. General principles of growing largesize single crystals of various silicon carbide polytypes. *Journal of Crystal Growth*, 52:146–150, 1981.

[18] Yu. M. Tairov. Growth of bulk sic. *Materials Science and Engineering*, B29:83–89, 1995.

[19] V. Balakrishna G. T. Dunne R. H. Hopkins R. N. Thomas W. A. Doolittle G. Augustine, H. M. Hobgood and A. Rohatgi. High purity and semi-insulating 4h-sic crystals grown by physical vapor transport. . *Materials Science Forum*, . 264-268:. 9–12, . 1998.

[20] O. Danielssona M.K. Linnarssonc A. Henrya E. Janzen J. Zhanga, A. Ellisonb. Epitaxial growth of 4h sic in a vertical hot-wall cvd reactor: Comparison between up and down-flow orientations. *Journal of Crystal Growth*, 241:421–430, 2002.

[21] T. Kimoto. *Step-controlled epitaxial growth of a-SiC and device applications*. PhD thesis, Kyoto University, Japan, 1995.

[22] J. Sumakeris H. S. Kong M. J. Paisley O. Kordina, K. Irvine and C. H. Carter. Growth of thick epitaxial 4h-sic layers by chemical vapor deposition. *Materials Science Forum*, 264-268:107–110, 1998.

[23] D.J. Larkin J.A. Powell. Process-induced morphological defects in epitaxial cvd silicon carbide. *Phys. Stat. Sol*, B202:529, 1997.

[24] K. Irmscher G. Wagner. Influence of the growth conditions on the layer parameters of 4h-sic epilayers grown in a hot-wall reactor. *Material Science Forum Science Forum*, 353-356:95, 2001.

[25] H. Behner A. Wiedenhofer R. Rupp, Yu. N. Makarov. Silicon carbide epitaxy in a vertical cvd reactor: experimental results and numerical process simulation. *Physica Status Solidi (B)*, 202:281–304, 1997.

[26] H. D. Nordby A. A. BurkJr., M. J. O'Loughlin. Sic epitaxial layer growth in a novel multi-wafer vapor-phase epitaxial (vpe) reactor. *Journal of Crystal Growth, Volume 200, Issues 3-4, April 1999, Pages 458-466*, Volume 200, Issues 3-4:458–466, 1999.

[27] T. Kimoto K. Fujihira and H. Matsunami. High-purity and high-quality 4h-sic grown at high speed by chimney-type vertical hot-wall chemical vapor deposition. *Appl. Phys. Lett.*, 80:1586, 2002.

[28] T. Jikimoto K. Izumi H. Tsuchida, I. Kamata. Growth of thick 4h-sic epilayers in a vertical radiant-heating reactor. *Mat. Res. Soc. Symp.*, 640:H2.12.1, 2001.

[29] T. Kimoto K. Fujihira1 and H. Matsunami. Fast epitaxial growth of high-quality 4h-sic by vertical hot-wall cvd. *materials Science Forum*, 433-436:161–164, 2002.

[30] A. Henry E. Janzen A. Ellison, J. Zhang. Epitaxial growth of sic in a chimney cvd reactor. *Journal of Crystal Growth*, 236, Issues 1-3:225–238, 2002.

[31] A. Ellison A. S. Bakin I. G. Ivanov A. Henry R. Yakimova M. Touminen A. Veanen E. Janzen O. Kordina, C. Hallein. High temperature chemical vapor deposition of sic. *Appl. Phys. Lett.*, 69:No. 10, 1996.

[32] B. Sundqqvist Pozina J. P. Bergman E. Janzen A. Elisson, B. Magnusson and Veanen. Sic crystal growth by htcvd. *Materials Science Forum*, 457-460:9–14, 2004.

[33] Donald L. Smith. *Thin-Film Deposition*. 1995.

[34] J. Peterson A. Henry Q. Wahab J.P. Bergman Y.N. Makarov A. Vorob A. Vehanen E. Janzen A. Ellison, J. Zhang. High temperature cvd growth of sic. *Materials Science and Engineering*, B61-62:113–120, 1999.

[35] A. Itoh T. Kimoto and H. Matsunami. Step-controlled epitaxial growth of high-quality sic layers. *Physica Status Solidi (b)*, 202:247, 1997.

[36] J.T. Glass H. S. Kong and R.F. Davis. Chemical vapor deposition and characterization of 6h-sic thin films on off-axis 6h-sic substrates. *Journal of Applied Physics,*, 64:2672, 1988.

[37] Zhang Chuanping b Huang Ximin b Yu Xiling Yang Bailiang a, M. Isshiki a. In-situ measurement of growth rate by laser diffraction during cdte single crystal growth from the vapour phase. *Journal of Crystal Growth*, 147:399–402, 1995.

[38] O. A. Nerushev M. Jönsson and E. E. B. Campbell. In situ growth rate measurements during plasma-enhanced chemical vapour deposition of vertically aligned multiwall carbon nanotube films. *Nanotechnology*, 18:305702 5pp, 2007.

[39] J.R. Elliot S.A. Gokoglu M.J.Purdy S. Bammidipati, G.D. Stewart. Chemical vapor deposition of carbon on graphite by methane pyrolysis. *AIChE Journal*, 42, no11:3123–3132 (25 ref.), 1996.

[40] A.M. Weiner S.J. Harris. Pressure and temperature effects on the kinetics and quality of diamond films. *J. Appl. Phys.*, 75:5026, 1994.

[41] J.C. Angus E.A. Evans. Microbalance studies of diamond nucleation and growth rates. *Diamond and related materials*, 5, no 3-5 (394 p.) (18 ref.), [Notes: Part 1]:200–205, 1996.

[42] Edward A. Evans A. Salifu, G. Zhang. In situ growth rate measurements for plasma processing of opaque materials. *Thin Solid Films*, 418:151–155, 2002.

[43] D. Neuschütz M. Schierling, E. Zimmermann. Deposition kinetics of al2o3 from alcl3-co2-h2-hcl gas mixtures by thermal cvd in a hot-wall reactor. *J. Phys. IV France*, 8:85–91, 1999.

[44] I.G. Ivanov O. Kordina J. Zhang C.G. Hemmingson C. Yu. Gu M.R. Leys. A. Ellison, T. Kimoto and E. Janzen. Growth and characterisation of thick epilayers by high temperature cvd. *Material Science Forum*, 264-268:103–106, 1998.

[45] J. Schoonman F.E. Kruis and B. Scarlett. Homogeneous nuculeation of silcon. *Aerosol Sci., Vol. 25, No. 7, pp. 1291 130,1, 1994*, Vol. 25, No. 7:1291 130,1,, 1994.

[46] Hrsg.:Verein Deutscher Ingenieure, editor. *VDI-Wärmeatlas*. Verein Deutscher Ingenieure, 2006.

[47] M. Klimenkov W. Matz E. Theodossiu, H. Baumann and K. Bethge. Characterization of crystallinity of sic surface layers produced by ion implantation. *phys. stat. sol.(a)*, 182:635, 2000.

[48] P. Mh-tenssorf A. Ellison A. Konstantinov 0. Kordinaa E. Janzha C. Hallin, F. Owman. In situ substrate preparation for high-quality sic chemical vapour deposition. *Journal of Crystal Growth*, 18:241–253, 1997.

[49] A. Gerlitzke G. Wagner, J. Doerschel. Surface preparation of 4h-sic substrates for hot-wall cvd of sic layers. *Applied Surface Science*, 184:55–59, 2001.

[50] U. Starke J. Schardt, J. Bernhardt and K. Heinz. Crystallography of the (3x3) surface reconstruction of 3c-sic(111), 4h-sic(0001), and 6h-sic(0001) surfaces retrieved by low-energy electron diffraction. *Physical Review B*, 62:15, 2000.

[51] U. Starke-K. Heinz J. Bernhardt, M. Nerding. Stable surface reconstructions on 6h-sic(0001). *Materials Science and Engineering*, B61-62:207–211, 1999.

[52] S. NISHINO W. S. YOO and H. MATSUNAMI. Single crystal growth of hexagonal sic on cubic sic by intentional polytypes. *Journal of Crystal Growth*, 99:278–283, 1990.

Der Lebenslauf ist in der Online-Version aus Gründen
des Datenschutzes nicht enthalten